1975

A GEOPHYSICAL INVESTIGATION IN THE BITTERROOT VALLEY WESTERN MONTANA

Robert W. Lankston

The University of Montana

76-12,193

LANKSTON, Robert Wayne, 1946-
A GEOPHYSICAL INVESTIGATION IN THE BITTERROOT VALLEY, WESTERN MONTANA.

University of Montana, Ph.D., 1975
Geophysics

Xerox University Microfilms, Ann Arbor, Michigan 48106

A GEOPHYSICAL INVESTIGATION IN THE BITTERROOT VALLEY, WESTERN MONTANA

by

Robert Wayne Lankston

B.S., Indiana University, 1969
M.A., Indiana University, 1971

Presented in partial fulfillment of the requirements for the degree of

Doctor of Philosophy

UNIVERSITY OF MONTANA

1975

Approved by:

Anthony Qamar
Chairman, Board of Examiners

John M. Stewart
Dean, Graduate School

Dec 3, 1975
Date

ABSTRACT

Lankston, Robert Wayne, Ph.D., April 1975 Geology

A Geophysical Investigation in the Bitterroot Valley, Western Montana (112 p.)

Director: Anthony Qamar

A map of the complete Bouguer anomaly for the Bitterroot Valley in western Montana is produced and interpreted to yield the general geometry of Cenozoic valley fill sediments. Various steps in processing the gravity data are discussed including lowpass, frequency domain filtering and two and three dimensional modeling.

Refraction and reflection seismic data are analyzed for the area north of Stevensville to verify the models generated from the gravity data and to investigate the possibility of using seismic methods to gain meaningful data for ground water prospecting.

A map of the total magnetic intensity is presented for the area north of Stevensville. Depth estimates based upon the magnetic data indicate anomalies originating from several levels in the subsurface in the vicinity of Ambrose Creek. Three dimensional modeling of the magnetic field verified the existence of a multilayer anomalous body.

Integrated geophysical analysis combining gravity and magnetics models, downward continuation of the magnetic field, and seismic refraction data indicates the existence of a continuous surface which extends from the eastern face of the Bitterroot Range and intersects the anomalous magnetic body in the Ambrose Creek area. This surface may be a gravity glide surface.

The study introduces a set of basic geophysical data which can be used for further studies in groundwater, economic geology, or regional structural geology in western Montana.

TABLE OF CONTENTS

LIST OF FIGURES

Figure Page

LIST OF PLATES

LIST OF TABLES

ACKNOWLEDGEMENTS

The completion of this study has been made possible through the combined efforts of numerous individuals and institutions. The geophysical field and laboratory work was marginally funded by the Water Resources Research Center, Bozeman, Montana through an account administered by the University of Montana. The University of Montana provided the geophysical field equipment, laboratory space and computer time.

Individuals from across the United States who contributed to the production of this study include Robert F. Blakely, Indiana Geological Survey, Jim Jordan, Western Geophysical Company, Richard I. Gibson and Jeffrey Friedberg, Aero Service Corporation, Jesse K. Douglas and others at Gulf Research and Development Company, Marvin Miller, Montana State Bureau of Mines and Geology, James A. Ferguson, Burlington Northern, Inc., Robert Twist, Federal Bureau of Wildlife and Fisheries, Anthony Qamar and Kenneth Gordon, University of Montana, and the many ranchers in the Bitterroot Valley who allowed access to their lands during the course of the study, in particular Ernest Bolin and the Brechbill family.

Several fellow students freely contributed time to perform field assistant duties including Richard Asher, Ellen Gressitt, Kathleen Hawley, Kathleen Huguet, David Millen, K. M. Nolan, Gene Suko, and Thomas Williams.

A project with the scope of this one with its volumes of data compilation, analysis and presentation should not have been attempted without the aid of a full time geophysical technician. Special recognition and thanks are due Marian Millen Lankston for her numerous days

spent as field assistant, data reducer, a job which included the tedious terrain corrections, digitizer and key puncher, draftswoman and typist. Without Marian's continuous moral and exceptional technical support, this study would never have been completed.

Chapter I

INTRODUCTION

Purpose and Scope

The Bitterroot Valley in western Montana is an area undergoing rapid growth (Montana Almanac, 1957). Related to the growth are problems of planning, zoning, and resource management. Groundwater and surface water are two resources intimately involved in these problems. Only two hydrogeologic studies have been conducted in the Bitterroot Valley (McMurtry, et al., 1959, and Nolan, 1973).

Although the present study was undertaken with the intention of providing geophysical data relevant to groundwater resources, problems which developed during the course of the research limited direct data on the amount of groundwater in the valley. On the other hand this study does present basic geophysical data collected in the Bitterroot Valley which allow large scale structures observed around the valley to be mapped in the subsurface and which subsequently act as a basis for more detailed studies of groundwater and regional geologic structure. This study provides an example of some of the geophysical programs and procedures which can be useful in valley fill studies in western Montana.

In addition to providing relevant geophysical data on groundwater resources, a second intention of this study was to investigate the utilization of basic, inexpensive surface geophysical techniques. Engineering methods of seismic exploration can provide direct data on groundwater conditions in the Bitterroot Valley. Gravimetric and surface magnetic methods yield data on regional geologic structure. The engineering seismic and potential field methods of geophysical exploration are relatively inexpensive and, when they are coupled with proper computer processing of the field data and synergistic evaluation, models of the subsurface can be constructed which are useful to the groundwater hydrologist, stratigrapher, and structural geologist.

No attempt is made in this study to relate the calculated geophysical models of the Bitterroot Valley to all of the known structures in the region surrounding the valley. The only previous geophysical study in the valley (Manghnani and Hower, 1962) is so limited that no attempt has been made to relate its results to the results of the present study. The three parts of this study, 1) potential field surveys, 2) seismic surveys, and 3) computer modeling and analysis, provide data on formation densities, magnetic susceptibilities, porosities, seismic velocities, and water storage volume and provide supporting data for regional structural geologic studies.

Geologic Setting

The Bitterroot Valley, south of Missoula, Montana, is approximately fifty miles (80 km) long and up to twelve miles (19 km) wide with the long axis extending in a generally north-south direction. The valley is bounded on the west and south by the Bitterroot Mountain Range and on the east by the Sapphire Mountain Range. The Bitterroot Mountains comprise the Idaho Batholith in the southern two thirds of the range, metamorphosed Precambrian sediments in the northern third of the range, and the Frontal Zone Gneiss along the entire eastern edge of the range. The Idaho Batholith is a complex late Cretaceous to early Tertiary granitic intrusive (Ferguson, 1972). The Frontal Zone Gneiss which bounds the west margin of the valley may represent a gravity glide "plane" along which rocks now comprising the Sapphire Mountain Range slid off of the rising Idaho Batholith (Ron Chase, personal communication). The Sapphire Mountains are composed largely of Precambrian Belt Group sedimentary rocks.

The surface of the Bitterroot Valley is generally flat and is mantled by a veneer of less than 500' (153 km) of Quaternary alluvium. The present course of the Bitterroot River trends northward with a gradient of approximately 30'/mile (5.6m/km). Under the Quaternary sediments is a section of valley fill sediments up to 4000 feet (1220 m) thick.

The Bouguer gravity anomaly map of the entire valley is interpreted to yield valley fill thicknesses for most of the valley (Plates 1 and 2). However, this study concentrates the geophysical field investigations and computer analyses in the area between Ambrose and Kootenai Creeks north of Stevensville. The geology of the concentrated study is presented in Figure 1. This area was selected for detailed investigations on the basis of the relatively flat gravity anomaly and the strong magnetic anomaly observed in reconnaisance surveys over the area and the ready access to the area.

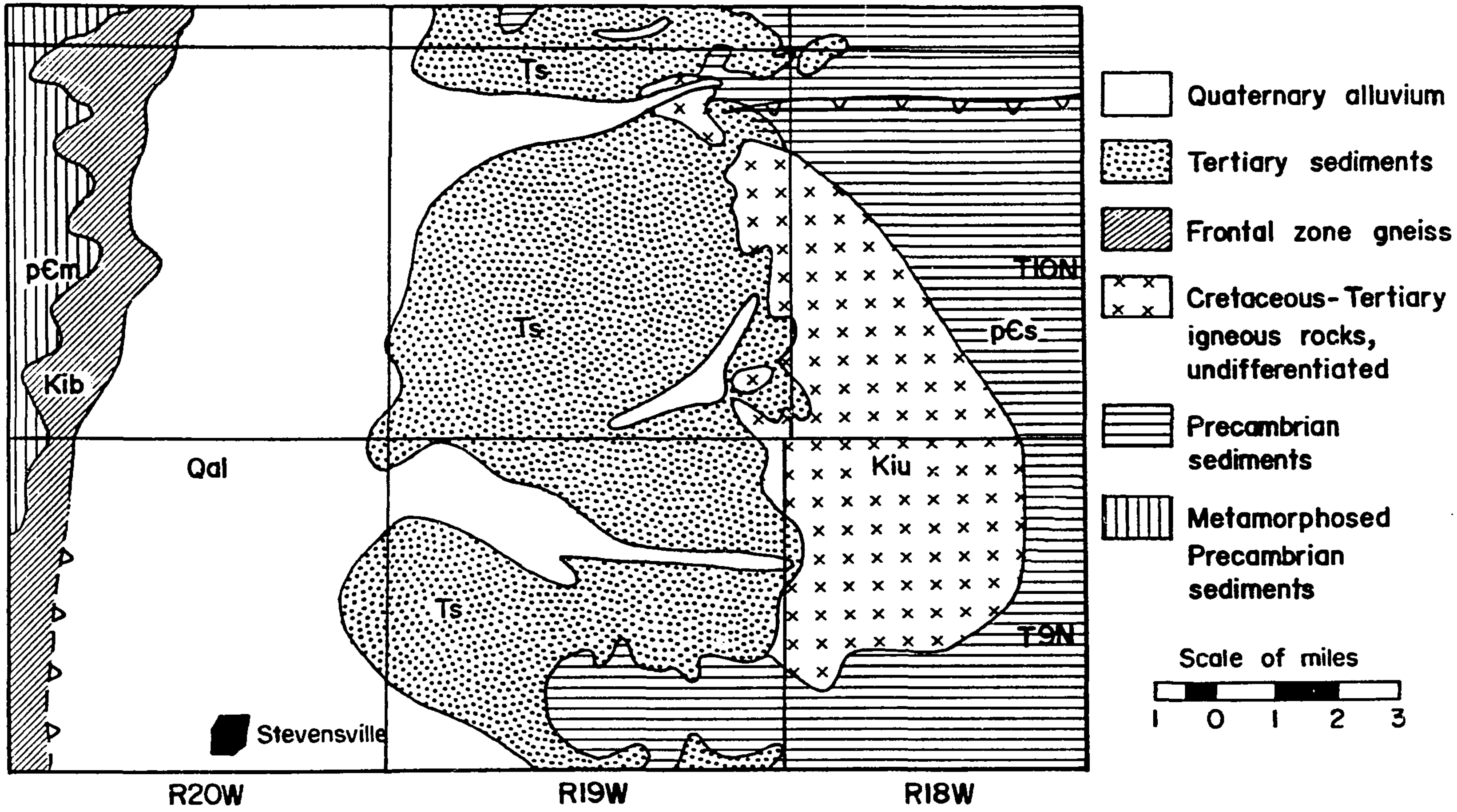

Figure 1. Generalized geologic map of the Ambrose and Kootenai Creek areas north of Stevensville, Montana in the Bitterroot Valley (from unpublished maps, University of Montana).

Chapter II

DATA COLLECTION AND REDUCTION

Gravimetric Survey

The gravimetric survey of the Bitterroot Valley was conducted as outlined by Dobrin (1960) using a Worden gravimeter. The survey covered the surface of the valley within the bedrock boundaries on a grid of approximately one mile (1.6 km) intervals. Only a few (approximately 5%) of the more than 400 gravity stations were occupied in the side canyons off of the main valley. The rationale for this will be discussed in later sections.

Reductions of the field data to the Bouguer anomaly were made with respect to the established gravity station at Johnson-Bell Airport in Missoula (980 443.844 milligals, Jesse Douglas, personal communication, 1972). Station elevations and latitudes were taken directly from published USGS topographic maps. Instrumental and diurnal drifts were determined by reoccupying daily base stations at intervals of two to three hours.

The Bouguer gravity anomaly was evaluated with the aid of a programmable desk calculator and a program written by Sidney Prahl. The program evaluated the complete Bouguer anomaly (g_B) for each station using the relationship

$$g_B = g_0 + \text{elevation correction} + \text{terrain correction} - g_T$$

where g_0 is the observed gravity defined as the difference between the gravity value at the Johnson-Bell Airport base and the gravity difference between the base and the station and g_T is the calculated theoretical gravity at the station calculated from the international gravity formula

$$g_T = 978.049(1 + 0.0052884 \sin^2\phi - 0.0000059 \sin^2 2\phi) \text{ gals}$$

(Grant and West, 1966) where ϕ is the station latitude. The free air and Bouguer effects were combined into the elevation correction. The datum was sea level and the density was assumed to be 2.67 grams/cubic centimeter. The elevation correction was 0.060 mgals/ft (0.183 mgals/m). Terrain corrections were obtained using templates after Hammer (1939) and tables presented by Douglas and Prahl (1972). The terrain correction was determined to Zone K (32,490 feet, 9.903 km).

The Bouguer anomaly map of the Bitterroot Valley (Plate 1) has several known uncertainties. These arise as a result of the quality of the topographic maps available and the necessity of making terrain corrections. Problems of gravimetric surveying in western Montana are discussed in detail by Burfeind (1967) and Smith (1967).

The greatest problems in gravimetric surveying in the Bitterroot Valley and, consequently the greatest uncertainties, are caused by the elevation and terrain corrections. Minimum station elevation uncertainty along the eastern margins of the valley is $\pm$ 50 feet (16.4 m) on the Sapphire (30 minute) quadrangle and $\pm$ 40 feet (13.1 m) on the Cleveland Mountain (15 minute) quadrangle where the contour intervals are 100 feet and 80 feet respectively. These elevation uncertainties alone may contribute an error of $\pm$ 3 milligals in the Bouguer anomaly in areas where the expected residual anomaly is between zero and five milligals. Though three milligals is small compared to the total anomaly across the valley of up to 30 milligals (Plate 1), this possible error reduces the reliability of the calculated valley fill thicknesses in the eastern areas. Calculated thicknesses in the central and western portions of the valley are more reliable because the locations and elevations can be interpolated more precisely from the available 7½ minute maps (contour intervals between 5 and 20 feet).

A second problem in gravimetric surveying in western Montana and particularly the Bitterroot Valley area is the uncertainty introduced into the Bouguer anomaly because of the necessity of making terrain corrections. Although care was exercised in selecting gravity station locations to reduce the effects of Zones A through D (Hammer, 1939) (distances up to 558 feet, 170 m from the gravimeter), the rugged terrain surrounding the valley, the poor quality maps along the east edge of the valley, and the subjectivity inherent in generating a terrain correction allowed the introduction of an uncertainty of as much as ± 0.1 milligal in the center of the valley and ± 5 milligals near the valley margins with the possible error increasing with distance into the mountains until the probable error exceeds ± 20 milligals. These ranges were determined by two methods: a) having the terrain correction calculated at a point by more than one person and b) calculating the terrain correction at a point by using only the highest or only the lowest elevation in each of the terrain correction template segments. The combined problems of location, elevation, and terrain correction discouraged establishing gravity stations outside the bedrock boundaries of the valley. Numerical modeling produced gravity anomalies which indicated that no usable information for the scope of the study of the Bitterroot Valley was lost by having so few stations in the mountains.

Magnetic Survey

Reconnaisance magnetic surveying with a Barringer total field precession magnetometer (± 10 gammas) through the northern third of the Bitterroot Valley indicated a magnetic high near the mouth of Ambrose Creek canyon on the east side of the valley north of Stevensville. Detailed magnetic surveying with a Geometrics Model G-816 total field precession magnetometer (± 1.0 gamma) delineated a relative anomaly of more than 500 gammas (Figs. 2 and 14). The reconnaisance survey and the detailed survey were tied together by the reoccupation of stations with both of the recording instruments. The ground level survey agrees very closely in anomaly shape with the aeromagnetic maps presented by Douglas (1972), USGS (1966), and Zietz, et al., (1971).

No latitude or longitude corrections were applied to the data because of the small size of the study area. Diurnal variations were determined by repeated occupation of base stations at intervals of two to three hours.

Seismic Survey

Seismic surveying of the Bitterroot Valley was conducted using an Independent Exploration Company 24 channel analog recording system which incorporated an Electro-Tech oscillograph and a Southwestern Industrial Electronics (SIE) analog magnetic tape recorder and playback unit. A single channel Bison Model 1570 engineering seismograph was also used.

The seismic survey was undertaken to check the large scale geologic

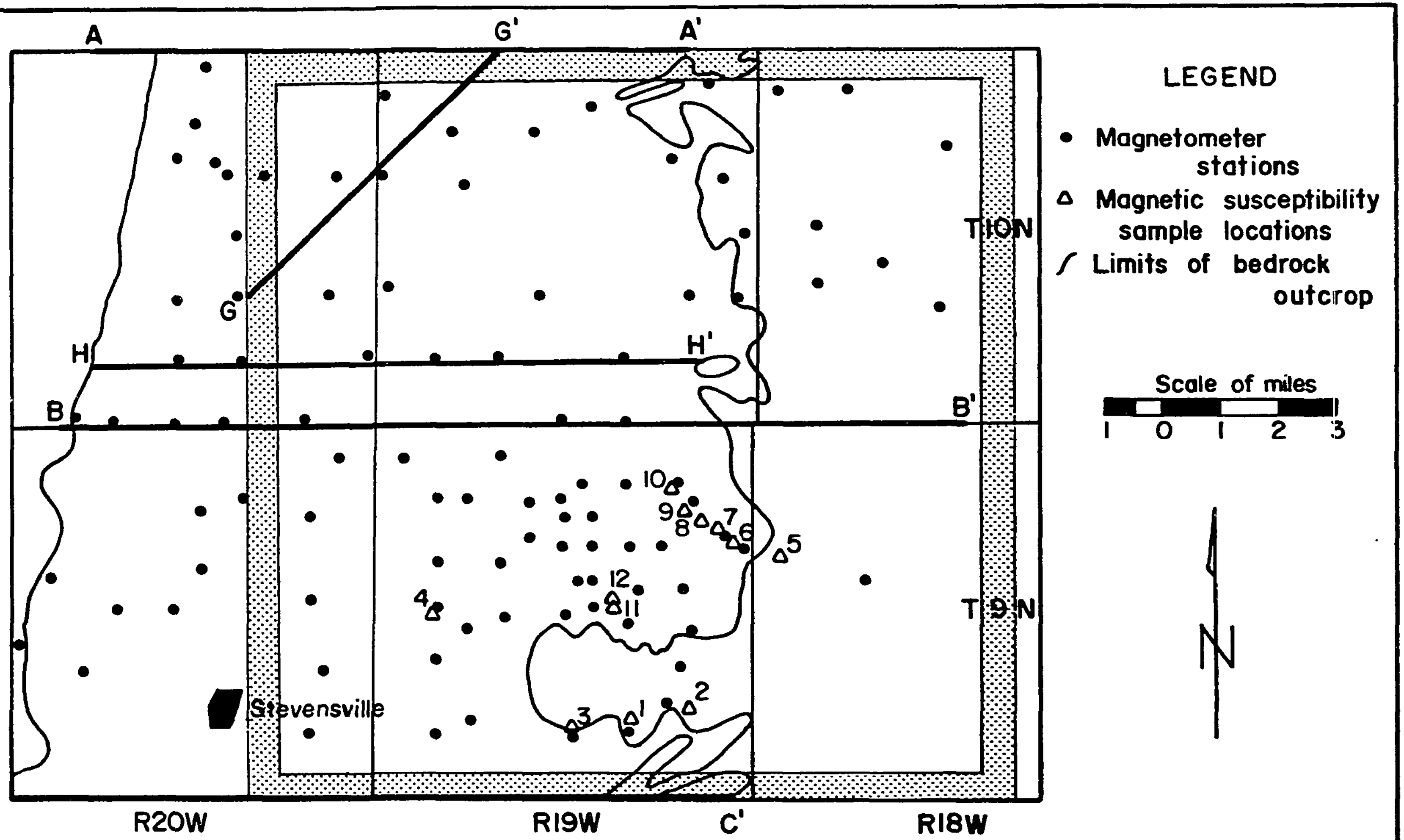

Figure 2. Magnetic field measurement locations and magnetic susceptibility sample locations. The shaded area outlines the margin of the area modeled with the Talwani and Ewing program (calculated map Figure 16). GG' is location of downward continuation profile (Figure 23).

models generated from the potential field data. In addition, the engineering refraction seismic method is a basic exploration technique which provides a fast and economical means for developing groundwater information along continuous profiles or at isolated locations. Refraction and reflection seismic data can be correlated directly to existing well data for extrapolation of groundwater conditions throughout a large area.

Both refraction and reflection seismic techniques were used to collect data from the areas near Ambrose Creek and Kootenai Creek north of Stevensville (Figs. 3 and 4). Problems in equipment condition and design reduced the ability of the seismic experiments to conclusively demonstrate the value of exploration seismic techniques for groundwater prospecting.

The Bison seismic system is limited in that it is designed for shallow refraction investigations with a hammer signal source (Axel Fritz, personal communication). Several of the problems described in a California Division of Highways report (Stevens, 1973) were encountered while using the Bison system in the Bitterroot Valley. In comparing the Bison system to other systems including a multichannel Electro-Tech analog system, the California researchers found problems in non-uniformity of time scales from one sweep rate to another, different arrival times when hammer and explosive sources were used, and different travel time plots from data generated with the Bison and a multichannel system. Though these problems were encountered in the survey in the Bitterroot Valley, no concerted attempt was made to duplicate the results of the Stevens (1973) report.

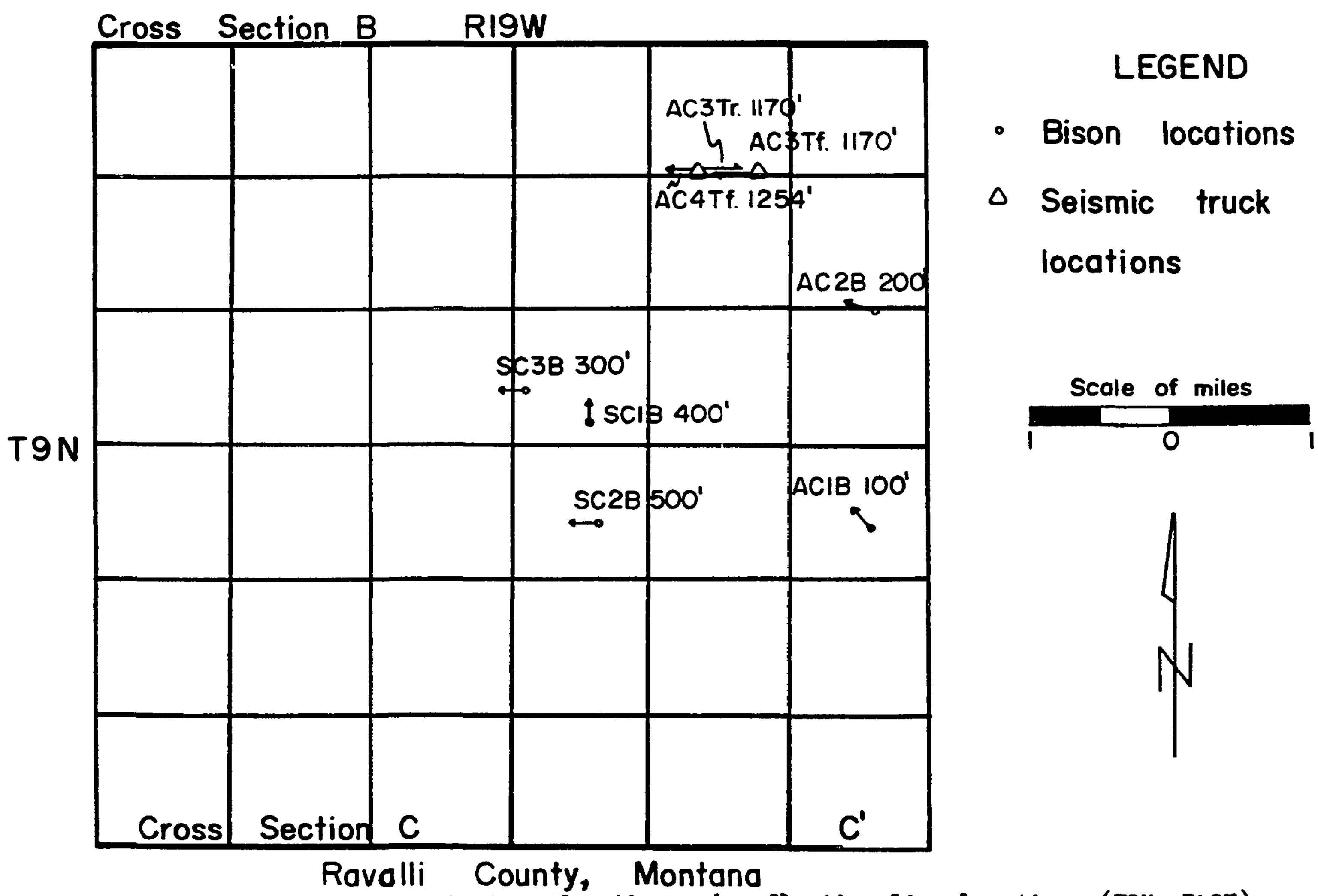

Figure 3. Index map showing seismic refraction and reflection line locations (T9N, R19W). (Arrows indicating line directions not drawn to scale.)

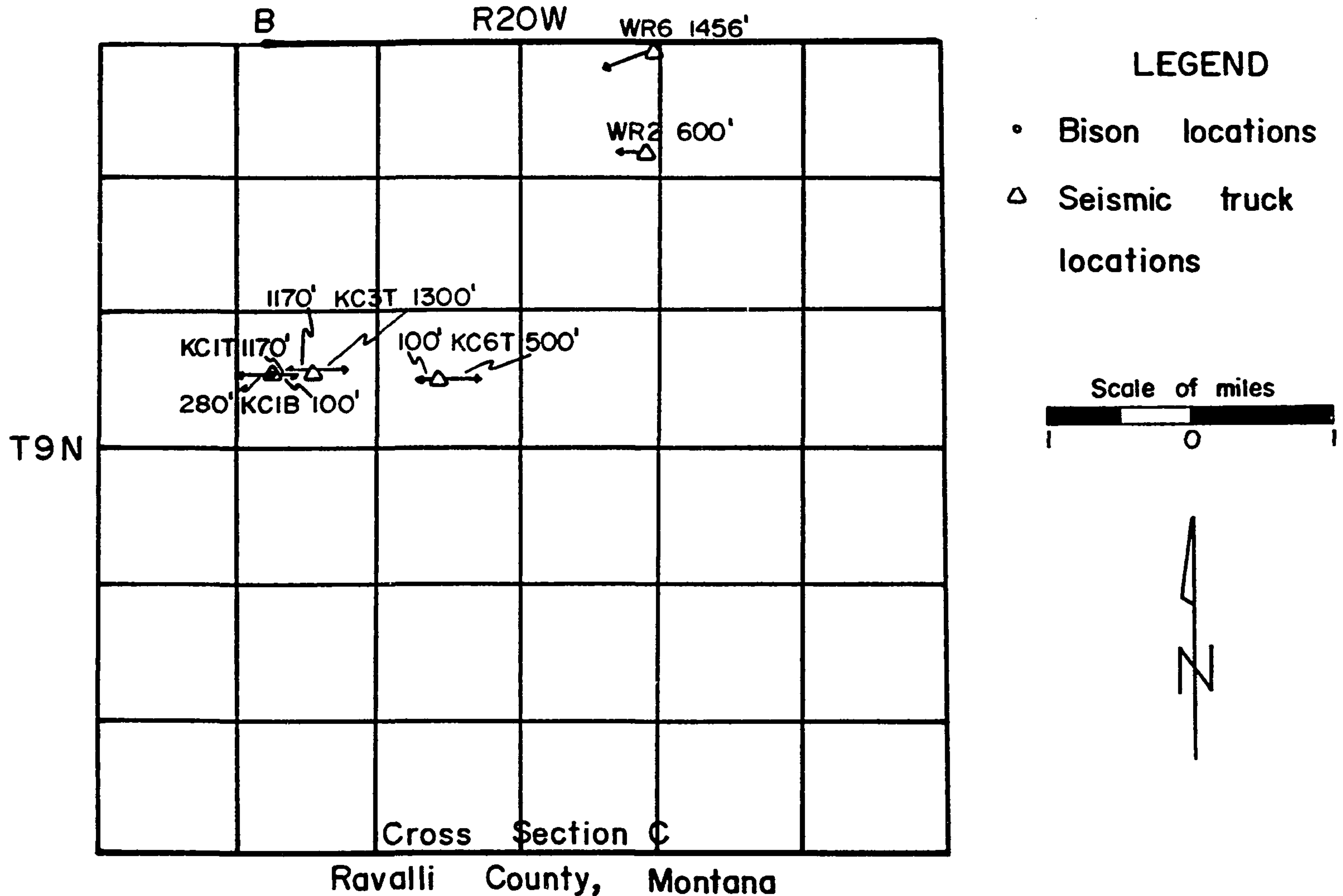

Figure 4. Index map showing seismic refraction and reflection line locations (T9N, R20W). (Arrows indicating line directions are not drawn to scale.)

For the seismic investigations in the Bitterroot Valley, the Bison system was used to measure near surface velocities by refraction techniques. Spread lengths up to 550 feet were attained with a sledge hammer as a signal source. However, signal return at more than 300 feet was minimal. The signal enhancement feature of the instrument had little effect because of the weak signal source and the generally poor transmissivity of the near-surface materials. For spread lengths greater than 300 feet, a pattern of ten geophones was used instead of a single geophone for signal reception. The ten-geophone pattern increased the signal-to-noise ratio by partially cancelling random high frequency noise near the pattern while adding the more coherent seismic signal. The ten-geophone pattern was usually arranged in a circle with a diameter of 10-15 feet (3-5 m). The Bison system was not used for any reflection experiments because its amplifier and filter circuits are not designed to record reflected seismic energy.

The 24 channel permanent recording system was used for refraction lines up to 2000 feet and for reflection experiments. One test using the Bison and the multichannel system simultaneously checked the reproducibility of the California tests in the Bitterroot Valley. Figure 5 indicates a difference of 20-30% between the velocities measured with the Bison and the multichannel system. A similar difference between calculated layer thicknesses suggests that care should be taken in interpreting Bison data gathered when using the hammer as a signal source.

Recording seismic reflections from the base of the valley fill section was limited by two basic problems. The condition and age of

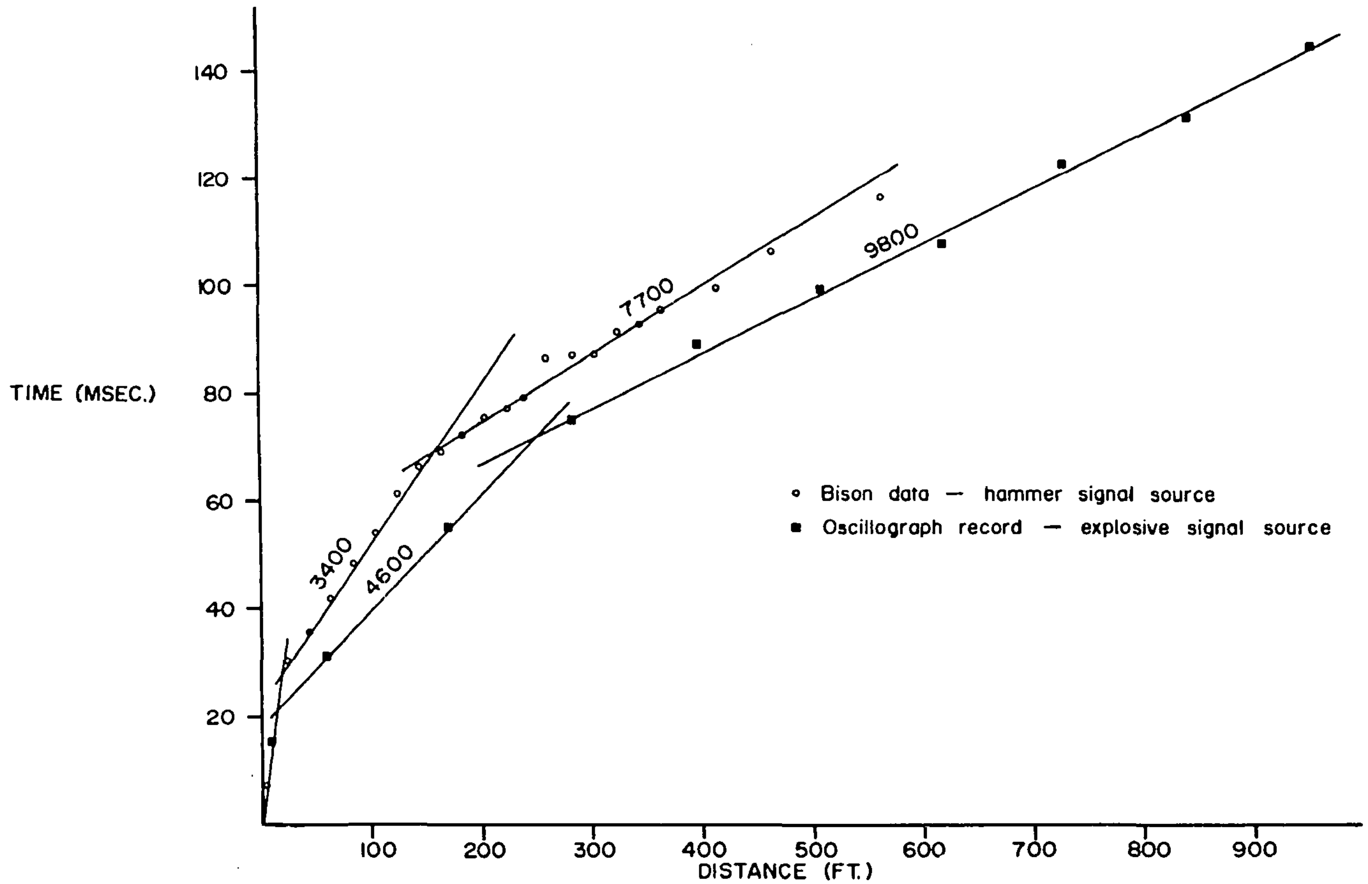

Figure 5. Comparison of seismic refraction data generated with the Bison seismograph and the multichannel seismograph near the mouth of Kootenai Creek Canyon. Velocities are in feet per second. Layer thicknesses calculated from these data differ by 20-30%.

the University of Montana multichannel seismic system is such that considerable work needs to be done to restore it to an "on line" status. Unfortunately little information is now available on operating and maintaining the system. The second problem is energy coupling to the ground. The Kinepak explosives used in this study when detonated at the ground surface have the disadvantage of expense, extreme noise, and at best moderate energy transfer to the ground. The present study was tied to surface charges because of the expense of drilling blast holes. Stevens (1973) reported the same disadvantages to Kinepak explosives.

The general field procedure for multichannel refraction surveying is to lay the geophone cable out to its full length, place one geophone per channel, and record at fairly high gain with the filter and mixer circuits out. For reflection recording the geophone cable is extended to various lengths ranging from 500 feet (150 m) to 2400 feet (730 m), the channel take-outs being evenly spaced along the total length of the cable. A pattern of eight geophones was connected to each channel take-out and each pattern was set in a small circle near the take-out. Best reflection records were obtained when the amplitude modulation level of the SIE tape recorder was set at 30% using the recording system's internal oscillator as a reference signal. The galvonometer level controls were set at 50 and the amplifier gains at 20-30 on the Independent Exploration Company amplifiers. In addition to paper oscillograph records, magnetic tape records were produced with the filters and mixers out.

Standard procedures for analyzing the seismic data (Appendix 3) were employed. Travel time plots were made and analyzed (Henbest, et al., 1969) for the forward and reverse refraction lines. Depths to interfaces and angles of dip were calculated with the aid of a program presented by Mooney (1973). Reflection data were analyzed with the aid of x^2-t^2 plots (Grant and West, 1966, and Dix, 1955). Few of the field oscillograph records showed clear reflection arrivals. The reflections were in general picked from playbacks of the magnetic tape records which were filtered and mixed to enhance each reflection arrival. (As many as three distinct reflection arrivals were seen on some records.)

CHAPTER III

COMPUTER ANALYSIS OF GRAVITY AND MAGNETIC DATA

Three FORTRAN programs were utilized in this study to analyze the gravity and magnetic data gathered in the Bitterroot Valley. An iterative program for determining the thickness of the valley fill section from the Bouguer gravity anomaly was modified from its original form (Bott, 1960) while the Talwani and Ewing (1960) algorithm for calculating gravity and vertical magnetic anomalies over irregular three dimensional bodies and the Henderson (1960) algorithm for continuing potential fields were followed exactly as presented.

The Bott Program

The Bott program was modified for application to the study of the Bitterroot Valley. As originally presented by Bott (1960) the program assumes a flat valley surface. This is reasonable only in the center of the Bitterroot Valley. Because of the desirability of analyzing the gravity data from the ground surface (Burfeind, 1967), the program was modified to account for irregularities in the topography of the present valley surface. This modification provided considerable improvement in endpoint agreement at the valley margins (Fig. 6).

As originally presented, the computer program calculates the thickness of the valley fill by iteratively applying the equation for the gravitational attraction of a vertical sheet of mass presented by Heiland (1940). A cross section of the valley is divided into a series of vertical, two dimensional sheets (Fig. 7). The Bouguer anomaly over each of the sheets in the series is calculated. The program cal-

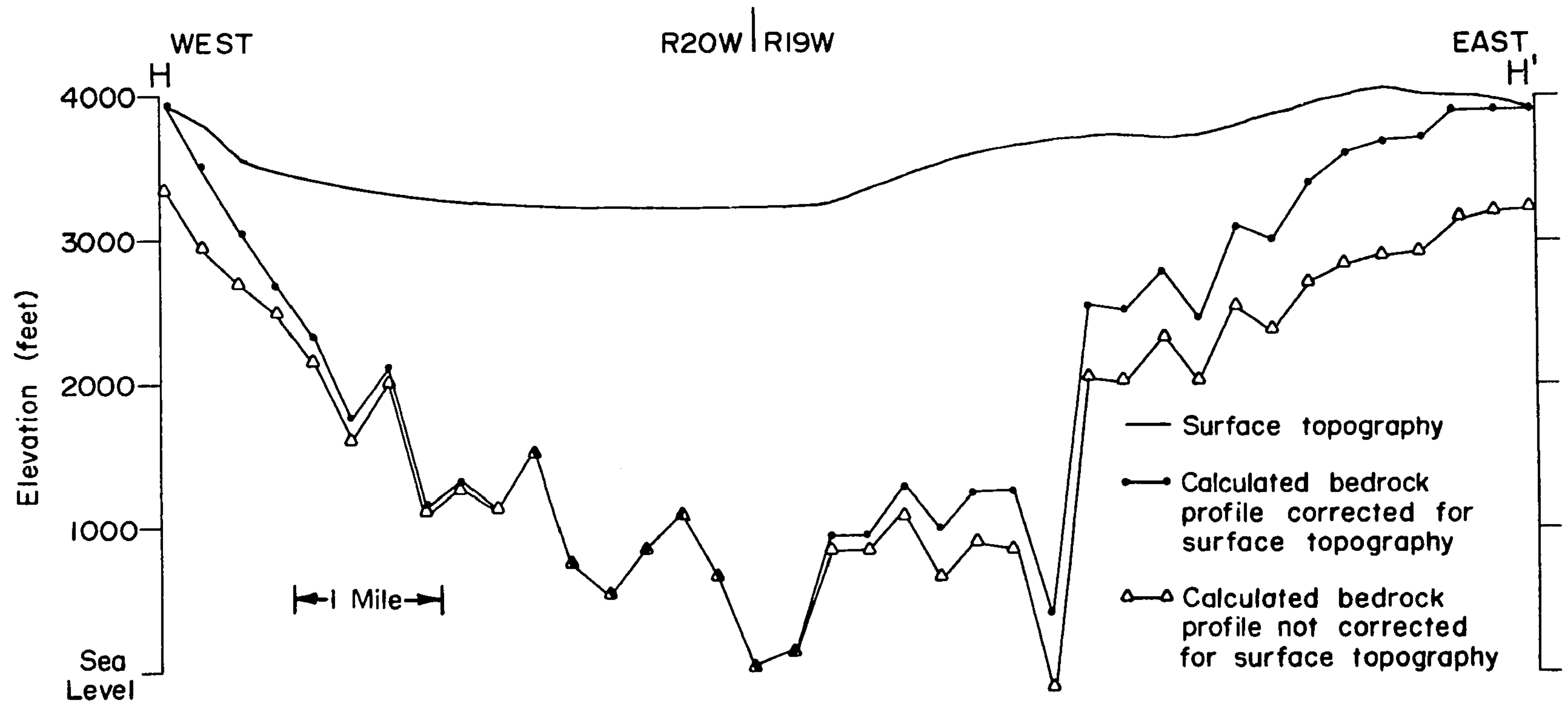

Figure 6. Comparison of bedrock profiles calculated by the Bott program with and without the correction for the surface topography. Note that the high amplitude irregularities in the central two thirds of the profile are unaffected by the topographic correction.

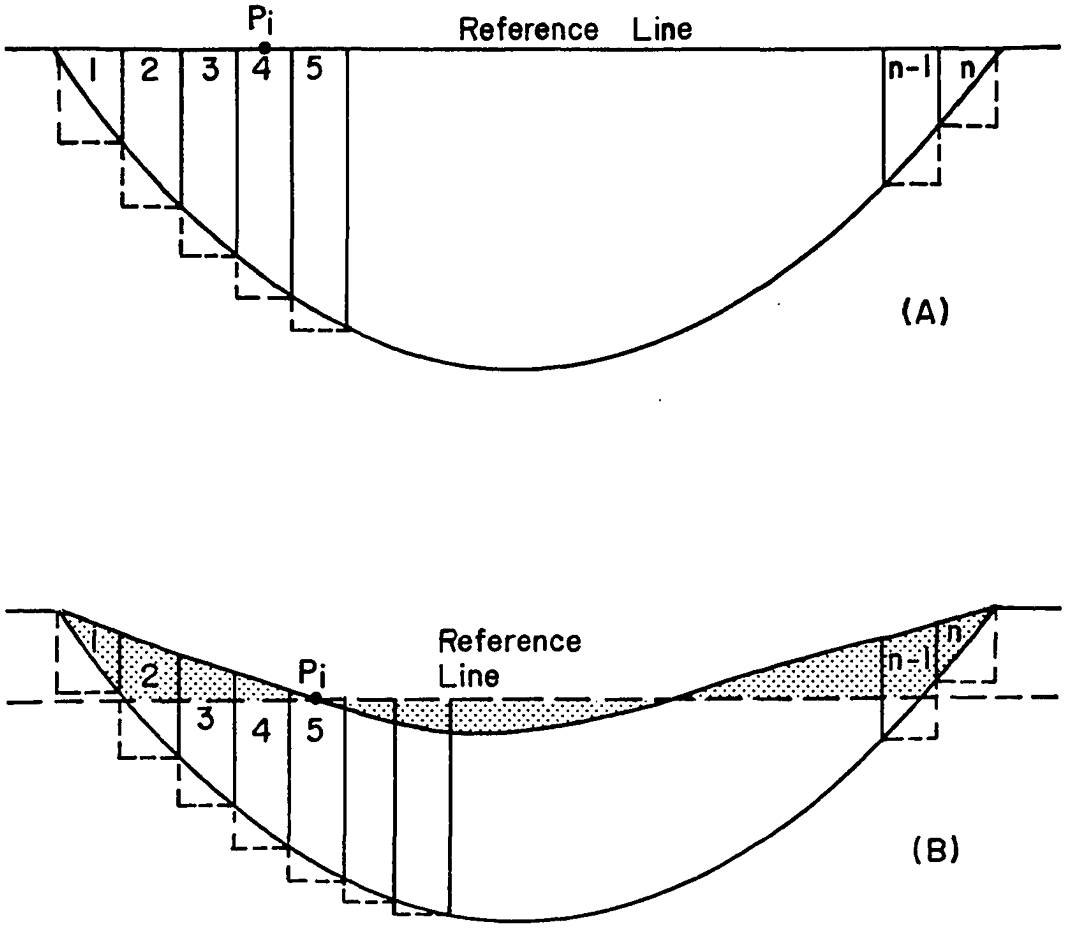

Figure 7. Assumed sedimentary valley configuration for application of the Bott program. (A) Original version of the program assumes a flat valley surface. The vertical thickness of each sheet is calculated at the sheets' centerpoints (P_i). The calculated anomaly at each P_i is the sum of the effects of each of the n sheets. The difference between the calculated and observed anomalies is used to adjust the calculated sheet thickness. The calculation, comparison, and recalculation proceeds through eight iterations. (B) Modified version of the program corrects for surface topography. All the steps in the original version are followed. In addition, the gravitational effects of the shaded areas are calculated and subtracted from the calculated effect in the original version. Thus, the adjusted sheet thickness is based upon anomalies that are related to a geometry of sheets that is more correct giving a more correct subsurface profile.

culates the mismatch between the observed anomaly and the calculated anomaly and modifies the thickness of each sheet in an effort to reduce the mismatch. The calculation of the anomaly and modification of the thicknesses continues through eight iterations as suggested by Bott (1960). To account for surface topographic variations, the vertical sheet equation is applied twice in each iteration; once for the valley fill material which is below a horizontal reference line through the point under consideration as in the original version, and second for the excess valley fill material that is above the reference line (Fig. 7).

For calculating sediment thickness in the Bitterroot Valley, the Bouguer gravity anomaly map was initially digitized at one quarter mile intervals along west to east trending profiles. The profiles were visually inspected, and an anticipated geologic cross section was imagined bearing in mind that to a first approximation the gravity anomaly was directly reflecting the bedrock topography multiplied by a constant. The geologic cross sections resulting from executions of the modified Bott program were difficult to interpret in light of the anticipated geologic results because of high amplitude irregularities (noise) in the calculated bedrock profiles (Fig. 6). The smooth Bouguer anomalies (Plates 3a-3f, for example) were expected to yield smooth bedrock topography profiles. In addition to not agreeing with the anticipated results the calculated profiles led the interpreter to a geologic conclusion which was not reasonable. The two dimensional assumption required by the Bott program would force the conclusion that the pre-Tertiary floor of the Bitterroot Valley is a series of sheer cliffs with faces as high as 5000 feet (1.52 km) and extending for distances of several miles in directions perpendicular to the plane of the profile. Although such a geometry is a geologic possibility, it was dismissed in this case because of the preliminary inspection of the gravity anomaly profiles and because no correlation of the irregularities could be found between parallel lines as little as one mile apart.

The noise was assumed to be inherent in the Bott algorithm. Both the original and modified Bott programs yielded noisy profiles (Fig. 6). In attempting to solve the noise problem, the program was changed to allow more than the eight iterations Bott suggested in 1960. It was assumed that more iterations would improve convergence of the algorithm and thus provide a smoother profile. However, more iterations increased the amplitude of the irregularities while fewer iterations reduced the amplitude of the irregularities (Fig. 8). No attempt was made to solve this problem, though the following discussion illustrates one approach toward the solution which is analogous to one published by Oldenburg (1974).

The Bouguer anomaly above each of the vertical sheets of mass into which a profile of the valley was subdivided for application of the Bott program is the sum of the gravity effects of all the sheets of mass in the profile. Thus the calculated elevation at each point is related to the calculated elevation at every other point. Any attempt to remove the noise from one elevation point must take into account the effect the removal at that point has upon all the other points in the profile. It is assumed, therefore, that a noise function

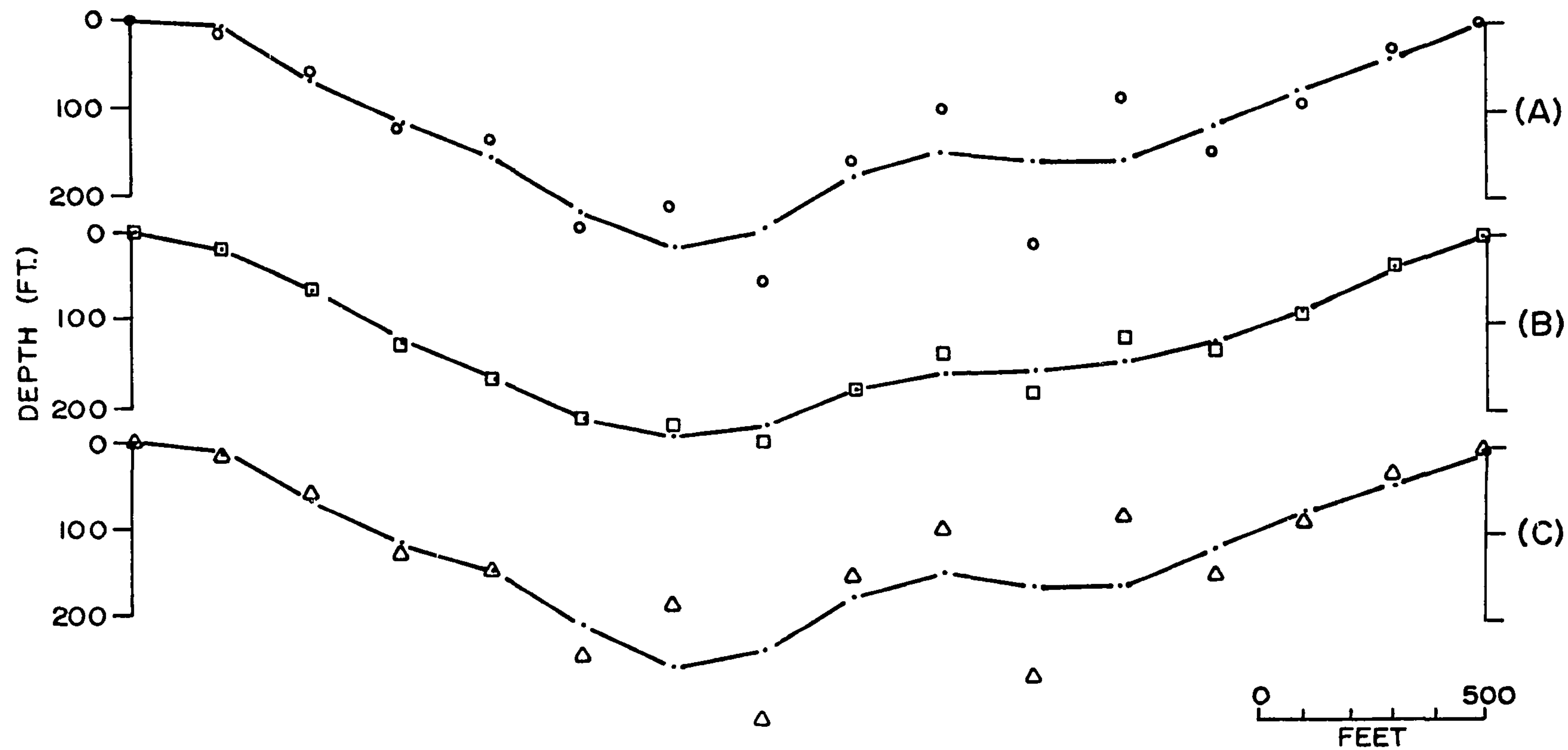

Figure 8. Outputs of the Bott program and the lowpass filter. The symbols in each case are the calculated thicknesses from the Bott program. The lines represent the output of the filter when the corresponding output of the Bott program was input to the filter. (A) Output of the original version of the Bott program with eight iterations. (B) Output of the Bott program with five iterations. (C) Output of the Bott program with ten iterations. The cutoff wavelength for the filter in each case is 750 feet/cycle (228.6 m/cycle).

exists which is the noise amplitude at each point in the profile. The assumption is made, based upon the shape of the Bouguer anomaly profiles, that the desired, true topography function is a low frequency function while the noise is a higher frequency function. The calculated bedrock topography is thus the sum, point for point, of the noise and the true topography functions.

One method of separating low frequency components out of a function is by the application of a lowpass filter to the function. A very sharp, one dimensional, frequency domain, zero phase-shift, lowpass filter was designed for application to the topographic output of the Bott program (after Bendix, 1966, Dean, 1958, Fuller, 1967, Seismograph Service Corp., 1969, Nettleton, 1973, Cooley and Tukey, 1965, and Zurflueh, 1967).

The lowpass filter smoothed the input topography profile. Output of the filter showed only the topography related to the low frequency components whose wavelengths were equal to or longer than the cutoff wavelength. Figure 8 shows the results of three different iteration schemes in the Bott program. Each output from the Bott program was used as input to the lowpass filter (cutoff wavelength equal to 750 feet, 218 m). The number of iterations was varied in the second part of the Bott program which employed an assumption of infinite planes of mass to make corrections in the calculated valley fill thicknesses.

To test the validity of applying the lowpass filter to the topography calculated by the Bott program, the Bouguer anomaly was calculated from the topographies input and output from the filter program. The Bouguer anomalies were calculated using equations and nomographs presented by Nettleton (1942). The root mean square (RMS) error between the observed Bouguer anomaly and the anomaly calculated from the topography output by the Bott program (filter input) is 1.73 milligals/21 stations. The RMS error for the output of the filter program is 1.76 milligals/21 stations. These are the same number considering the uncertainty in the Bouguer anomaly. The observed and the two calculated Bouguer anomaly curves are presented in Figure 9. Because the two methods converge numerically to the same value, the topographic output of the Bott program versus the output of the filter program must be weighed on their geologic credibility. Taking into account the general shape of the anomaly and the two dimensional assumptions employed by the inversion procedure the filtered topography is superior.

Because the Bouguer anomaly data collected in the Bitterroot Valley should not be used to resolve features with horizontal dimensions less than one mile (1.6 km), the Bouguer anomaly was digitized at a one mile (1.6 km) sample spacing and input to the Bott program. A comparison between the one mile sampled input and the quarter mile sampled input high cut filtered at one mile is presented in Figure 10. The disadvantage of using one mile digitization is the loss of model detail that might be available from the Bouguer anomaly map. However, both the filtering approach and the one mile digitization approach minimize problems of using one data point for each model point.

All of the elevations on the bedrock topography map (Plate 2) were generated by the original Bott program as modified to account for surface topography and by digitizing the Bouguer anomaly map at one

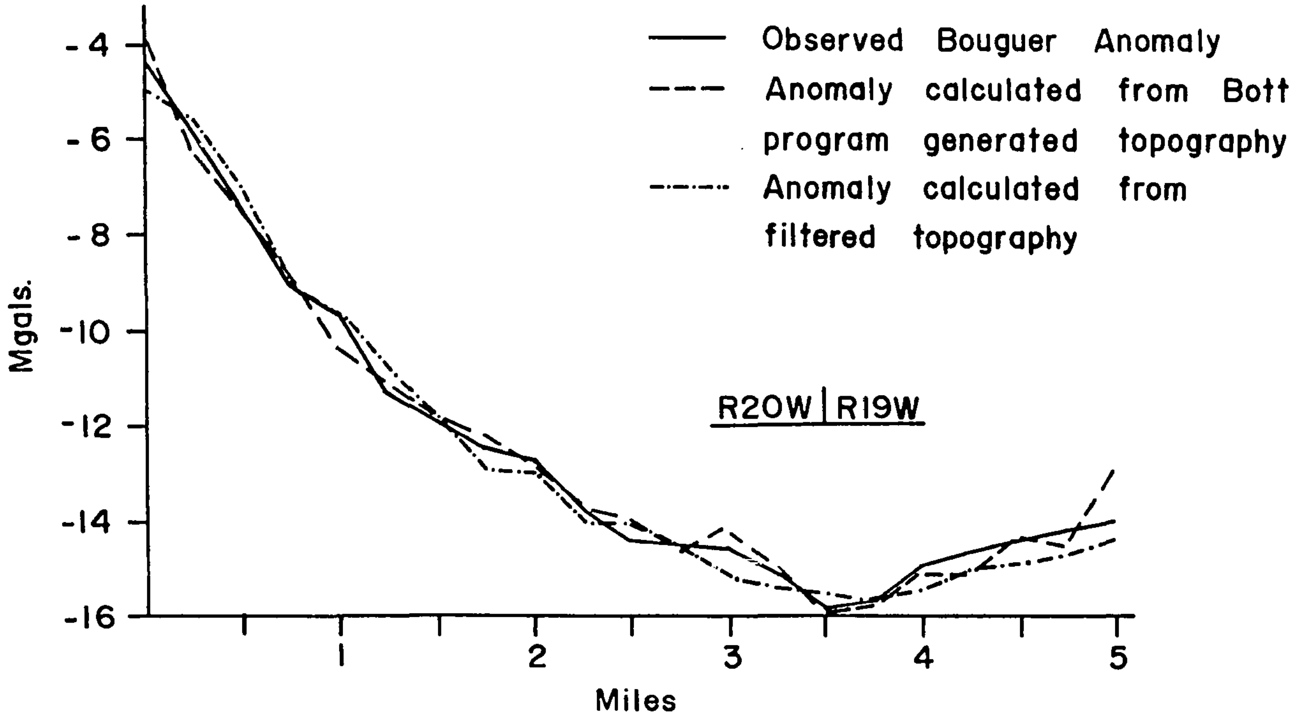

Figure 9. Comparison of observed and calculated Bouguer Anomalies along a portion of Cross Section H.

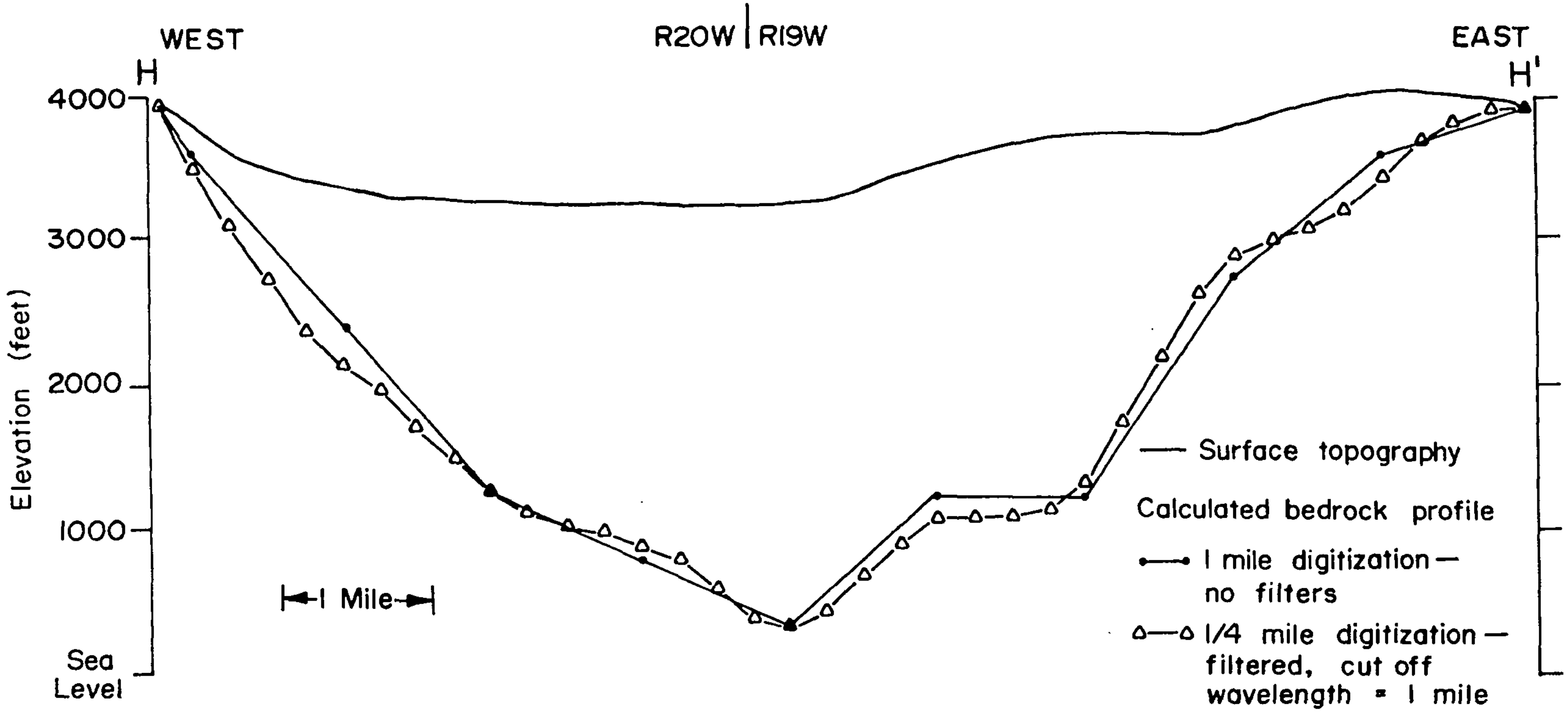

Figure 10. Comparison of the Bott program output and the lowpass filter output. The filter used input data digitized at one quarter mile intervals while the Bott program data interval was one mile. The cutoff wavelength for the filter was one mile/cycle (1.6 km/cycle).

mile intervals along profiles extending from west to east, the area of less uncertainty in the Bouguer anomaly to the area of more uncertainty. The distance between the west-east profiles was one mile (1.6 km). All of the calculations assume a constant bedrock to valley fill density contrast of -0.5 gm/cc (Burfeind, 1967, and Cook, et al., 1967).

The above mentioned topographic irregularities appear when the ratio of the horizontal width of the sheet of mass to its vertical thickness is small. If the gravity data can be digitized reliably at short intervals, the analysis program should provide a comparably reliable output. The noise observed in this study should not occur. The Bott program consists of two parts, of which the second appears to introduce the irregularities. The second part of the program iteratively applies the equation for an infinite horizontal sheet of mass to reduce the error between the calculated anomaly and the observed anomaly by modifying the thickness of the valley fill. Figure 8 suggests that fewer iterations through the second part of the program would reduce the noise problem. Perhaps the iterations in the second part of the program using the horizontal sheet equation should be replaced with calculations using the vertical sheet equation as is used in part one of the program. Initial tests of this hypothesis indicate it to be correct,though no complete study was attempted.

The Talwani and Ewing Program

The Talwani and Ewing (1960) program calculates the Bouguer gravity and the vertical magnetic anomalies over any irregular, three dimensional body (Fig. 11).

This versatile program has the ability of summing the effects of more than one anomalous body. However, the coordinates of the polygonal vertices of each lamina of each body must be read into the program in the same sense, i.e., all clockwise, because the sign of the calculated anomaly is dependent upon the direction in which the vertices are read. Because the program incorporates Simpson's Rule for integration, the effects of at least four laminae must be summed to begin to obtain a good numerical solution. The program can generate several forms of output. The form used in this study assumed all the output data to be on a flat, horizontal surface. The output surface was a 25X25 point grid. The grid spacing was varied for different models from 0.1 to 0.5 miles (0.16 to 0.8 km).

The Talwani and Ewing program was used to generate a gravity field over a hypothetical valley fill situation (grid spacing equal to 0.25 miles, 0.4 km). The generated Bouguer anomaly, digitized at one quarter mile (0.4 km) intervals was input to the Bott program. As was predictable from potential field theory, the modeled geologic section output of the Bott program agreed very closely with a cross section of the three dimensional Talwani and Ewing model (Fig. 12). In addition, 93.7 per cent of the total gravity anomaly due to the valley fill was seen between the bedrock boundaries of the model valley. This test illustrated that the Bott program could yield satisfactory geologic cross sections, even at short digitization intervals if the anomaly is smooth. However, the test suggested that care must be taken when applying the Bott program to actual field data in which are compounded the uncertainties of surveying plus the unknown lateral and vertical density changes in the valley

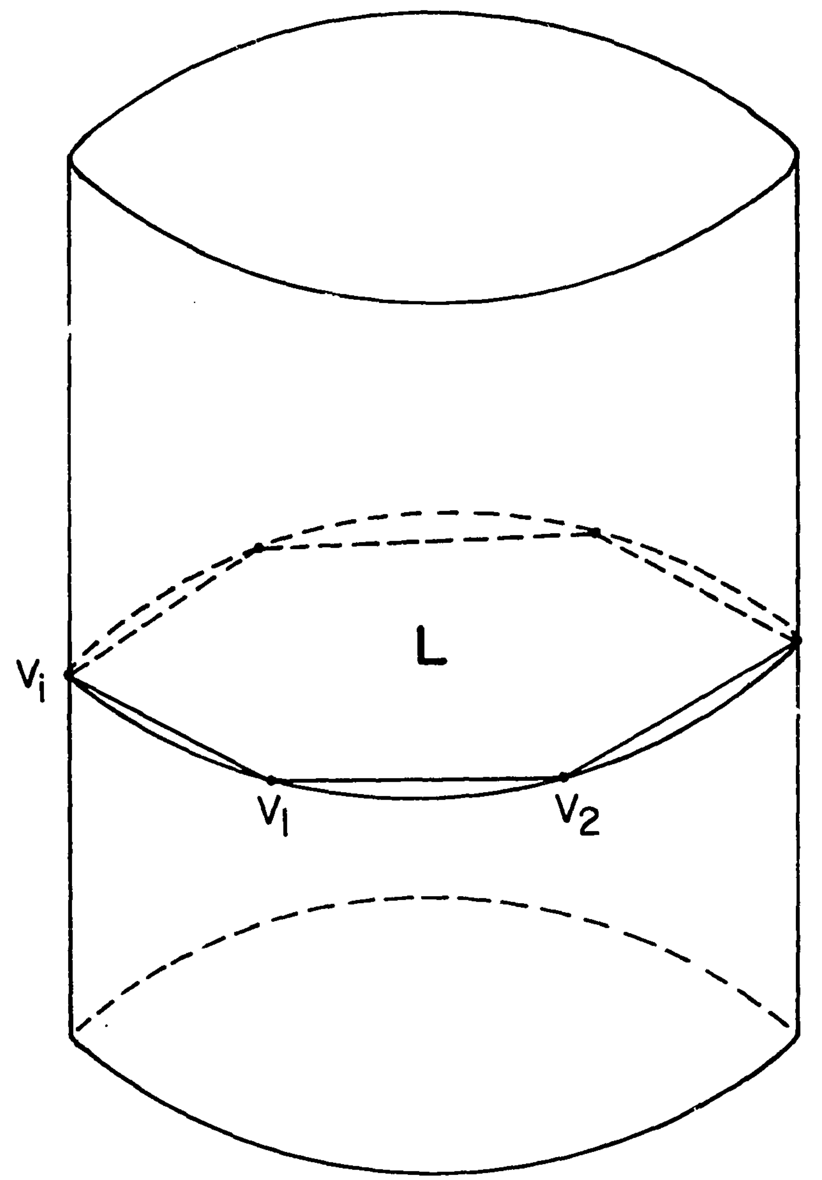

Figure 11. A sample lamina for the Talwani and Ewing three-dimensional modeling program. Lamina (L) represents one of the several laminae which would be used to approximate the cylinder to be modeled. Of course, the more vertices (V_i) which are incorporated into each lamina, the closer the lamina will approximate the cross section of the body. Furthermore, the more laminae used in the model, the more the calculated anomaly will approach the true anomaly of the body. Output options of the program allow the anomaly to be calculated on any horizontal plane or at any selected discrete points in space for which the x-y-z coordinates are given.

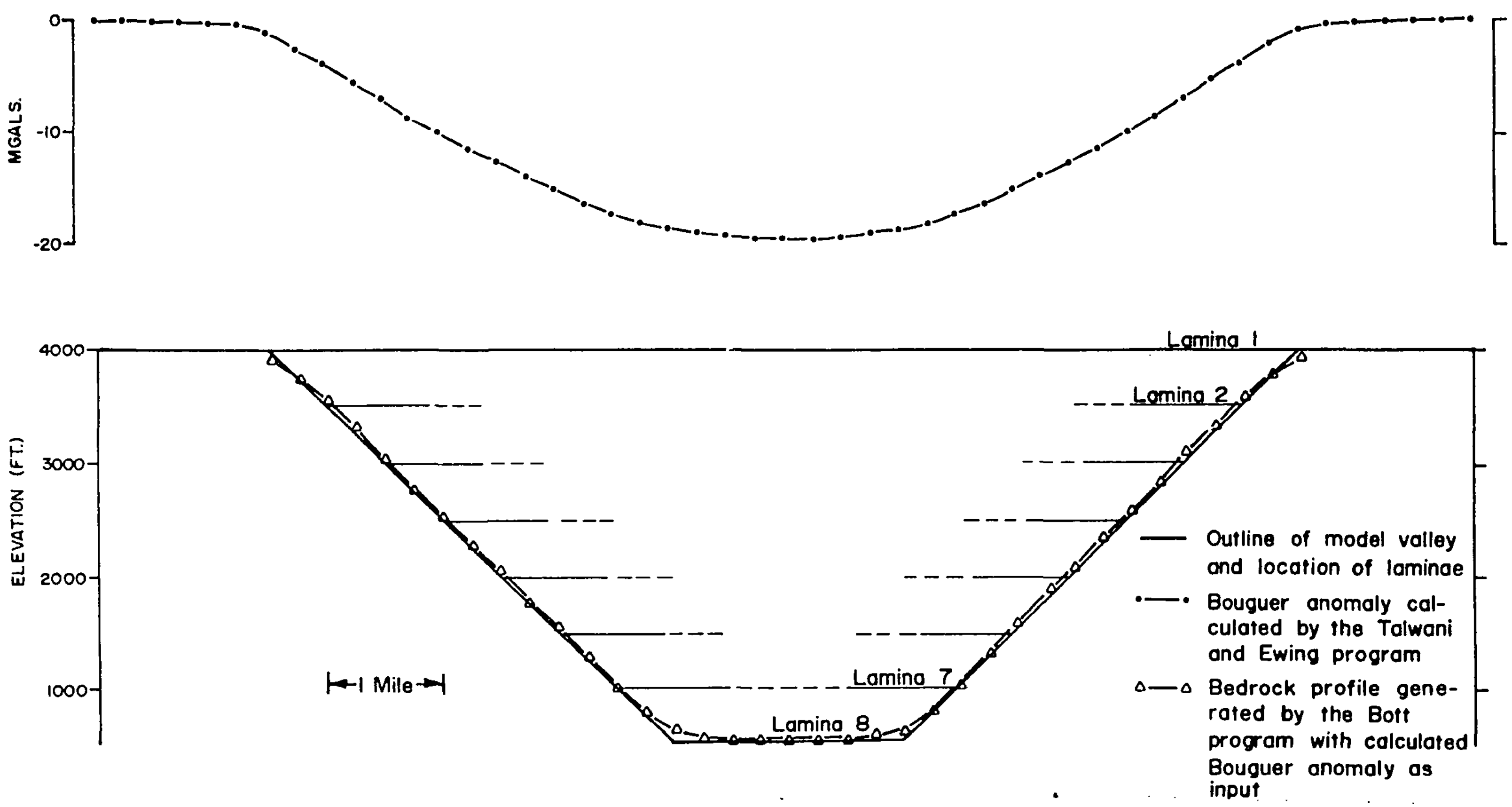

Figure 12. Vertical cross section through the three dimensional model of a hypothetical valley. The modeled valley continues along an axis extending into the page for a distance of at least ten miles (16 km) on each side of this cross section. The positions of the eight laminae used for this model are indicated. The Bouguer gravity anomaly for this model is presented above the cross section. The Bouguer anomaly was input to the Bott program, which is plotted for comparison to the original model.

fill and the surrounding bedrock as well as the bedrock topographic changes. For the width and thickness of the hypothetical valley (dimensions chosen to be similar to the Bitterroot Valley), the length of the valley had to be twenty miles (32 km) before the anomaly in the center of the valley showed negligible effects of the ends of the valley. Application of the Bott program to model data from profiles not in the center of the model valley yielded valley fill thicknesses that varied by more than 10 per cent from the expected values. This is also predictable because the Bott program is based upon the assumption that the valley has an infinitely long axis.

Another calculation of the gravity anomaly with the Talwani and Ewing program involved a hypothetical gravel body buried within the valley fill section (grid spacing equal to 0.5 miles, 0.8 km). The gravel body, approximately one mile (1.6 km) long, 1000 feet (305 m) wide, and 100 feet (30.5 m) thick, was assumed to have a density of 0.1 grams per cubic centimeter less than the valley fill sediments surrounding it. These calculations were necessary to determine the possibility of finding potential underground water storage aquifers with gravimetric techniques (Hall and Hajnal, 1962). The results of the test are presented in digital map form in Figure 13. Figure 13a and Figure 13b show the slight differences between the valley fill model and the valley fill with the gravel stringer in it. The residual map (Fig. 13c), the difference between Figures 13a and 13b, indicate a 0.41 mgal maximum anomaly over the gravel body and suggests that for this situation, gravimetry is unable to delineate the potential aquifer. Figure 13d is the total anomaly calculated with the gravel body at the surface. The

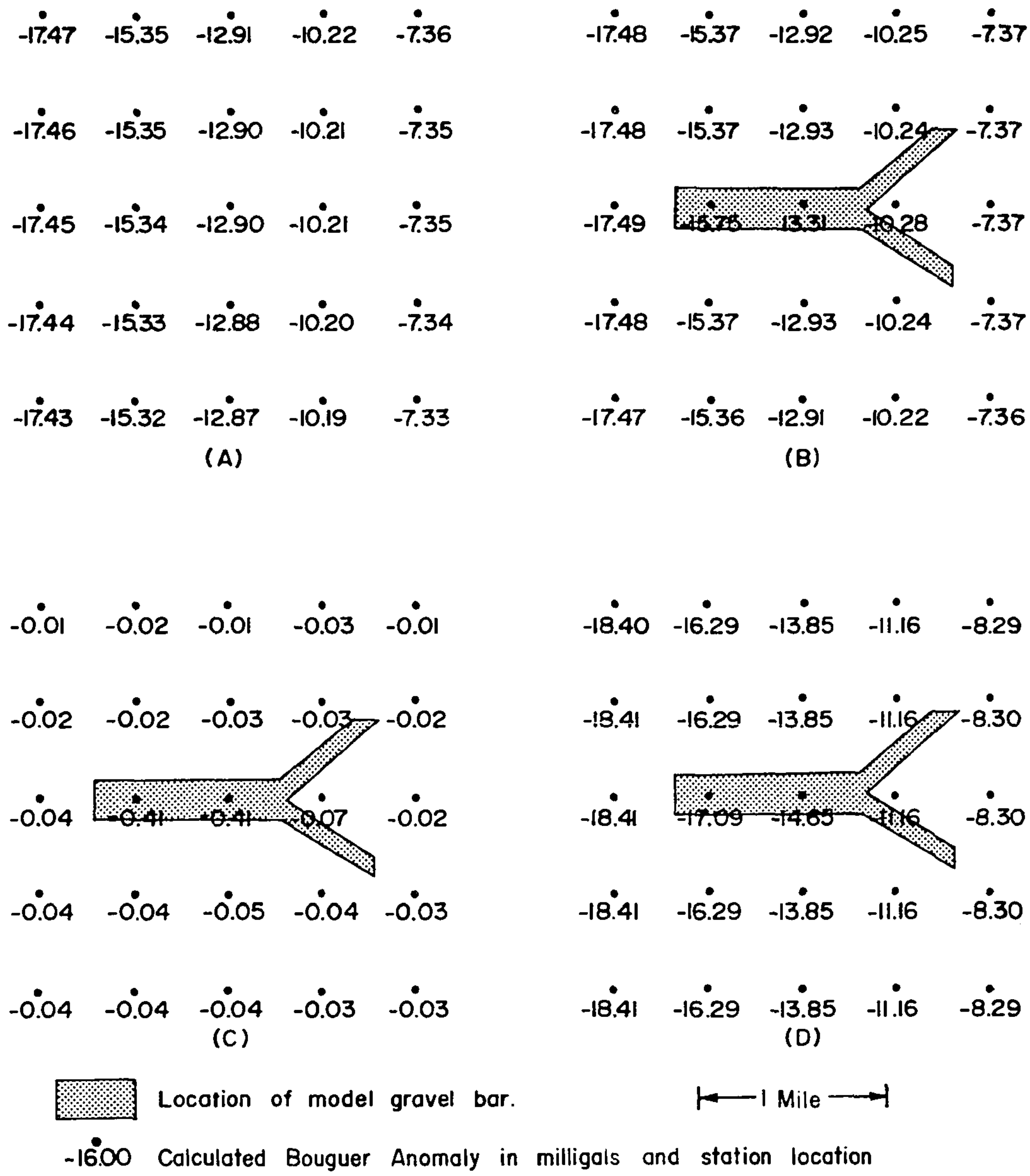

Figure 13. Digital map output for the gravel bar models. (A) Model of hypothetical valley without the gravel bar. (B) Model of valley with gravel bar. (C) Residual map, Map A - Map B. (D) Model with gravel bar at the surface. The main part of the gravel body is 1000 feet (305 m) wide and 100 feet (31 m) thick. The density of the gravel body was assumed to be 0.1 grams/cubic centimeter less than the surrounding valley fill sediments.

calculated anomalies indicate that even the effects of surface stream gravels are difficult to separate from the anomaly of the whole valley fill section. In order to see the anomaly of either gravel body, the field data would have to be generated at 0.1 mile (0.16 km) intervals and have a reliability of $\pm$ 0.01 milligals. In addition, the true thickness of the valley fill sediments would have to be known on a similarly dense grid to enable the separation of the anomaly due to variations in depth to bedrock from the anomaly due to the gravel body.

The Talwani and Ewing program was used extensively to find a set of physical and geological parameters that would yield a magnetic anomaly map that corresponded closely to the observed field in the vicinity of Ambrose Creek (Fig. 14).

The assumption was made that the calculated vertical magnetic anomaly would be within 5% of an observed total field anomaly because of the inclination of the magnetic field in the area (71°)(Deel and Howe, 1948). The observed field is presented in Figure 14. One possible anomalous body is presented in Figure 15 and its calculated field is presented in Figure 16. The susceptibilities used in the modeling are not all observed at the surface. The average value of the susceptibilities (Table 1) measured at the surface is 300×10^{-6}cgs. This value was used for the surface layer of the anomalous body. The lower layers of the body are assumed to have a magnetic susceptibility of 3000×10^{-6} cgs. This susceptibility was chosen on the basis of depth estimates using Peters' (1949) and Nettleton's (1942) methods. In addition to using the average value of the surface susceptibilities, the polygonal outline of the surface layer was held fixed to the outline of the igneous body

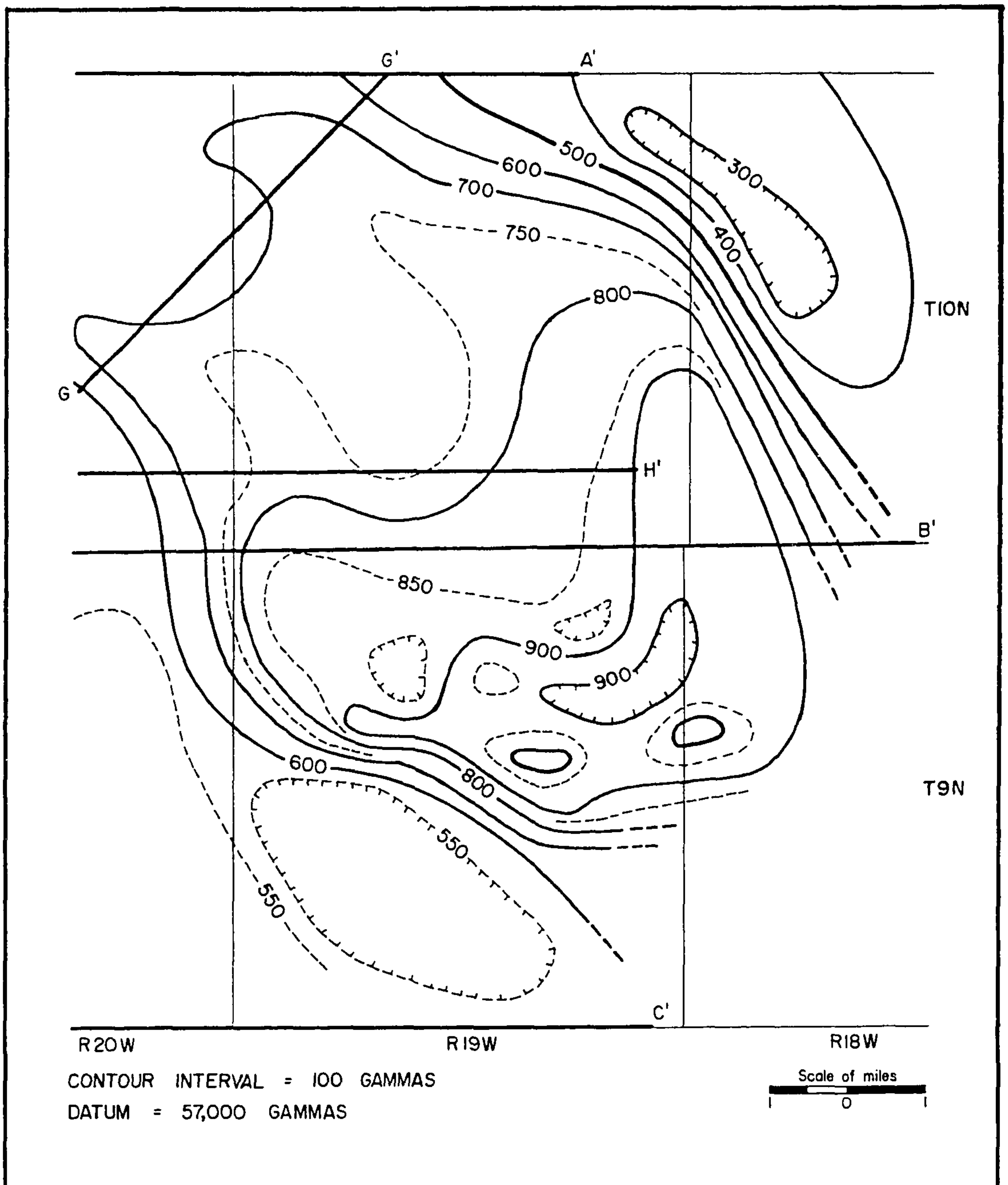

Figure 14. Total magnetic intensity map of the Ambrose Creek area. Station locations are presented in Figure 2.

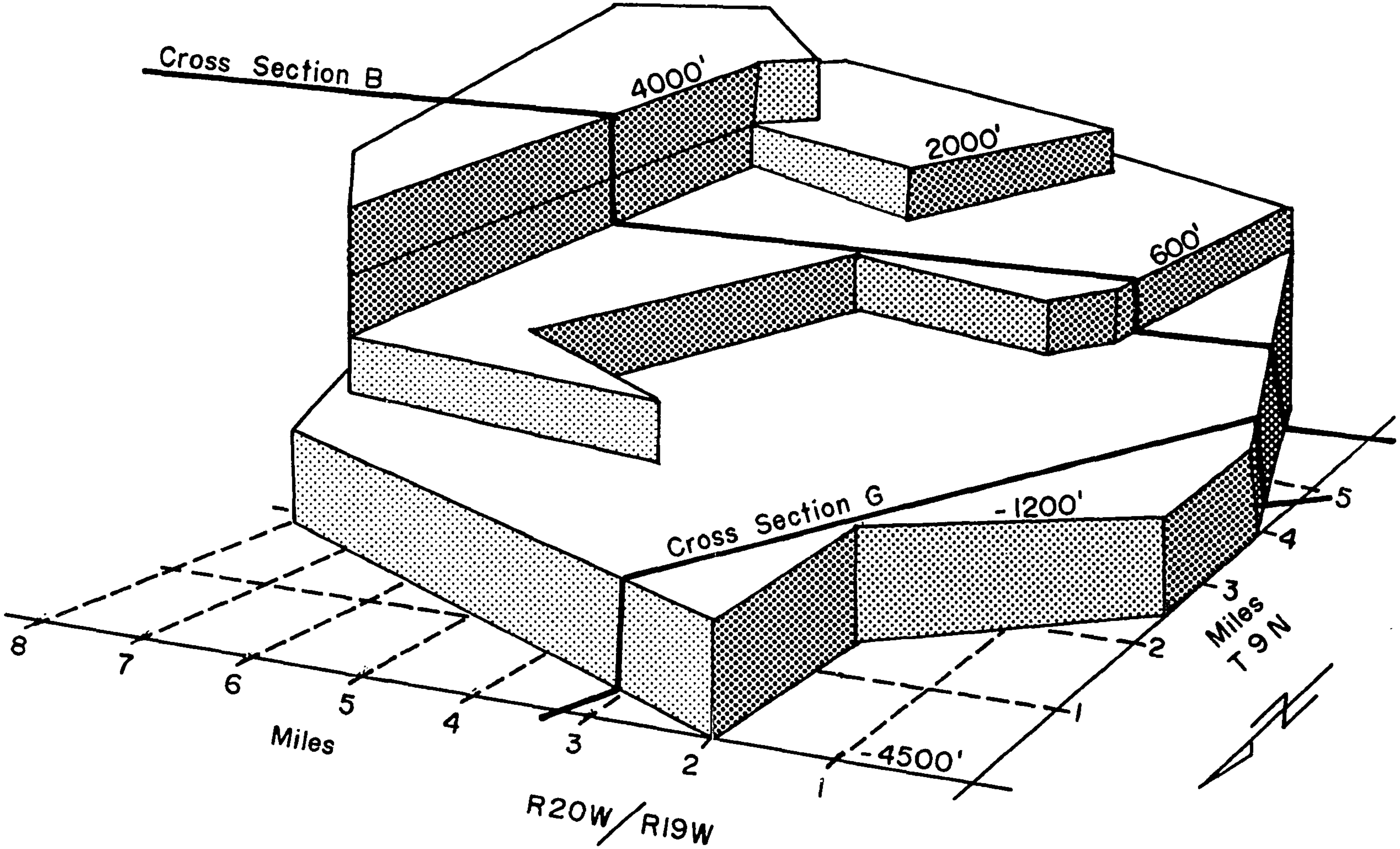

Figure 15. Isometric view of the proposed magnetic body in the Ambrose Creek area. The body is assumed to have vertical sides. The outline of the top layer follows the outcrop pattern of the large granitic body mapped in the vicinity of Ambrose Creek. The susceptibility of the upper layer is 300×10^{-6} cgs. The susceptibilities of the lower layers are assumed to be 3000×10^{-6} cgs.

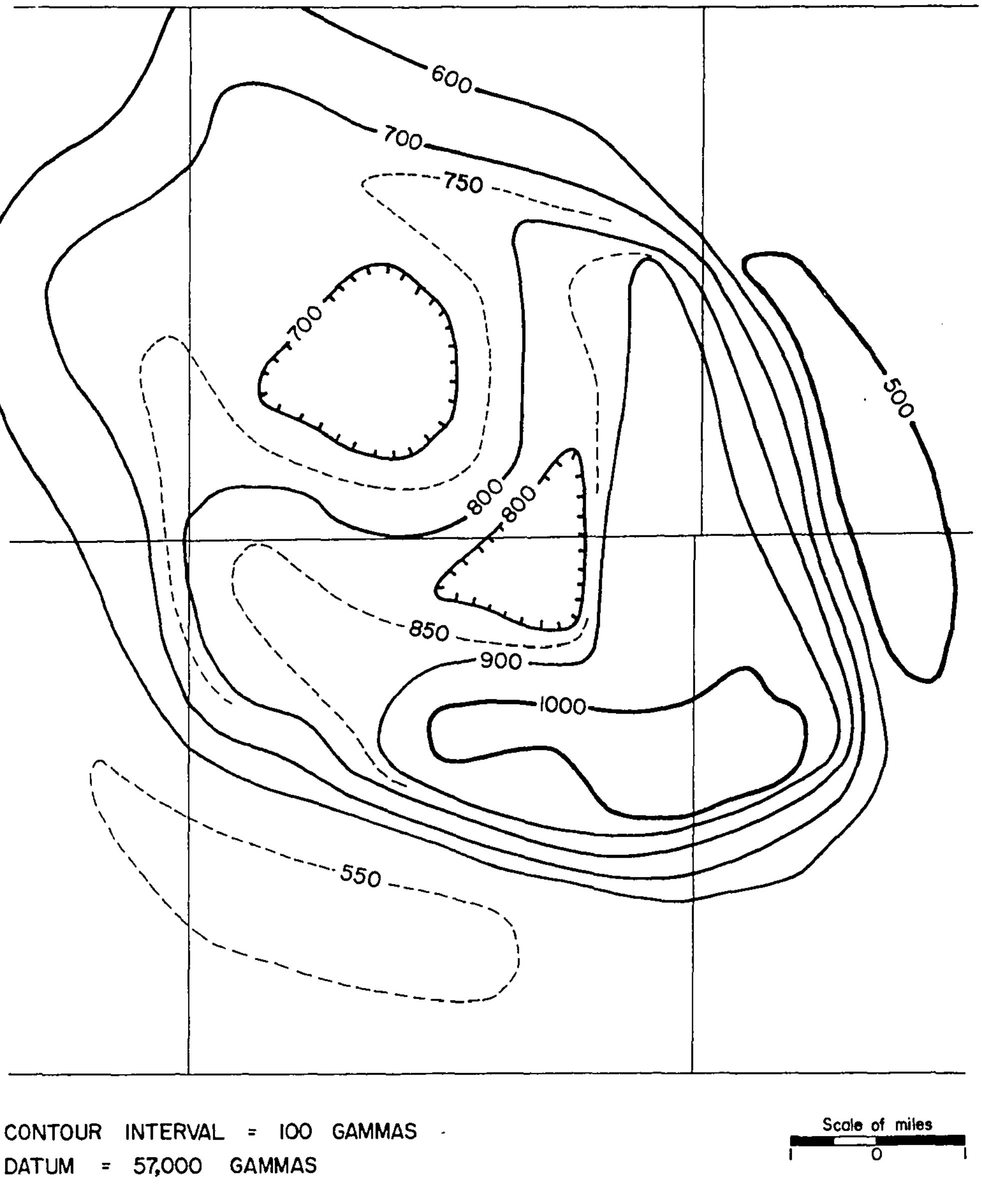

Figure 16. Calculated vertical magnetic field over the proposed magnetic body in the Ambrose Creek area.

Table 1. Magnetic susceptibilities from samples collected in the vicinity of Ambrose Creek. The susceptibilities were measured on a Bison susceptibility bridge. All samples were rock chips or soil and were measured in standardized sample bottles. No cores were measured. Sample locations are indicated in Figure 2.

Sample Number	Calculated Susceptibility	Rock Type	Remarks
SS-1	0	Granodiorite chips	Weathered sample
SS-2	0	Metamorphosed Belt	
SS-3	0	Metamorphosed Belt	
SS-4	52 X 10^{-6} cgs	Soil sample	
SS-5a	1316 X 10^{-6} cgs	Granite	
SS-5b	490 X 10^{-6} cgs	Granite	
SS-5b'	312 X 10^{-6} cgs	Granite	
SS-6a	0	Metasediment	Float sample
SS-6b	121 X 10^{-6} cgs	Granite	Fresh sample
SS-6c	0	Amphibolite	Weathered sample
SS-6d	177 X 10^{-6} cgs	Basic sill	Highly weathered
SS-7a	0	Tertiary sediments	Sand unit
SS-7b	0	Tertiary sediments	Volcanic ash
SS-7b'	0	Tertiary sediments	Volcanic ash
SS-7c	0	Tertiary sediments	Calcite cemented sand
SS-7d'	0	Tertiary sediments	Sand below soil
SS-8	48 X 10^{-6} cgs	Soil sample	
SS-9	0	Soil sample	
SS-10	127 X 10^{-6} cgs	Soil sample	
SS-11	0	Tertiary sediments	Volcanic ash
SS-12	0	Tertiary sediments	Volcanic ash

observed at the surface in the vicinity of Ambrose Creek. Nevertheless, the model presented is nonunique though the observed and calculated anomalies are very similar in amplitude and contour pattern. Differences in the two anomalies can be attributed in part to the different density of data points on the two maps. To eliminate this possible problem, an output option of the Talwani and Ewing program could be used that calculates the magnetic field only at the points where measurements of the total field were actually observed. This option was not used because of the poor control on subsurface rock types and magnetic susceptibilities.

The Henderson Program

A third FORTRAN program, employed in analyzing the magnetic data, followed an algorithm and set of coefficients presented by Henderson (1960) for upward and downward continuation and first and second derivatives. Continuation involves the application of a mathematical operator to the observed anomaly such that a new anomaly is calculated at a higher or lower datum. The observed magnetic field in the Ambrose Creek area was continued downward in order to locate the top of the proposed anomalous body in the center of the valley. The top of the body was located above the level at which the continued data showed oscillations (after suggestions by Peters, 1949, and Rudman, et al., 1971). A limitation of this program is that the field can be continued up or down only in integer multiples of the input data grid spacing.

Cross section GG' (Fig. 23) presents the results of downward continuing the magnetic data observed in the northern Bitterroot Valley.

by one and two grid units, 0.5 and 1.0 miles (0.8 and 1.6 km), respectively.

Chapter IV

RESULTS

Inspection of the Bouguer gravity map (Plate 1) indicates several general features. The anomaly pattern follows the bedrock outcrop pattern very closely on the western margin of the valley. The anomaly pattern along the east margin of the valley is very irregular indicating that the eastern wall of the Bitterroot Valley has a different structural origin than the western margin. The Bouguer gravity anomaly map of this study and the Montana gravity map presented by Bonini, et al., (1973) generally agree with respect to the north south trend of the anomaly and the irregular contour pattern on the east side of the valley.

Two geologic features along the east side of the valley probably account for the large negative anomalies near Ambrose Creek north of Stevensville and near Willow Creek north of Hamilton. In both areas, the depression in the Bouguer anomaly corresponds very closely to igneous bodies observed at the surface in the two areas.

Bedrock appears to extend continuously from the exposed face of the Bitterroot Range under the western half of the valley with no discernible, high amplitude, high angle normal faults. However, a several mile wide zone of low amplitude, high angle faults may exist. The gravity data of this study can not be used to distinguish between a smoothly sloping bedrock surface and an intricately faulted surface with low amplitude faults (Fig. 17).

The apparent bedrock high north of Victor is probably related to a thinner section of valley fill rather than a bedrock density change.

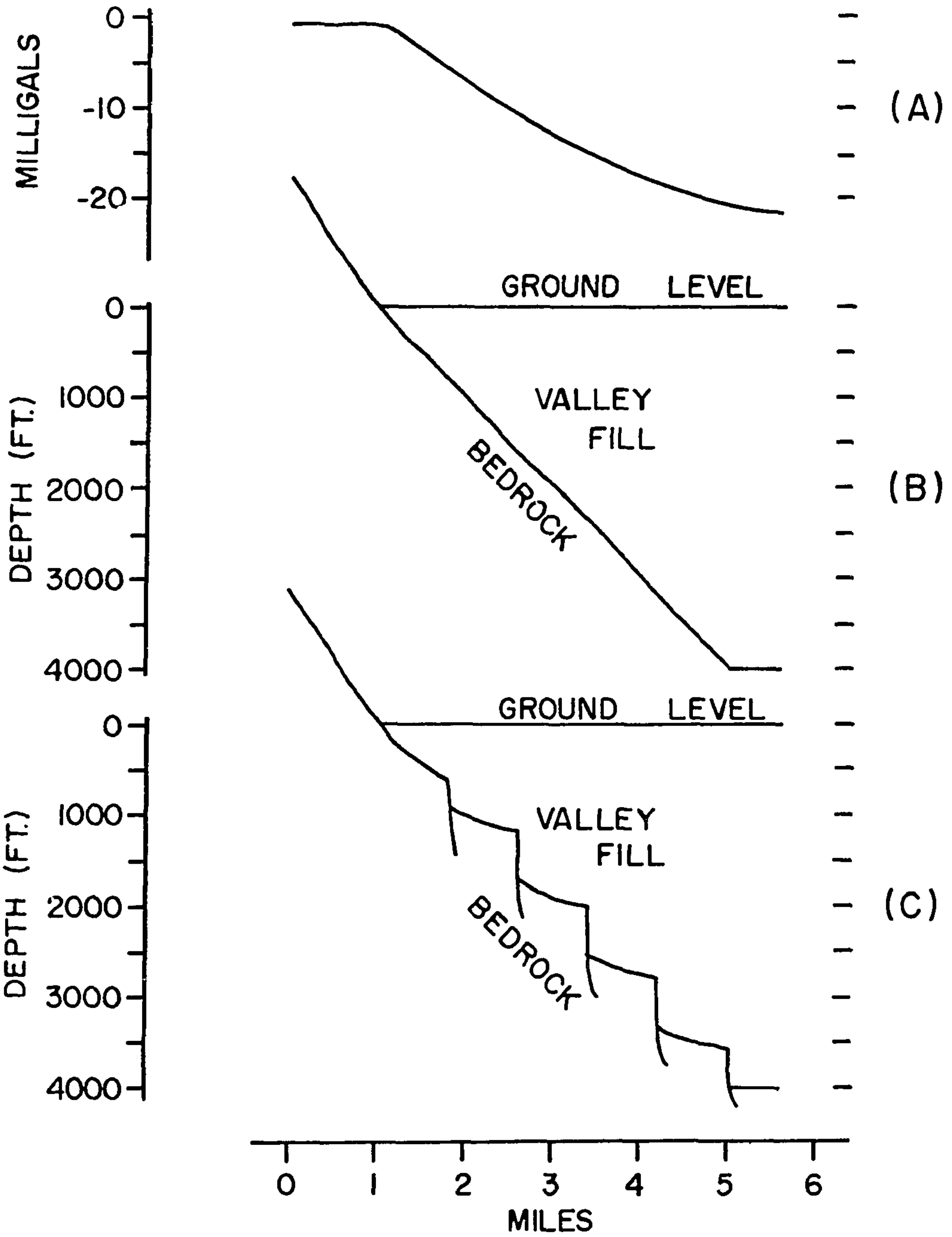

Figure 17. Calculated Bouguer anomaly over sloping and intricately faulted surfaces. (A) Calculated Bouguer anomaly. (B) Two dimensional model of smoothly sloping bedrock surface. (C) Two dimensional model showing intricately faulted bedrock surface. Note that vertical exaggeration is greater than 5X. Both models yield the same calculated Bouguer anomaly.

The high occurs in an area where the gravity data is as precise as possible in this study. The elevation, location and terrain correction errors were minimal in this area. A thinner section of valley fill is preferred over a denser bedrock because the increase in density would have to be on the order of 1.5 to 2 grams/cubic centimeter. This increase would certainly place the underlying rocks in a range of densities not commonly found in crustal rocks. The density increase was calculated using Nettleton's (1940) method.

The calculated valley fill thicknesses along the eastern edge of the valley have some uncertainty as discussed in a previous section. This uncertainty is compounded by the large igneous bodies in Ambrose and Willow Creeks. The densities of the granite are slightly less (Presley, 1970) than the 2.67 grams/cubic centimeter density used in this study to calculate the Bouguer anomaly. Therefore, part of the depression in the gravity anomaly is due to the lower density in the igneous body (Bott, 1962) and not to the lower density in valley fill material. Because the igneous bodies are at the surface, a much smaller density change can account for the observed anomaly than in the case above for the Victor area.

The dip of the Frontal Zone Gneiss on the eastern front of the Bitterroot Range varies from 20-30°. The calculated dip of the bedrock surface as it continues under the western part of the valley is 10-20°. This dip is verified both from gravimetric and seismic data (Fig. 18 and 19). In addition to verification of the average dip of the bedrock surface, the correspondence of the gravity and seismic results indicates that the assumed average density contrast of 0.5 grams/cubic centimeter

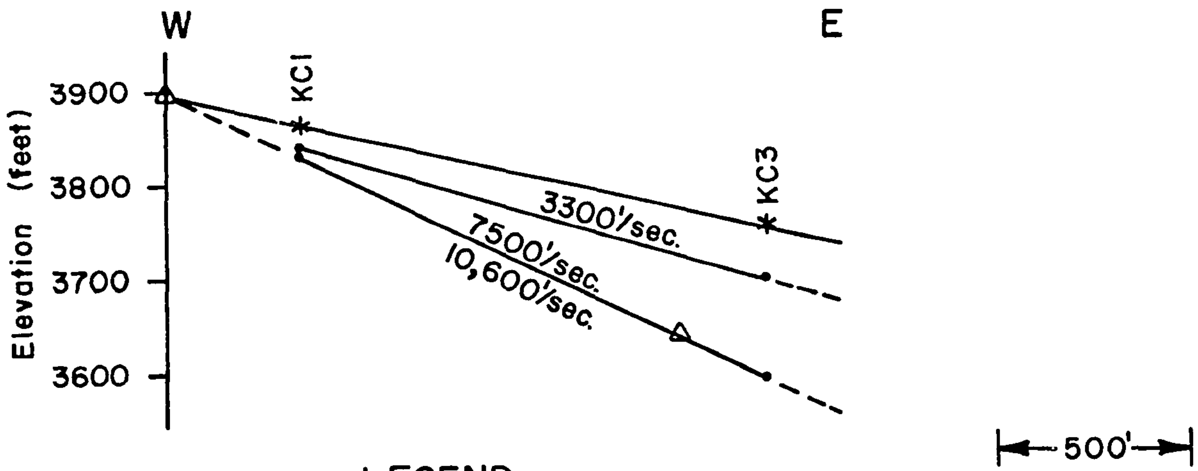

LEGEND

- • Depth point calculated from refraction data
- Δ Depth point calculated from gravity data
- ∗KCI Shot point and number

Figure 18. Comparison of depths calculated from gravimetric and seismic refraction data in the Ambrose Creek area.

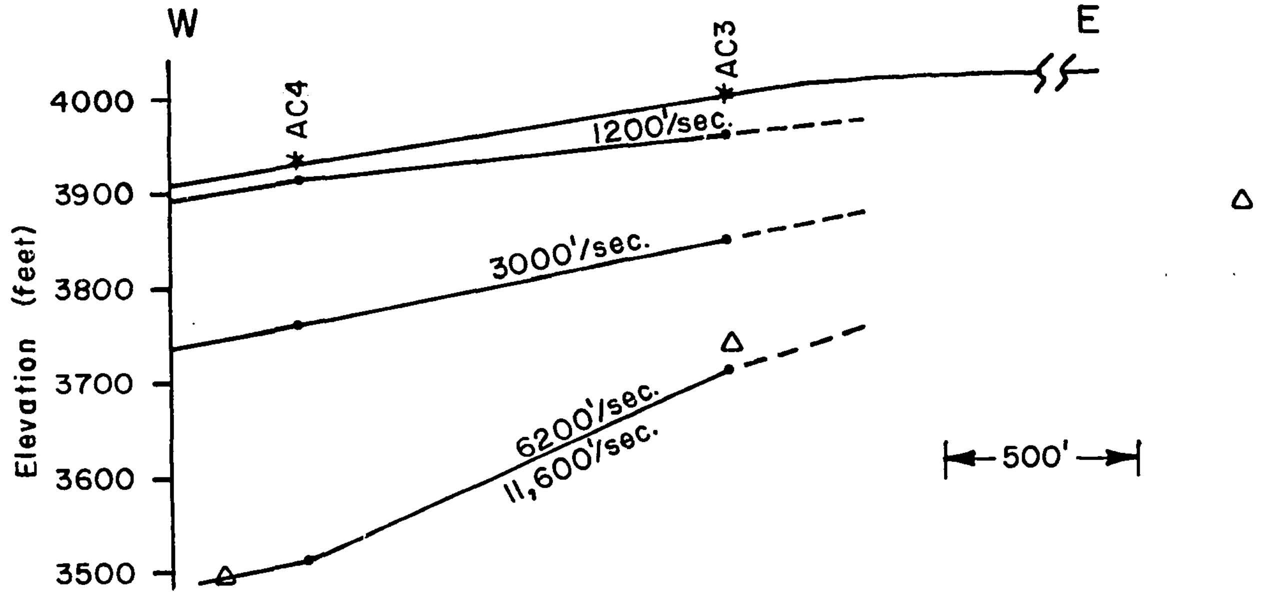

LEGEND

- • Depth point calculated from refraction data
- Δ Depth point calculated from gravity data
- *AC3 Shot point and number

Figure 19. Comparison of depths calculated from gravimetric and refraction seismic data in the Kootenai Creek area.

between the valley fill and the bedrock is an adequate assumption for the Bitterroot Valley (Figs. 18 and 19).

Refraction data from the Ambrose and Kootenai Creek areas indicate four formation velocity ranges (Table 2). Though Table 2 appears simplistic, such a tabulation is required if the refraction method is to satisfy the requirement of being an economical and viable method for measuring the groundwater reserves. A comparison of seismic refraction results with existing well data (Fig. 20) indicates that the wells penetrated into the 7000-8000 feet per second velocity zone and appear to be producing groundwater from that zone. More data is needed to extend the correlation to other parts of the valley.

Table 2. Formation velocities and geologic interpretation, Kootenai and Ambrose Creek areas.

Velocity	Interpretation
700-2000 ft/sec	Dry, near surface weathered zone
2000-4000 ft/sec	Dry, less weathered Cenozoic deposits
4000-8000 ft/sec	Water saturated, possibly Tertiary deposits
above 10000 ft/sec	Bedrock

Although the gravity data may be insufficient to resolve structural features with dimensions less than one square mile (2.56 square kilometers), they can test regional tectonic theories. A popular idea is that the Sapphire Mountain Range slid off of the rising Idaho Batholith. The Frontal Zone Gneiss is hypothesized as the zone of deformation along which the overlying plate of Belt sediments and batholithic rocks was transported. The face of the Bitterroot Range exposed at the western edge of the valley may represent the zone of maximum deformation with

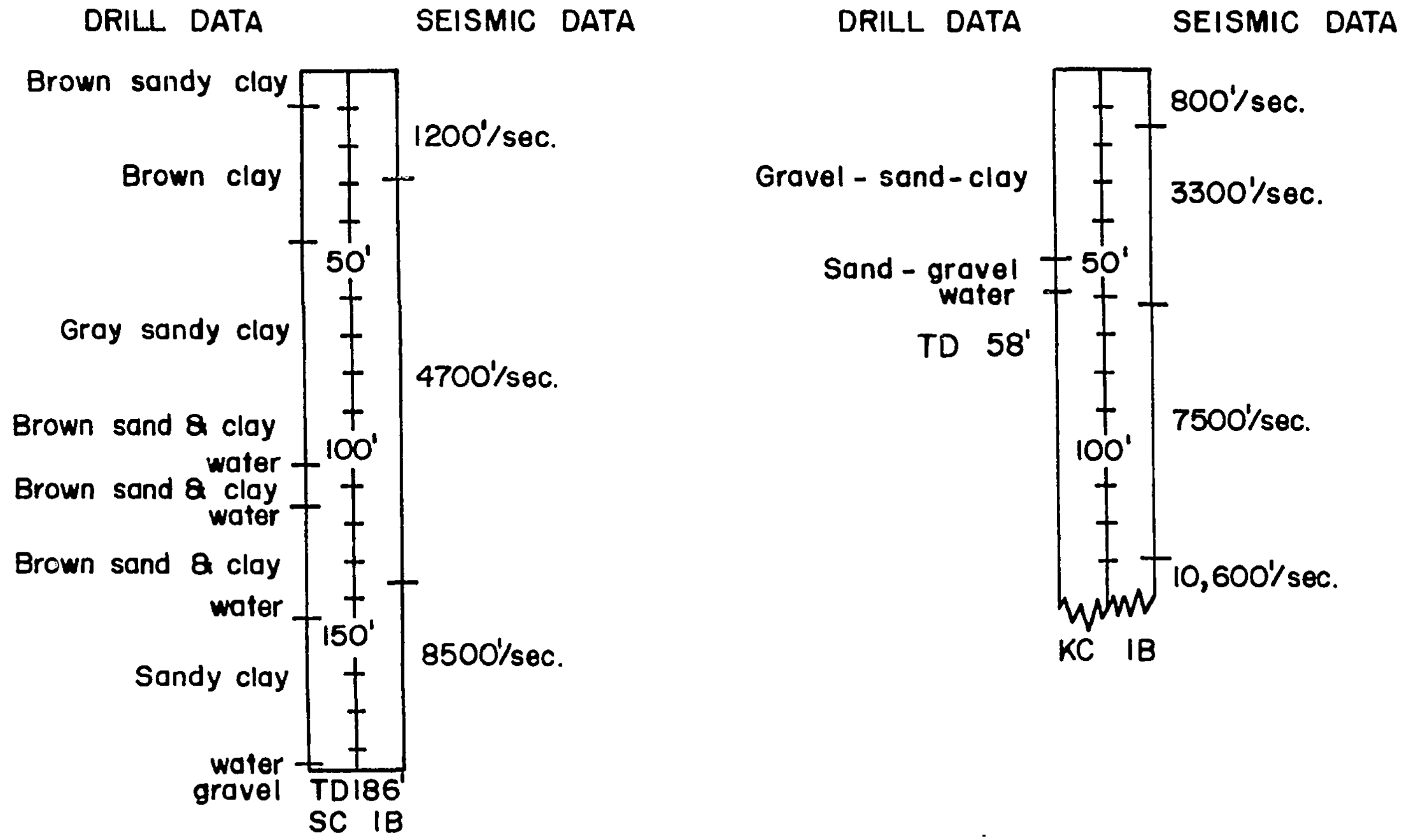

Figure 20. Comparison of seismic refraction results with existing well data.

the extent of deformation decreasing westward into the range (Ron Chase, personal communication). Thus the total thickness of the Frontal Zone Gneiss may be as much as 1.25 miles (2 km) or more. Such an extensive unit should be traceable with geophysical techniques. Three lines of evidence developed in this study allow the surface which comprises the eastern face of the Bitterroot Range to be continuously traced at depth beneath the valley fill sediments. A fourth line of evidence verifies the position of the surface in the western portions of the valley and suggests a possible thickness for the Frontal Zone Gneiss in that area.

The first line of evidence is based upon the assumption that there is little high amplitude, high angle faulting in the western part of the Bitterroot Valley (Plate 2). Also, the assumption is made that the glide surface can be described by a fairly simple mathematical expression. One possible expression is based upon a power curve of the form:

$$Z = C_1 X^{C_2}$$

where Z is the vertical position, X is horizontal position and C_1 and C_2 are two constants to be determined. The major geologic assumption is that the surface exposed at the front of the Bitterroot Range extends under the Bitterroot Valley and is the contact that divides the valley fill sediments from the bedrock. By plotting the calculated bedrock elevations with respect to distance from the mountain front on full logarithmic scales and fitting a straight line to the points, the relationship between the elevation and distance can be determined. By extending the line to greater distances from the mountain front, the position of the surface can be computed anywhere. Figure 21 illustrates

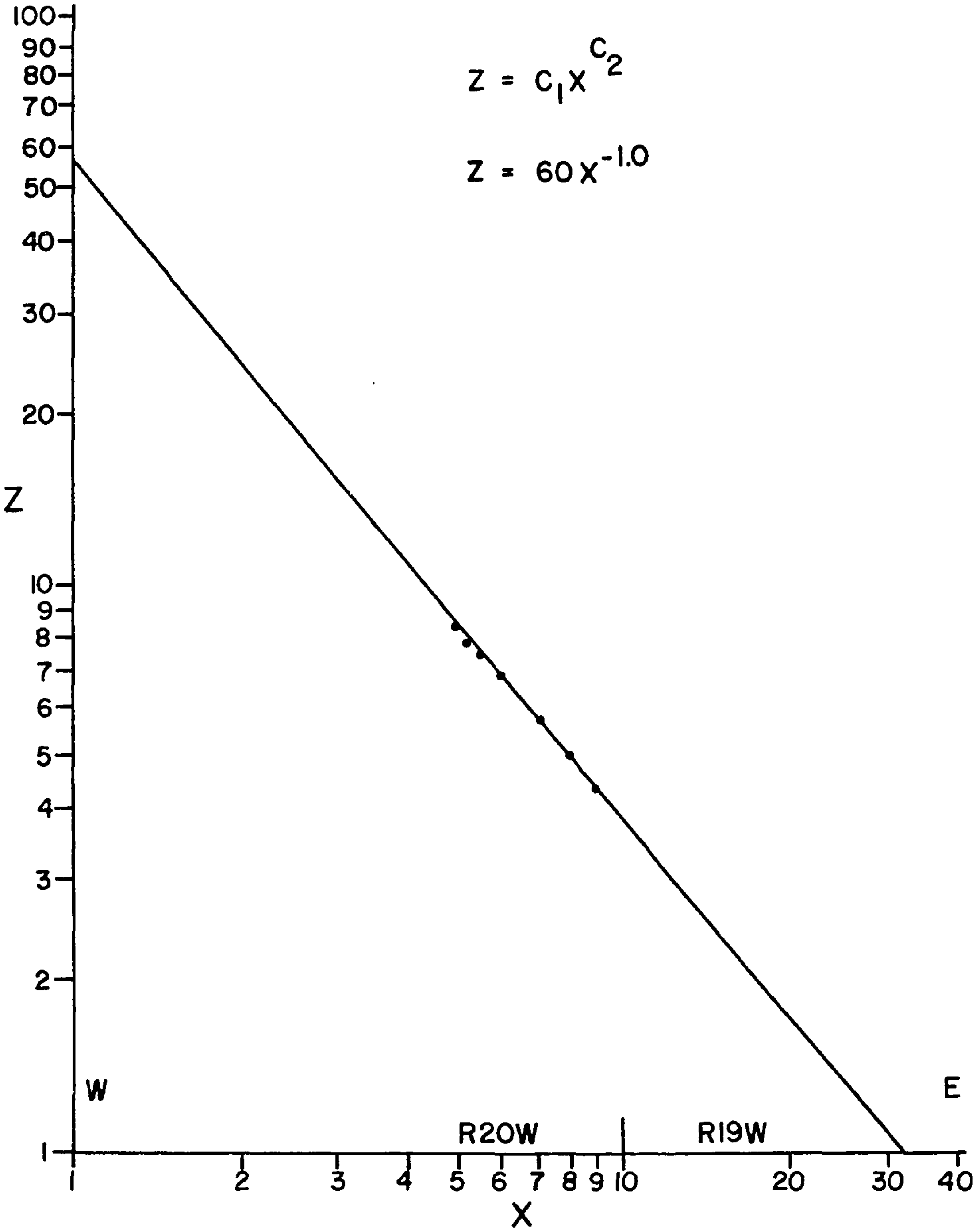

Figure 21. Power curve fit of calculated bedrock elevations. This plot is an average of several such graphs prepared in the Kootenai-Ambrose Creek areas. The Z-axis is in kilofeet with respect to an arbitrary datum. The elevations plotted are bedrock elevations calculated by the Bott program and taken from the topographic map of the area. Figure 22 shows where the power curve from this approximation would lie along cross section BB'.

the plotting procedure and Figure 22 illustrates how the surface would plot with respect to the western part of the valley and also its location relative to the proposed magnetic body in the east. Similar analyses of other cross sections through the magnetic body follow Figure 22 very closely.

The second line of evidence for the existence of the glide surface is seen in the downward continuation of the observed magnetic field in the Ambrose Creek area. Figure 23 shows the observed field and two levels of downward continuation, 2640 and 5280 (0.8 and 1.6 km) below the surface. The observed profile and the profile from the 2640 foot (0.8 km) level have the same anomaly pattern. The lower profile, however, has a slightly higher amplitude as expected. The profile at the 5280 foot (1.6 km) level, though, shows some oscillation, an indication that the field has been continued below the surface of the disturbing body (Peters, 1949). The 5280 foot (1.6 km) level corresponds to a plane 100-200 feet (30.5 to 61 m) below the surface of the lower most layer in the proposed magnetic body.

Though the shape of the calculated anomalous body is nonunique, the correspondence of the three surfaces, 1) the surface between the third and fourth layers in the model (elevation = 1200 feet, 366 m, below sea level), 2) the "glide surface" from the power curve approximation (elevation ≈ 1000 feet, 305 m, below sea level), and 3) the surface from the downward continuation (elevation = 1280 feet, 390 m, below sea level, indicate that a geophysical discontinuity of some nature exists in that area.

The reflection seismic data lends limited evidence to the existence

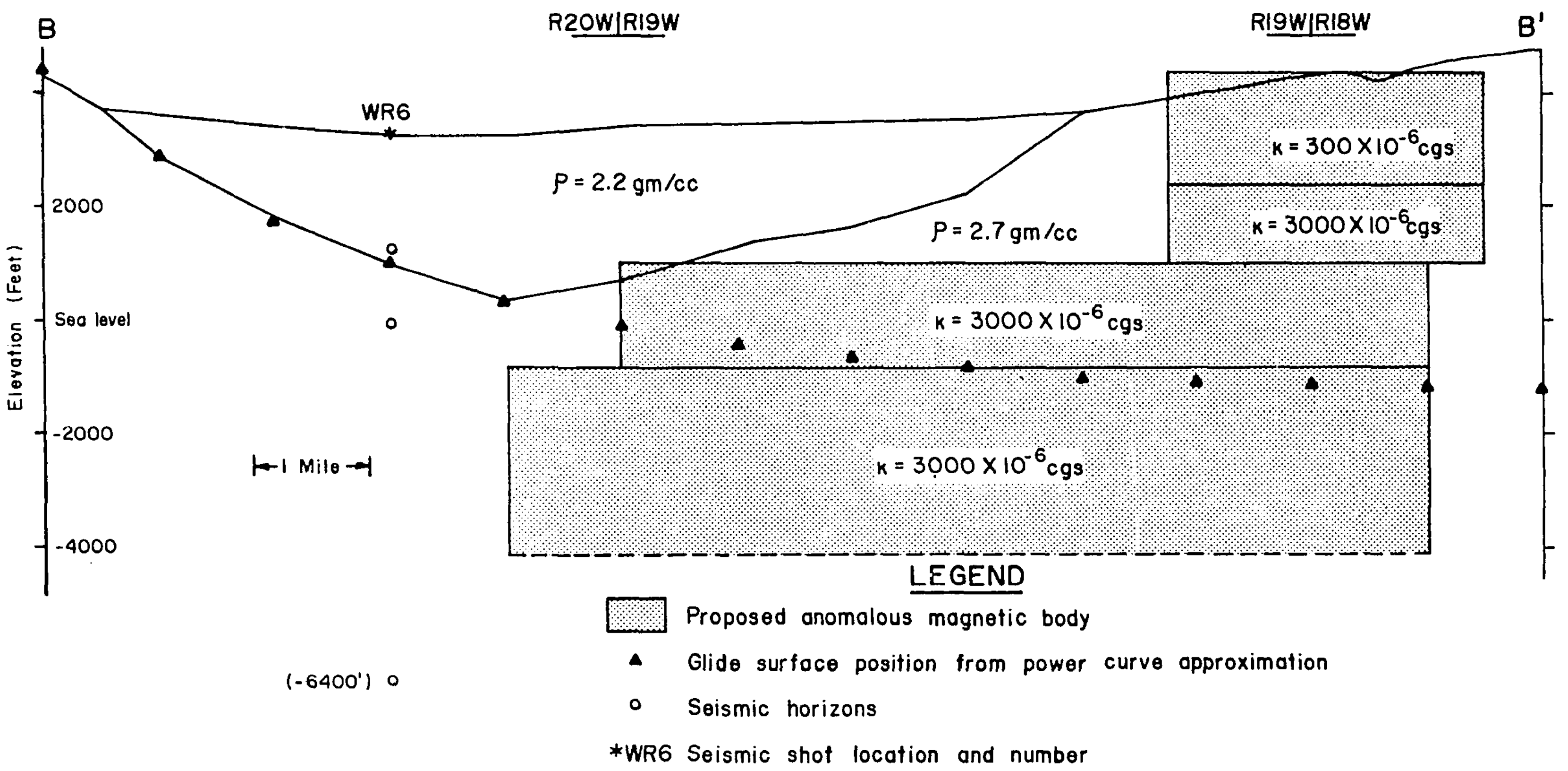

Figure 22. Cross section of the Bitterroot Valley along line BB'. This cross section is not dissimilar from others in the vicinity of Kootenai and Ambrose Creeks. The lower most layer in the proposed magnetic body may continue westward into the Bitterroot Mountains. The model was not extended to the west because of lack of observed data in that area.

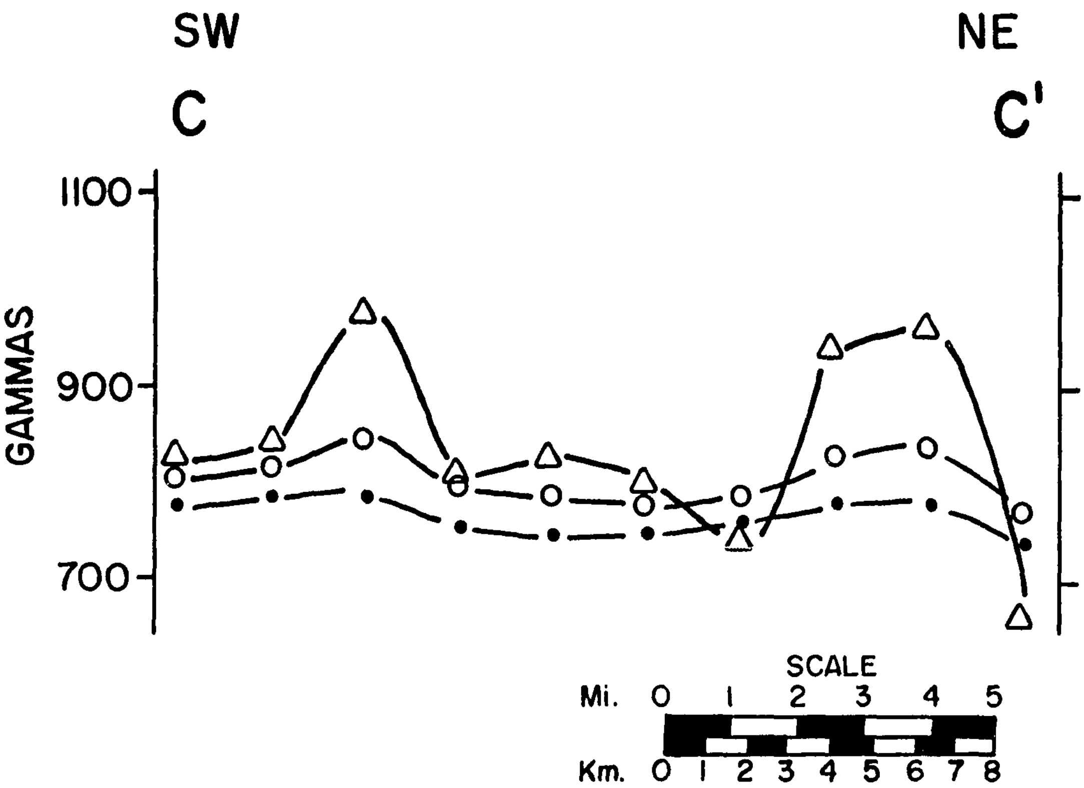

LEGEND

- • Observed anomaly at the surface
- o Anomaly continued downward 2640' (805m.) to elevation of 1360' (450m.)
- △ Anomaly continued downward 5280' (1610m.) to elevation of -1280' (-420m.)

Figure 23. Comparison of two levels of downward continuation with observed total intensity magnetic data in the center of the Bitterroot Valley. The anomaly continued to 1370 feet (418 m) retains most of the character of the original anomaly. However, the anomaly continued to -1280 feet (-390 m) shows high frequency oscillations, an indication that the primary assumption of downward continuation has been violated; e.g., the level of continuation is below the surface of the anomalous body.

of the above surface because the reflection experiments were conducted too far to the west. However, the seismic data collected near the Bitterroot River between Kootenai and Ambrose Creeks indicates three reflecting horizons (Table 3, Figure 22, and Appendix III).

Table 3. Results of reflection seismic experiments on the Ravalli National Wildlife Refuge. Shot location, NE corner, Sec. 3, T9N, R20W.

Interval	Interval Velocity	Interpretation
Surface - 2000 ft.	7500 ft/sec	Cenozoic valley fill
2000 - 3300 ft.	13200 ft/sec	Frontal Zone Gneiss
3300 - 9600 ft.	12700 ft/sec	Frontal Zone Gneiss
9600 - ?		Idaho Batholith

The first reflecting horizon is the valley fill-bedrock interface. The depth to this interface agrees within 10 percent of the depth calculated from the gravity data (Fig. 22). The second reflecting horizon is presumed to be a surface within the Frontal Zone Gneiss. The lowest reflecting horizon may represent the base of the Frontal Zone Gneiss. The total thickness agrees fairly closely to thicknesses of the Frontal Zone Gneiss measured near the front of the Bitterroot Range (Ron Chase, personal communication).

Planimetric analysis of the calculated bedrock topography map (Plate 2) indicates that the total volume of Cenozoic deposits in the Bitterroot Valley is of the order of 70 cubic miles (290 cubic kilometers). Assuming an average porosity of 20 percent, and assuming that all of that is filled with groundwater, the valley could potentially hold 14 cubic miles (57 cubic kilometers) of water. Of this, four cubic miles (16 cubic kilometers) of groundwater would be within the top 400 feet

(122 m) of the valley fill section.

Chapter V

CONCLUSIONS

Basic surface geophysical techniques, as outlined in this study, are an inexpensive means of generating subsurface information in the search for groundwater resources. Unfortunately, the volume of data provided by such methods does not yield any firm information that can be used entirely as a replacement for actual well drilling. Seismic refraction and well log data can be correlated, and the seismic refraction method appears to be the best of the geophysical methods investigated in this study for locating groundwater reserves. Gravity and magnetic techniques do not give direct information on groundwater resources, but they do yield regional structural information. The data of this study say nothing about how much groundwater is actually contained within the valley fill sediments, nor do they say anything about the volume of water which can be produced or what percentage of that produced would be usable. Permeability of an aquifer is best evaluated in downhole tests either by pumping or geophysical logging, and water quality can be determined only after a sample is obtained.

The seismic refraction method offers the best possibilities for generating subsurface data that can be used as a guide to water well drilling. Certainly the refraction data from two sites can not be considered as a guide for groundwater prospecting in the whole valley. Perhaps a program of reporting all refraction data to the Montana Bureau of Mines and Geology, as is required for driller's data, could be established. This would allow a correlation of refraction data and driller's data to be made and subsequently provide an improved guide to geophysical groundwater prospecting. A complication might exist, however, before the correlation of the two sets of data could be confidently undertaken. That is, few of the water well logs submitted to the state are prepared by trained geologists or groundwater hydrologists.

In addition to the limited information generated on groundwater reserves, the seismic data in this study provide two pieces of information valuable in regional structural geologic studies. Seismic results from the Kootenai and Ambrose Creek areas indicate that the depth to bedrock calculated from gravity data is very close to that calculated from the seismic data. Thus, the assumed average density of the valley fill section of 0.5 grams/cubic centimeter less than the surrounding bedrock is correct.

Furthermore, the presence of at least two reflecting horizons in the western part of the valley indicates that the Frontal Zone Gneiss can be traced at depth with seismic reflection techniques. The dip of the gneiss appears to decrease from 20° at the western margin of the valley to as little as 15° three miles (5 km) east of the mountain front.

The average formation velocity of the valley fill sediments ranges from 6500 to 8500 feet per second. The lowest velocities are observed in the center of the valley. This is explained by suggesting that the Bitterroot River has always favored the center of the valley. The less consolidated and more water saturated sediments there would be expected to have a lower velocity than the more strongly cemented sediments outside the central portions of the valley.

With the block of geophysical data available through the present study in the Bitterroot Valley, future studies will have a definite starting point. The groundwater prospector can combine new and existing well data and new engineering seismic data to help reduce the number of dry wells drilled for groundwater in the valley.

The present preliminary geophysical study in the Bitterroot Valley invites further geophysical research to define the regional geologic structure. The two best tools for such future studies will be the reflection seismograph and the magnetometer. Both tools could be combined to define precisely the configuration of the proposed magnetic body and the Frontal Zone Gneiss at depth. The high precision now available in airborne magnetometry and digital seismic recording and processing should allow even subtle features like low amplitude normal faults in the valley floor to be interpreted. The answer to the complicated question of the regional geology in western Montana will only be obtained when synergistic geophysical data are thoroughly integrated with surface geologic data.

Appendix I

GRAVITY DATA

The following tabulation contains the information compiled to present the Bouguer gravity anomaly map (Plate 1) of the Bitterroot Valley. The field notes, map of station locations, and preliminary Bouguer anomaly map are available through the University of Montana Department of Geology.

Station numbers in the tabulation between 400 and 500 are in the Ambrose Creek area and are called AC-1 through AC-99 in the field notes. Station numbers greater than 500 were incorporated from a small survey initiated by Gary Crosby. These stations correspond to stations numbered 390 to 500 in the field notes. Stations 1 through 61 were also incorporated from a survey initiated by Gary Crosby. Station numbers 158 through 174 are from a survey conducted by Jesse K. Douglas in the presentation of his master's thesis (1972).

Station numbers not appearing in the following table indicate that these stations were not used in this study. All field readings have been referred to the established base station at Johnson-Bell Airport in Missoula. The column labeled observed gravity is the milligal difference between the field observation station and the airport station.

Several base stations were carried forward from the airport station to reduce the necessity of traveling to the airport during the surveying. All but one of these base stations were used in the determination of the Bouguer anomaly and therefore appear in the following table. It is not recommended that the field observation stations be used as bases for subsequent studies because positioning the gravimeter on the absolute location of the base station may not be possible.

The one base station that could be used in future studies is in the basement of the Science Complex on the campus of the University of Montana. The gravity value is 980,446.583 milligals in the center of the north edge of the pier in the Earthquake Laboratory.

The small circles on Plate 2 indicate station locations.

STATION NUMBER	STATION ELEVATION [METERS]	STATION LATITUDE [DEG. N]	STATION LONGITUDE [DEG. W]	OBSERVED GRAVITY [MGALS]	BOUGUER ANOMALY [MGALS]
1	1103.4	46.5738	114.0925	-47.281	-176.3
2	1033.6	46.5738	114.1080	-53.289	-173.5
3	1075.9	46.5738	114.1242	-59.328	-170.0
4	1098.5	46.5738	114.1301	-62.555	-168.2
5	1143.0	46.5760	114.1427	-59.367	-153.9
6	1252.7	46.5789	114.1555	-90.570	-159.5
7	1353.3	46.5802	114.1761	-107.625	-152.0
8	1389.9	46.5825	114.1814	-124.602	-161.6
9	983.9	46.5738	114.0654	-49.883	-181.4
10	1067.4	46.5662	114.0546	-55.648	-170.2
11	1021.7	46.5662	114.0329	-58.281	-181.9
12	1057.4	46.5662	114.0020	-63.562	-180.0
13	990.0	46.5892	114.0884	-43.492	-174.6
14	991.5	46.6030	114.0864	-41.133	-173.0
15	995.8	46.6174	114.0880	-41.852	-173.9
16	993.6	46.6317	114.0784	-41.477	-175.2
17	1090.6	46.4370	114.1516	-61.477	-160.9
18	1121.7	46.4370	114.1611	-71.625	-159.1
19	1205.5	46.5910	114.1792	-91.797	-148.2
20	1243.6	46.5430	114.1977	-100.375	-159.9
21	1034.8	46.5300	114.1304	-57.703	-173.5
22	1009.2	46.5300	114.1115	-55.625	-177.2
23	1004.0	46.5280	114.0867	-59.086	-182.6
24	1037.5	46.5200	114.0656	-66.961	-183.1
25	1104.6	46.1590	114.0453	-81.930	-184.6
26	1132.0	46.5190	114.0236	-80.344	-177.7
27	1161.3	46.5180	114.0018	-80.242	-171.0
28	972.0	46.7570	114.0822	-6.523	-156.1
29	972.0	46.7480	114.0830	-7.750	-156.2
30	965.0	46.7360	114.0801	-9.414	-157.8
31	964.7	46.7230	114.0774	-16.047	-163.3
32	1003.1	46.5170	114.0967	-60.625	-183.0
33	1000.7	46.5190	114.1183	-56.891	-179.0
34	1024.1	46.5130	114.0809	-65.820	-184.0
35	1021.4	46.5340	114.0654	-62.203	-182.7
36	998.5	46.5540	114.0654	-54.898	-181.8
37	992.4	46.5880	114.0465	-49.789	-180.9
38	994.9	46.6110	114.0380	-46.477	-179.1
39	995.2	46.6310	114.0385	-42.273	-176.5
40	1042.4	46.6410	114.0166	-46.258	-171.8

STATION NUMBER	STATION ELEVATION [METERS]	STATION LATITUDE [DEG. N]	STATION LONGITUDE [DEG. W]	OBSERVED GRAVITY [MGALS]	BOUGUER ANOMALY [MGALS]
41	1093.9	46.6430	113.9904	-53.844	-169.3
42	1143.6	46.6470	113.9699	-58.937	-164.7
43	1240.8	46.6380	113.9445	-80.086	-164.5
44	1310.9	46.6320	113.9271	-94.187	-163.5
45	981.5	46.6750	114.0812	-23.008	-161.1
46	1075.9	46.8070	114.0350	-75.414	-159.1
47	1033.3	46.7940	114.0462	-65.117	-156.2
48	1146.7	46.7780	113.9570	-91.586	-157.1
49	1195.1	46.7530	113.9409	-104.828	-155.0
50	1269.8	46.7230	113.9023	-124.500	-158.6
51	1241.5	46.7340	113.9161	-117.281	-157.7
52	1229.3	46.7370	113.9344	-112.617	-156.0
53	1177.7	46.7650	113.9400	-100.289	-154.5
54	1158.8	46.7740	113.9444	-94.852	-157.1
55	1143.0	46.7800	113.9651	-89.789	-156.2
56	1124.1	46.7830	113.9826	-86.172	-157.2
57	1095.1	46.7830	114.0022	-89.352	-165.6
58	1061.9	46.7840	114.0264	-72.039	-155.5
59	986.6	46.8030	114.0663	-58.016	-159.1
60	972.9	46.8060	114.0814	-52.469	-156.4
61	960.7	46.8180	114.0644	-51.141	-158.9
63	957.4	46.7870	114.0925	-.133	-155.8
64	963.2	46.7640	114.0623	-3.305	-155.0
65	970.8	46.7580	114.0734	2.578	-147.1
68	1046.7	46.7910	114.0365	-16.484	-154.5
69	1097.3	46.7830	114.0389	-27.461	-154.3
70	1084.5	46.7790	114.0424	-25.734	-154.5
71	969.3	46.7710	114.0590	-5.305	-156.5
72	1138.4	46.7680	114.0455	-20.641	-137.0
73	975.4	46.8150	114.0920	-2.312	-156.5
74	975.4	46.7950	114.0997	-5.125	-156.8
75	972.3	46.7690	114.0792	-3.266	-154.1
76	963.2	46.7480	114.0648	-5.805	-155.9
77	972.3	46.7030	114.0772	-25.875	-169.8
78	970.8	46.6880	114.0782	-24.141	-166.6
79	978.4	46.6690	114.0789	-28.875	-167.7
80	1055.2	46.6960	114.0917	-41.258	-166.5
81	1055.5	46.6810	114.0922	-32.813	-154.2
82	1115.6	46.6740	114.1045	-48.406	-155.2
83	972.0	46.6690	114.0563	-28.031	-170.1

STATION NUMBER	STATION ELEVATION [METERS]	STATION LATITUDE [DEG. N]	STATION LONGITUDE [DEG. W]	OBSERVED GRAVITY [MGALS]	BOUGUER ANOMALY [MGALS]
84	995.2	46.6460	114.0789	-38.375	-173.2
85	977.2	46.6300	114.0535	-38.773	-176.4
86	1008.3	46.6480	114.0385	-38.531	-171.6
87	1021.1	46.6580	114.0312	-34.828	-166.1
88	1024.1	46.6690	114.0257	-30.781	-161.9
89	1164.3	46.6760	114.0035	-57.430	-160.4
90	986.0	46.6810	114.0299	-23.711	-163.0
91	1040.9	46.6950	114.0334	-30.195	-158.7
92	1115.6	46.6920	114.0233	-43.750	-156.6
93	1277.1	46.6990	114.0037	-73.672	-153.1
94	1426.5	46.7080	113.9980	-102.906	-153.0
95	982.4	46.7070	114.0337	-19.523	-160.8
96	963.2	46.7350	114.0711	-10.367	-159.5
97	963.2	46.7280	114.0532	-10.828	-159.2
98	963.2	46.7210	114.0478	-12.031	-159.6
99	996.1	46.7310	114.0437	-16.492	-158.2
100	1072.9	46.7340	114.0216	-31.102	-157.0
101	1130.8	46.7400	114.0017	-43.781	-159.0
102	1197.9	46.7400	113.9804	-57.508	-159.4
103	963.2	46.7160	114.0546	-15.016	-162.4
104	1103.4	46.7220	114.0229	-38.820	-157.1
105	1182.6	46.6990	114.1146	-62.273	-160.0
106	1249.7	46.6880	114.1164	-77.523	-158.9
107	1170.4	46.6630	114.1061	-61.242	-156.1
108	1200.9	46.6570	114.1075	-70.547	-158.9
109	1106.4	46.6560	114.0993	-51.977	-161.0
110	1025.7	46.5010	114.0826	-67.039	-183.8
111	1053.1	46.5010	114.0654	-71.336	-182.7
112	1082.0	46.5010	114.0455	-74.086	-179.7
113	1112.5	46.5010	114.0238	-76.812	-176.4
114	1141.5	46.5010	114.0018	-78.922	-172.1
115	1204.0	46.4840	113.9776	-93.078	-172.3
116	1234.4	46.4790	113.9576	-104.625	-177.0
117	1298.4	46.4630	113.9387	-114.898	-173.4
118	1325.9	46.4530	113.9221	-126.172	-176.2
119	1356.4	46.4410	113.9123	-134.523	-176.4
120	1402.1	46.4270	113.9057	-148.531	-179.6
122	1216.2	46.4760	113.9929	-98.375	-174.5
123	1129.3	46.4840	114.0234	-84.820	-179.4
124	1164.3	46.4770	114.0027	-91.289	-178.0

STATION NUMBER	STATION ELEVATION [METERS]	STATION LATITUDE [DEG. N]	STATION LONGITUDE [DEG. W]	OBSERVED GRAVITY [MGALS]	BOUGUER ANOMALY [MGALS]
125	1216.2	46.4720	114.0095	-101.836	-172.4
126	1231.4	46.4580	114.0080	-101.445	-172.8
127	1188.7	46.4570	114.0299	-95.867	-175.9
128	1178.1	46.4720	114.0301	-94.859	-178.6
129	1103.4	46.4820	114.0485	-82.375	-182.0
130	1051.6	46.4850	114.0664	-71.812	-182.0
131	1019.6	46.4850	114.0897	-65.445	-182.0
132	979.9	46.4720	114.0897	-64.656	-187.9
133	1012.9	46.4570	114.0912	-65.680	-181.0
134	1033.3	46.4570	114.0777	-69.766	-180.1
135	1015.0	46.4420	114.0940	-65.539	-179.1
136	1027.2	46.4420	114.0731	-68.141	-179.2
137	1143.0	46.4430	114.0536	-89.187	-177.2
138	1252.7	46.4520	113.9880	-112.125	-178.4
139	1319.8	46.4520	113.9666	-122.289	-175.0
140	1022.3	46.4240	114.0967	-67.844	-178.3
141	1033.0	46.4240	114.0728	-67.750	-176.0
142	1086.6	46.4270	114.0515	-82.164	-176.9
143	1133.9	46.4270	114.0314	-92.148	-180.1
144	1065.3	46.4420	114.0528	-72.750	-173.4
145	1129.3	46.4420	114.0286	-82.930	-173.3
146	1015.3	46.4420	114.1154	-66.117	-179.4
147	1022.6	46.4420	114.1349	-67.180	-178.8
148	1034.6	46.4420	114.1462	-69.937	-178.9
149	1033.3	46.4270	114.1473	-70.648	-178.7
150	1036.3	46.4130	114.1437	-73.227	-179.7
151	1021.1	46.4130	114.1264	-69.227	-179.1
152	1024.1	46.4130	114.1121	-69.977	-179.2
153	1025.7	46.4090	114.0938	-70.805	-179.3
154	1029.6	46.3970	114.0933	-73.695	-180.3
155	1091.2	46.3970	114.0684	-84.031	-178.2
156	1129.6	46.3970	114.0508	-89.836	-176.2
157	1193.3	46.3970	114.0347	-100.242	-173.6
161	1059.5	46.5740	114.0018	-57.047	-171.0
173	1052.5	46.5600	114.0018	-54.656	-171.4
174	1034.5	46.5600	114.0236	-53.086	-173.4
175	1051.9	46.4137	114.1678	-77.172	-180.2
176	1083.3	46.4287	114.1678	-80.625	-177.7
177	1067.7	46.4465	114.1678	-75.875	-176.7
178	1127.8	46.4658	114.2141	-97.000	-165.6

STATION NUMBER	STATION ELEVATION [METERS]	STATION LATITUDE [DEG. N]	STATION LONGITUDE [DEG. W]	OBSERVED GRAVITY [MGALS]	BOUGUER ANOMALY [MGALS]
179	1228.3	46.4960	114.1920	-96.727	-165.4
182	1601.7	46.4370	114.2209	-173.492	-160.8
183	1074.4	46.4559	114.1679	-71.906	-171.7
184	1106.4	46.4721	114.1674	-74.789	-168.8
185	1050.0	46.4721	114.1448	-66.352	-173.5
186	1072.9	46.4903	114.1475	-67.344	-170.9
187	1037.5	46.5008	114.1463	-62.297	-174.0
188	1002.5	46.5000	114.1232	-56.977	-177.1
189	1004.3	46.4885	114.1271	-57.766	-176.6
190	1015.0	46.4721	114.1296	-61.719	-177.2
191	1086.6	46.4544	114.1362	-66.391	-166.3
192	1082.0	46.4175	114.1890	-78.844	-174.3
193	1117.1	46.4171	114.2093	-83.391	-170.4
194	1152.1	46.4155	114.2209	-87.219	-165.4
195	1116.8	46.3990	114.1997	-93.062	-180.9
196	1202.7	46.3940	114.2209	-103.250	-172.6
197	1123.5	46.3810	114.1993	-95.969	-181.1
198	1175.9	46.3810	114.2209	-99.406	-173.0
199	1243.6	46.3791	114.2405	-108.242	-163.0
200	1089.7	46.3854	114.1784	-94.562	-187.7
201	1085.7	46.3998	114.1782	-89.125	-184.2
202	1051.6	46.3998	114.1462	-81.672	-184.1
203	1048.5	46.3854	114.1465	-94.836	-196.6
204	1075.6	46.3782	114.1678	-93.766	-189.4
205	1120.1	46.3660	114.1940	-98.086	-183.2
206	1147.0	46.3530	114.1942	-106.297	-184.4
207	1238.1	46.3530	114.2146	-116.891	-175.6
208	1132.0	46.3421	114.1992	-103.539	-183.4
209	1082.0	46.3415	114.1709	-101.000	-191.7
210	1180.5	46.3330	114.2209	-105.148	-173.6
211	1228.3	46.3210	114.2209	-114.523	-172.0
212	1150.6	46.3240	114.1927	-108.094	-182.9
213	1079.0	46.3124	114.1737	-99.852	-188.5
214	1063.1	46.3134	114.1561	-99.719	-192.0
215	1056.4	46.3283	114.1560	-98.336	-193.4
216	1052.2	46.3421	114.1556	-96.430	-193.6
217	1058.0	46.3566	114.1558	-95.211	-190.8
218	1061.9	46.3710	114.1558	-92.680	-190.5
219	1098.8	46.3710	144.1777	-99.008	-189.1
220	1066.8	46.3259	144.1729	-98.047	-190.3

STATION NUMBER	STATION ELEVATION [METERS]	STATION LATITUDE [DEG. N]	STATION LONGITUDE [DEG. W]	OBSERVED GRAVITY [MGALS]	BOUGUER ANOMALY [MGALS]
221	1033.9	46.3819	114.1046	-80.062	-184.6
222	1036.3	46.3709	114.1046	-83.211	-186.2
223	1056.7	46.3709	114.0821	-86.766	-185.5
224	1092.7	46.3778	114.0623	-90.586	-182.8
225	1109.8	46.3888	114.0615	-93.937	-183.6
226	1167.4	46.3798	114.0399	-103.492	-180.7
227	1107.9	46.3620	114.0618	-92.344	-180.0
228	1115.6	46.3560	114.0608	-96.023	-181.6
229	1130.8	46.3400	114.0611	-92.789	-174.0
230	1072.6	46.3460	114.0829	-94.367	-187.7
231	1072.9	46.3570	114.0830	-91.336	-182.0
32	1041.5	46.3570	114.1046	-86.992	-187.7
233	1045.2	46.3460	114.1204	-93.586	-192.7
234	1053.1	46.3255	114.1196	-97.695	-193.4
235	1058.0	46.3129	114.1359	-100.617	-194.1
236	1057.4	46.3255	114.1030	-97.375	-192.1
237	1096.1	46.3255	114.0814	-103.180	-190.0
238	1141.8	46.3255	114.0618	-109.695	-186.9
239	1228.0	46.3246	114.0336	-125.047	-183.5
240	1289.3	46.3270	114.0188	-134.383	-181.1
241	1417.3	46.3393	113.9980	-165.164	-187.5
242	1341.1	46.3266	114.0086	-148.312	-184.6
243	1176.5	46.3130	114.0415	-115.828	-183.5
244	1117.1	46.3130	114.0615	-109.047	-190.2
245	1044.9	46.3132	114.1133	-99.742	-195.6
246	1077.5	46.2986	114.1678	-100.578	-188.4
247	1123.2	46.3024	114.1890	-104.211	-182.5
248	1181.4	46.3090	114.2113	-109.602	-175.4
249	1254.6	46.2986	114.2207	-123.187	-172.3
250	1225.3	46.2876	114.2206	-116.898	-170.5
251	1107.9	46.2876	114.1950	-100.750	-180.5
252	1231.4	46.2693	114.2209	-122.422	-172.6
253	1155.8	46.2692	114.1992	-111.742	-180.6
254	1150.6	46.2547	114.1993	-114.359	-182.6
255	1249.7	46.2554	114.2204	-127.523	-172.6
999	1109.5	46.2692	114.1779	-107.867	-186.4
256	1092.7	46.2550	114.1779	-107.109	-187.5
257	1065.3	46.2887	114.1628	-100.141	-189.7
258	1084.2	46.2552	114.1563	-109.172	-192.0
259	1074.4	46.2690	114.1561	-103.734	-189.6

STATION NUMBER	STATION ELEVATION [METERS]	STATION LATITUDE [DEG. N]	STATION LONGITUDE [DEG. W]	OBSERVED GRAVITY [MGALS]	BOUGUER ANOMALY [MGALS]
260	1067.1	46.2840	114.1399	-103.539	-192.5
261	1062.2	46.2986	114.1410	-101.820	-193.1
262	1083.9	46.3130	114.0872	-102.789	-191.0
263	1132.6	46.2985	114.0618	-110.867	-187.9
264	1185.1	46.2985	114.0412	-123.422	-188.6
265	1229.6	46.2980	114.0183	-132.789	-187.8
266	1258.8	46.2951	114.0017	-140.406	-189.1
267	1310.6	46.2960	113.9816	-154.203	-192.4
268	1386.8	46.2940	113.9570	-171.695	-194.4
269	1118.0	46.2952	114.0870	-113.656	-193.6
270	1065.9	46.2985	114.1146	-102.578	-193.2
271	1085.1	46.2841	114.1146	-107.773	-191.5
272	1118.6	46.2770	114.0930	-115.953	-194.0
273	1140.0	46.2770	114.0714	-119.055	-189.2
274	1200.3	46.2770	114.0312	-131.000	-192.4
275	1237.5	46.2770	114.0297	-138.281	-191.6
276	1338.1	46.2770	114.0073	-153.141	-185.1
277	1088.1	46.2681	114.1354	-111.680	-194.9
278	1101.9	46.2547	114.1359	-116.758	-196.0
279	1147.6	46.2541	114.0716	-121.672	-191.7
280	1030.5	46.5892	114.0234	-57.164	-180.9
281	1121.7	46.6032	113.9867	-72.539	-174.7
282	1094.2	46.5885	114.0018	-69.250	-180.3
283	1140.0	46.5883	113.9679	-72.164	-173.8
284	1194.8	46.6035	113.9380	-78.531	-170.7
285	1243.6	46.6180	113.9184	-85.891	-167.2
286	1341.1	46.6211	113.8954	-107.523	-170.2
287	1511.8	46.6015	113.8555	-138.367	-165.4
288	1658.1	46.6035	113.8256	-171.906	-168.8
289	1414.3	46.6100	113.8741	-122.414	-169.6
290	1255.8	46.6044	113.9209	-94.047	-171.7
291	1116.8	46.5736	113.9595	-67.008	-172.0
292	1084.5	46.5736	113.9806	-66.562	-178.2
293	990.0	46.5581	114.0864	-51.398	-180.3
294	998.2	46.5412	114.1005	-52.477	-177.6
295	1033.3	46.5519	114.1201	-55.281	-173.4
296	996.4	46.5581	114.1026	-50.617	-177.5
297	1095.1	46.5588	113.9814	-64.969	-173.0
298	1134.8	46.5588	113.9598	-76.258	-176.2
299	1255.8	46.5430	113.9183	-97.312	-171.4

STATION NUMBER	STATION ELEVATION [METERS]	STATION LATITUDE [DEG. N]	STATION LONGITUDE [DEG. W]	OBSERVED GRAVITY [MGALS]	BOUGUER ANOMALY [MGALS]
300	1341.1	46.5414	113.8970	-117.133	-173.8
301	1536.2	46.5339	113.8756	-160.422	-177.4
302	1731.3	46.5220	113.8618	-188.477	-164.7
303	1466.1	46.5472	113.8763	-143.516	-175.6
304	1524.0	46.5589	113.8756	-147.664	-169.6
305	1423.4	46.5657	113.8950	-131.711	-174.0
306	1240.5	46.5543	113.9380	-95.297	-173.7
307	1058.0	46.5448	114.0234	-65.078	-179.4
308	1098.2	46.5303	114.0246	-71.734	-176.7
309	1086.6	46.5337	114.0420	-72.359	-180.0
310	1645.9	46.2956	113.9199	-217.180	-188.3
311	1798.3	46.3129	113.9442	-241.687	-184.0
312	1767.8	46.3371	113.9576	-252.844	-203.7
313	1706.9	46.3394	113.9676	-257.281	-221.1
314	1090.9	46.2409	114.1563	-111.898	-192.1
315	1092.7	46.2265	114.1563	-112.305	-190.7
316	1100.0	46.2113	114.1561	-113.492	-183.7
317	1108.6	46.1968	114.1561	-115.062	-187.5
318	1118.0	46.1824	114.1561	-116.156	-185.1
319	1082.0	46.1682	114.1639	-114.781	-180.6
320	1146.0	46.1542	114.1375	-126.961	-185.8
321	1204.0	46.1444	114.0917	-143.977	-188.4
322	1216.2	46.1388	114.0731	-153.578	-190.1
323	1275.6	46.1301	114.0480	-165.937	-189.9
324	1200.9	46.1464	114.1138	-134.422	-179.7
325	1131.7	46.1968	114.1347	-121.352	-189.3
326	1149.1	46.1972	114.1143	-124.336	-189.0
327	1135.4	46.2115	114.1143	-124.500	-193.3
328	1124.7	46.2113	114.1304	-121.422	-192.3
329	1109.2	46.2371	114.1349	-120.414	-196.9
330	1145.1	46.2290	114.1113	-127.117	-195.5
331	1163.7	46.2262	114.0928	-122.195	-186.5
332	1206.4	46.2115	114.0927	-138.359	-192.7
333	1216.2	46.1972	114.0927	-138.250	-189.3
334	1156.7	46.1535	114.1636	-126.156	-181.8
335	1173.5	46.1384	114.1593	-131.773	-181.8
336	1161.3	46.1107	114.1694	-132.359	-179.3
337	1156.4	46.0956	114.1794	-129.945	-175.0
338	1248.2	46.0962	114.2056	-147.477	-174.3
339	1181.1	46.1064	114.2053	-134.703	-182.1

STATION NUMBER	STATION ELEVATION [METERS]	STATION LATITUDE [DEG. N]	STATION LONGITUDE [DEG. W]	OBSERVED GRAVITY [MGALS]	BOUGUER ANOMALY [MGALS]
340	1155.8	46.1107	114.1844	-126.641	-174.6
341	1190.9	46.1207	114.2038	-135.391	-178.3
342	1236.9	46.1207	114.2242	-137.844	-172.6
343	1143.0	46.1244	114.1827	-125.484	-179.3
344	1191.8	46.1276	114.2038	-135.906	-180.3
345	1219.2	46.2430	114.2209	-123.508	-173.5
346	1127.8	46.2404	114.1938	-112.047	-183.8
347	1151.8	46.2265	114.2078	-112.312	-175.5
348	1107.9	46.2265	114.1889	-109.148	-184.1
349	1116.2	46.2113	114.1781	-112.062	-184.8
350	1122.6	46.1968	114.1781	-114.523	-182.9
351	1123.2	46.1824	114.1842	-113.187	-179.6
352	1124.1	46.1680	114.1842	-114.023	-178.5
353	1130.8	46.1535	114.1844	-118.359	-179.2
354	1133.9	46.1384	114.1772	-123.109	-181.0
355	1141.5	46.1384	114.1975	-124.297	-180.7
356	1136.0	46.1535	114.2023	-118.922	-177.7
357	1186.3	46.1682	114.2040	-123.422	-174.6
358	1120.1	46.2442	114.1144	-122.125	-197.1
359	1141.5	46.2442	114.0930	-125.750	-196.2
360	1157.6	46.2371	114.0830	-125.570	-191.9
361	1204.0	46.1747	114.0714	-141.227	-191.8
362	1234.4	46.1718	114.0503	-150.695	-192.6
363	1248.2	46.1586	114.0081	-165.297	-199.3
377	1252.7	46.1623	114.0296	-156.000	-191.4
378	1304.5	46.2688	114.2415	-134.297	-165.0
379	1542.3	46.2526	114.2501	-134.617	-160.4
380	1143.0	46.5422	113.9522	-77.953	-174.7
381	1268.0	46.5257	113.9520	-104.383	-174.4
382	1377.7	46.5124	113.9565	-118.719	-165.8
383	1117.1	46.5430	114.0018	-156.766	-171.4
384	1066.8	46.6091	114.0136	-61.687	-179.8
385	1271.0	46.5874	114.1402	-90.766	-159.8
386	1706.9	46.5969	114.1646	-174.227	-152.5
387	1035.1	46.5892	114.1078	-48.375	-169.3
388	1033.3	46.6031	114.1078	-44.000	-167.9
389	981.5	46.6046	114.0585	-43.070	-177.7
390	979.0	46.6180	114.0651	-40.789	-177.0
401	1092.6	46.5575	113.9814	-67.312	-175.5
402	1088.1	46.5582	113.9814	-66.250	-175.5

STATION NUMBER	STATION ELEVATION [METERS]	STATION LATITUDE [DEG. N]	STATION LONGITUDE [DEG. W]	OBSERVED GRAVITY [MGALS]	BOUGUER ANOMALY [MGALS]
403	1083.2	46.5588	113.9814	-65.195	-175.5
404	1088.8	46.5588	113.9787	-65.531	-174.7
405	1095.1	46.5588	113.9760	-66.016	-173.8
406	1101.4	46.5588	113.9733	-66.422	-172.9
407	1117.6	46.5588	113.9706	-69.625	-172.8
408	1124.7	46.5588	113.9679	-71.266	-173.0
409	1132.5	46.5588	113.9652	-72.547	-172.6
410	1140.5	46.5588	113.9625	-73.664	-172.1
411	1155.1	46.5588	113.9598	-76.289	-171.7
412	1164.0	46.5588	113.9571	-78.406	-172.0
413	1172.8	46.5588	113.9544	-80.445	-172.2
414	1184.3	46.5588	113.9517	-82.898	-172.3
415	1196.6	46.5588	113.9490	-85.328	-172.3
416	1208.7	46.5588	113.9463	-87.227	-171.1
417	1218.0	46.5588	113.9436	-88.898	-171.4
418	1247.3	46.5543	113.9380	-95.109	-171.3
419	1101.9	46.5534	113.9814	-69.461	-175.5
420	1095.2	46.5526	113.9814	-68.289	-175.5
421	1099.1	46.5526	113.9787	-68.781	-175.1
422	1106.5	46.5526	113.9760	-70.062	-174.9
423	1122.5	46.5526	113.9733	-73.164	-174.8
424	1131.4	46.5526	113.9706	-74.656	-174.4
425	1127.5	46.5526	113.9679	-73.742	-174.2
426	1087.5	46.5504	113.9814	-66.719	-175.1
427	1089.6	46.5484	113.9814	-67.531	-175.3
428	1095.0	46.5467	113.9814	-69.336	-175.8
429	1098.7	46.5445	113.9814	-70.664	-176.2
430	1106.4	46.5445	113.9787	-72.219	-176.2
431	1115.7	46.5445	113.9760	-74.242	-176.3
432	1112.5	46.5445	113.9733	-71.695	-174.3
433	1115.6	46.5445	113.9706	-74.164	-176.2
434	1127.8	46.5445	113.9679	-77.852	-177.5
435	1149.1	46.5445	113.9652	-80.297	-175.7
526	1079.0	46.5165	114.1399	-68.156	-173.1
527	1231.4	46.5220	114.1614	-92.906	-162.0
528	1414.3	46.5216	114.1766	-131.055	-161.5
529	1527.0	46.5125	114.1727	-153.570	-162.5
536	1682.5	46.5006	114.1957	-184.930	-162.4
539	1101.2	46.4793	114.1561	-72.547	-169.1
540	1194.8	46.4772	114.1736	-88.727	-164.0

STATION NUMBER	STATION ELEVATION [METERS]	STATION LATITUDE [DEG. N]	STATION LONGITUDE [DEG. W]	OBSERVED GRAVITY [MGALS]	BOUGUER ANOMALY [MGALS]
541	1304.5	46.4930	114.1664	-109.195	-164.1
542	1450.8	46.5065	114.1716	-137.281	-161.8
543	1560.6	46.4988	114.1774	-161.789	-165.3
544	1284.7	46.4685	114.1829	-108.203	-164.5
545	1456.9	46.4803	114.1830	-141.625	-163.6
546	1662.7	46.4713	114.2003	-182.617	-160.5

Appendix II

COMPUTER PROGRAMS

Five FORTRAN programs were used in this study of the Bitterroot Valley. The Bott (1960) program for iteratively determining the thickness of valley fill from the Bouguer anomaly, the Talwani and Ewing program (1960) for calculating gravity and magnetic fields over arbitrary three dimensional bodies and the Henderson (1960) program for generating first and second derivatives and continued fields are fairly well documented within the bodies of the respective programs. Additional information on the Talwani and Ewing program and the Henderson program as used in this study is available through the Indiana Geological Survey, Bloomington, Indiana 47401. For flow charts of these three programs, the user is advised to refer to the original papers from which these programs were written.

The lowpass filter program used in this study is also included in this appendix. The program requires a Fourier transform subroutine to complete the filtering process. In general, the program reads the input signal in the spatial (time) domain, Fourier transforms into the frequency domain, applies the frequency domain filter function, and inverse transforms the data to yield the filtered signal. The filter function is defined to be a very sharp, zero-phase shift filter (Fig. 24). The Fourier transform subroutine used in this study followed the fast transform algorithm of Cooley and Tukey (1965). However, any Fourier transform program could be used with the filter program.

The following list of variables and explanations should help the user implement the lowpass filter program.

1. TITLE a 72 character title of the data to be filtered
2. N the number of equispaced points in the input signal
3. FREQ the cutoff frequency for the filter functions. This is expressed as a wavelength and must be in the range $2 \leq \text{FREQ} \leq (N - 1)/2$
4. SPACE the distance between the equispaced data points
5. A(I) the input signal array, not complex
6. DATA(I,J) the array used in the Fourier transform, complex
7. PLOT(I) the array used for a line printer plot of the power spectrum and the filtered and unfiltered time domain signals
8. B(I) the filtered output signal array, not complex
9. F(I) the distance from the origin of the input signal. This is related to SPACE.

The fifth program included in this appendix was used to calculate layer thicknesses and dips from the seismic refraction data. The program has been copied (with permission) exactly as it was presented by Mooney (1973). The input is documented in the program and the output is self explanatory. For a discussion of the theory and a flow chart of the program, the user should refer to the original paper.

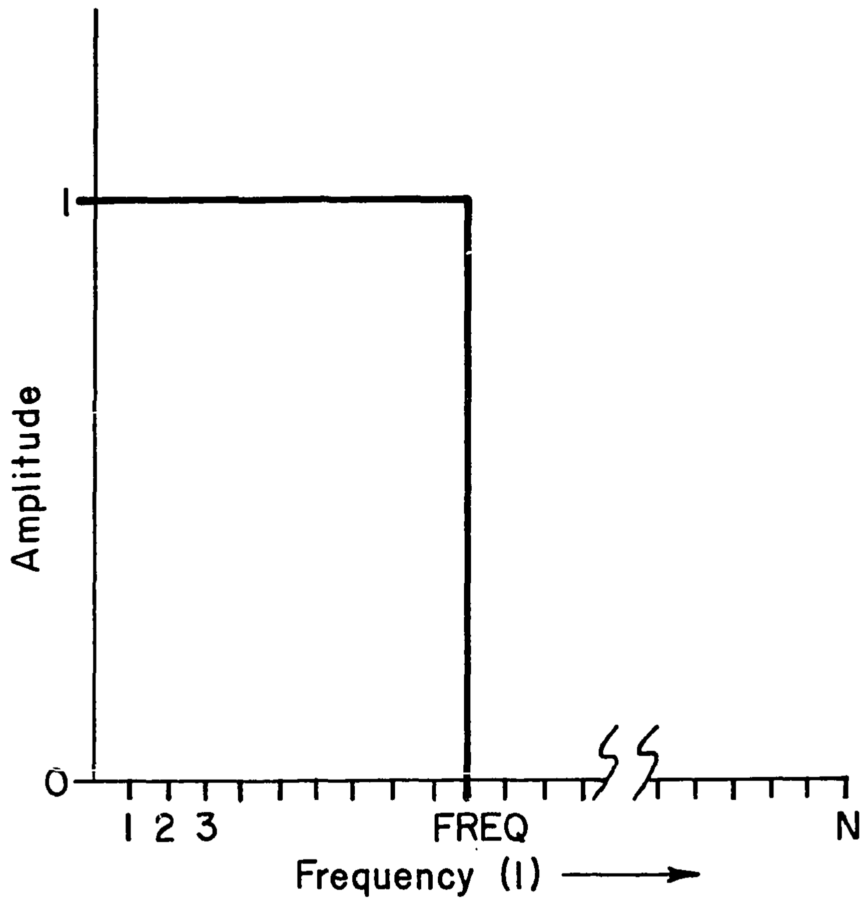

Figure 24. Frequency response curve of the lowpass filter. FREQ is the cutoff frequency as outlined in the text. N is the total number of frequencies output by the Fourier transform program and equals the number of equispaced input data points. Such a sharp filter can introduce a "ringing" in the output of the filter. A filter with sloping sides would minimize the ringing. Future users of the lowpass filter should consider modifying the filter response curve to have sloping sides.

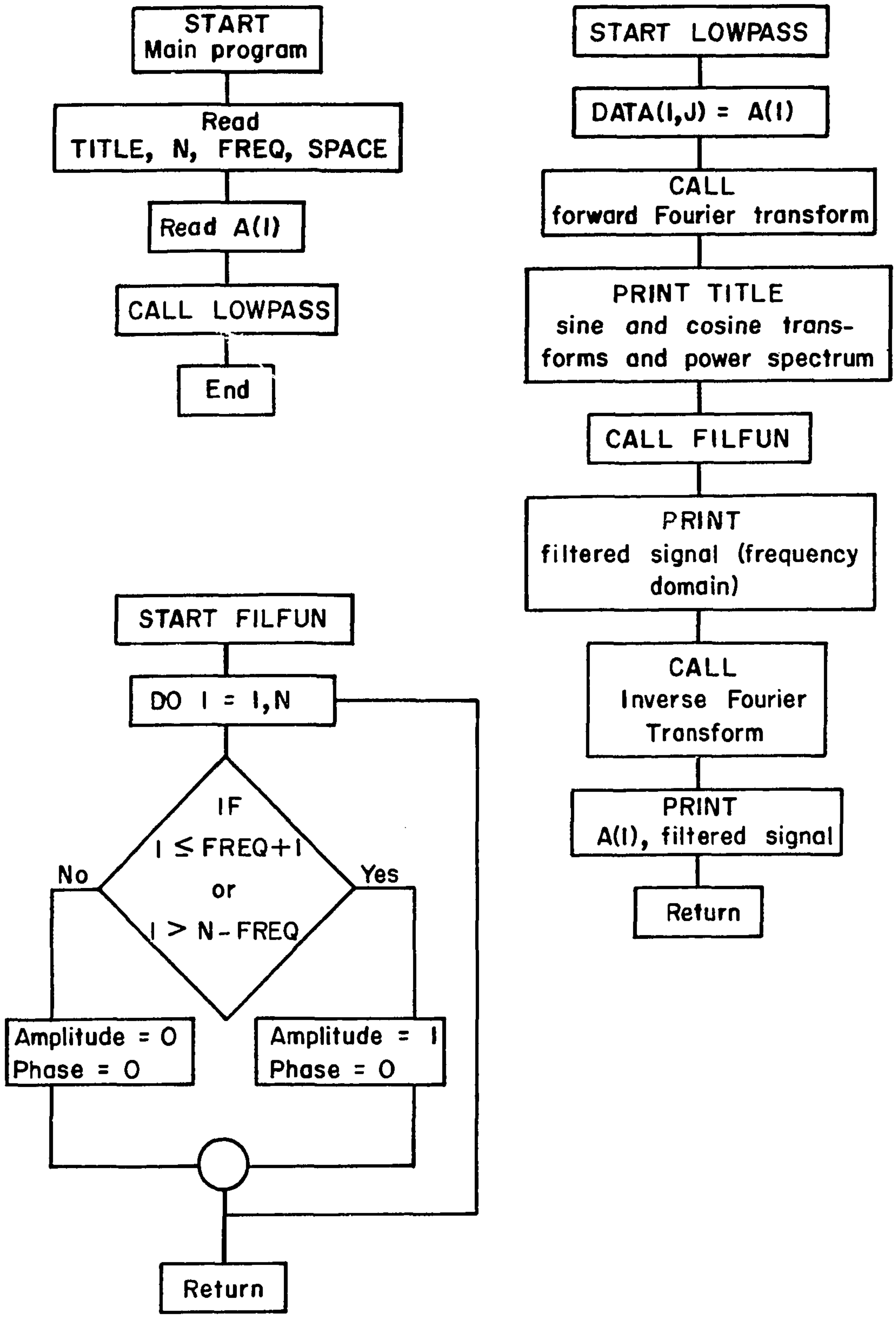

Figure 25. Flow chart for the lowpass filter program.

The Lowpass Filter Program

```
      DIMENSION  TITLE(12)
      DIMENSION A(400)
      DOUBLE PRECISION TITLE
      INTEGER SPACE
 1000 READ (2,3, END=1001) (TITLE(I),I = 1,12)
      READ(2,2) N,FREQ,SPACE
      READ(2,1) (A(I),I = 1,N)
      TEMP = 0.
    1 FORMAT(5F)
    3 FORMAT (12A6)
    2 FORMAT(2I,F)
      CALL LOPASS (N,A,FREQ,TEMP,SPACE,TITLE)
      GO TO 1000
 1001 CALL EXIT
      END
      SUBROUTINE LOPASS (N,A,FREQ,TEMP,SPACE,TITLE)
      DIMENSION TITLE(12), PLOT(75)
      DIMENSION F(400)
      DIMENSION A(400), DATA(400), WORK(400)
      DIMENSION B(400)
      DOUBLE PRECISION TITLE
      COMPLEX DATA,WORK

      INTEGER FREQ, TPLOT
      DO 1 I = 1,N
      DATA(I) = 0.
    1 DATA(I) = CMPLX(A(I)-TEMP,0.0)

  103 CALL FOURT(DATA,N,1,-1,1,WORK)
      PRINT 100,(TITLE(I),I = 1,12)
  100 FORMAT (1H1,///2X,12A6,//5X,'FOURIER TRANSFORM OF INPUT SIGNAL',/
     *5X,'I   ','FT/CYCLE',6X,'REAL',8X,
     1'IMAGINARY',5X,'AMPLITUDE',30X,'AMPLITUDE SPECTRUM',///)
      DO 3 I = 1,(N+1)/2
      POWER = SQRT((REAL(DATA(I))**2.) +(AIMAG(DATA(I))**2.))/N
      TI = N*SPACE/(I-1)
      J = I-1
      DO 106 JJ = 1,75
  106 PLOT(JJ) = 1H
      TPLOT = (POWER/2) +0.5
      DO 107 JJ = 1,TPLOT
  107 PLOT(JJ) = 1HX
    3 PRINT 2, J, TI, DATA(I), POWER,(PLOT(JJ), JJ = 1,75)
    2 FORMAT (1X,I5,F8.1,3F14.2,75A1)
      CALL FILFUN (DATA,N,FREQ,DATA)
      THETA = 0.
      DO 20 I = 1,N
      SUM = 0.
      FTHETA = 0.
      DO 22 J = 2,(N/2)
   22 SUM = SUM + REAL(DATA(J))*COSD((J-1)*THETA)+AIMAG(DATA(J))
     1 *SIND((J-1)*THETA)
      THETA = THETA - 360./N
      FTHETA = ( SUM + REAL(DATA(1))/2.)/(N/2)
   20 F(I) =  FTHETA + TEMP
      PRINT 5
    5 FORMAT (///'  FILTERED DATA, FREQUENCY DOMIAN. '/)
      DO 6 I = 1,(N+1)/2
      J = I-1
    6 PRINT 7, J ,DATA(I)
```

```
    7 FORMAT (2X,I5,2F20.2)
      WAVE = N*SPACE/FREQ
      CALL FOURT (DATA,N,1,1,1,WORK)
      PRINT 9, FREQ, WAVE
      DO 8 I = 1,N
      DATA(I) =  DATA(I)/FLOAT(N)
      B(I) = REAL(DATA(I)) + TEMP
      DO  23 J = 1,60
   23 PLOT(J) = 1H
      PLOT(30) = 1H.
      TPLOT = ((B(I) + 1500)/50.) +0.5
      PLOT(TPLOT) = 1H*
      TPLOT = ((A(I) + 1500)/50.) +0.5
      PLOT(TPLOT) = 1H+
  102 FORMAT (2XI5,3F15.2,'.....',60A1)
    8 PRINT 102, I, A(I), B(I),F(I),(PLOT(J),J = 1,60)
  104 CONTINUE
    9 FORMAT(///'  FILTERED DATA, TIME DOMAIN,'/'  CUTOFF FREQUENCY = '
     *,I,'  CYCLES/PERIOD   WAVELENGTH = ',F8.2,' FT/CYCLE'
     */,'    I',7X,
     1'INPUT +',15X,'OUTPUT *',10X,'....',6('I.........'),'I',/
     2,57X,'-1500',3X,'-1000',5X,'-500',8X,'0.0',8X,
     3'500',5X,'1000',5X,'1500'//)
      RETURN
      END
      SUBROUTINE FILFUN (C,N,FREQ,F)
      DIMENSION E(400,2),F(400)
      COMPLEX F
      INTEGER FREQ
      DIMENSION C(400),D(400)
      COMPLEX C,D
      DO 12 I = 1,N
      IF(I.LE.(FREQ+1).OR.I.GT.(N-FREQ)) GO TO 13
      P = 0
      R = -AIMAG(C(I))
      D(I) = CMPLX (P,R)
      GO TO 12
   13 P = 1
      R = 0
      D(I) = CMPLX(P,R)
   12 CONTINUE
      DO 10 I = 1,N
      A = REAL(C(I))*REAL(D(I))
      B = AIMAG(C(I))+AIMAG(D(I))
      E(I,1) = A
   10 E(I,2) = B
      DO 11 I = 1,N
   11 F(I) = CMPLX(E(I,1),E(I,2))
      RETURN
      END
```

The Bott Program

```
C     LABEL - GRAV1
C     PROGRAM FOR DIRECT GRAVITY INTERPRETATION OF SEDIMENTAPY BASINS.
C     AFTER BOTT, GEOPHYSICAL JOURNAL 3.
C     FORTRAN 4H  APRIL 1972 BY PRAHL.
C     FIRST DATA CARD SPECIFIES OPT, FLAT, SYSTEM, NUM, AND DEN.
C     IF FLAT=0, BASIN IS ASSUMED TO BE FLAT AND IF FLAT=1, INPUT
C     ELEVATIONS OF TOPS OF BLOCKS - ELEV(I) IN FEET OR METERS.
C     SYSTEM = 0 FOR ENGLISH OR SYSTEM = 1 FOR METRIC.
C     DEN=DENSITY CONTRAST IN GRAMS PER CUBIC CENTIMETER.
C     NUM=NUM OF ANOMALIES OR BLOCKS.
C
C     IF OPT=0, HALF WIDTH OF BLOCKS IS CONSTANT - W IN FEET OR METERS.
C     OBSERVED ANOMALIES MUST BE EVENLY SPACED ( 2W BETWEEN CONSECUTIVE
C     OBSERVED ANOMALIES ARE AT CENTER OF BLOCKS.
C     ANOMALIES ) AND MUST BE AT CENTER OF BLOCKS.
C     SECOND DATA CARD CONTAINS TITLE OF INPUTTED DATA.
C     FOR OPT=0 THIRD DATA CARD CONTAINS HALF WIDTH - W AND LAST DATA
C     CARDS CONTAIN THE ELEVATIONS,ELEV(I),AND/OR THE OBSERVED ANOMALIES,
C     AOBS(I), AT CENTER OF EACH BLOCK IN CONSECUTIVE ORDER FROM LEFT.
C
C     IF OPT=1, HALF WIDTHS OF BLOCKS ARE WW(I) IN FEET OR METERS.
C     SECOND DATA CARD CONTAINS TITLE OF INPUTTED DATA.
C     FOR OPT=1 NEXT DATA CARDS CONTAIN HALF WIDTH,WW(I),AND ELEVATIONS,
C     ELEV(I), AND/OR OBSERVED ANOMALIES,AOBS(I), AT CENTER OF EACH
C     BLOCK FOR EACH BLOCK IN CONSECUTIVE ORDER FROM LEFT.
C
C     AOBS(I)=OBSERVED ANOMALIES IN MILLIGALS--ORDER 10.
C     BE CAREFUL WITH THE ALGEBRAIC SIGNS OF DEN AND AOBS(I).
C     PROGRAM CAN HANDLE ANY NUMBER OF DATA SETS IN ANY ORDER.
C     OUTPUT IS DEPTH OF BLOCKS FROM SURFACE.
C     DEPTHS AT END OF PROFILES WILL BE ANOMALOUS BECAUSE OF END EFFECTS.
C
      DIMENSION T(100),AOBS(100),ACALC(100),AX(20),TT(100),XX(100),WW(10
     10),SYSTN(4),ELEV(100)
      DIMENSION ELSL(100), TEMP1(100), TEMP2(100)
      DATA SYSTN/'FEET','    ','METE','RS  '/
      INTEGER OPT,SYSTEM,FLAT, SET
      FELEV(X,W,ELDIFF)=ELDIFF*(ATAN((X-W)/ELDIFF)-ATAN((X+W)/ELDIFF))
C
    9 READ (5,200,END=30) (AX(I), I=1,20)
      READ(  5,103)          OPT,FLAT,SYSTEM,NUM,DEN
  305 WRITE(  8,203)(AX(I),I=1,20)
C     SEDIMENTARY INTERPRETATION
C     PART 1
      IF(OPT.EQ.0)GO TO 31
      IF(FLAT.EQ.0)GO TO 32
      READ(5,100)(WW(I),ELEV(I),AOBS(I),I=1,NUM)
      GO TO 18
   32 READ  (  5,100)(WW(I),AOBS(I),I=1,NUM)
   18 XX(1)=0.0
      DO 34 J=1,NUM-1
   34 XX(J+1)=XX(J)+WW(J)+WW(J+1)
      GO TO 33
   31 READ(  5,100) W
      IF(FLAT.EQ.0)GO TO 19
      READ (5,100) ( AOBS(I), ELEV(I), I = 1, NUM)
      GO TO 20
   19 READ(  5,100) (AOBS(I),I=1,NUM)
  320 DO 69 I=1,NUM
   69 ELEV(I)=0.0
```

```
   20 XX(1)=0.0
      DO 50 I=1,NUM-1
   50 XX(I+1)=XX(I)+2.*W
      DO 51 I=1,NUM
   51 WW(I)=W
   33 IF(SYSTEM.EQ.0)GO TO 25
      KK=3
      CON1=4.191E-02
      CON2=1.334E-02
      GO TO 26
   25 KK=1
      CON1=1.277E-02
      CON2=4.066E-03
   26 DO 1 I=1,NUM
      T(I)=0.0
    1 ACALC(I)=0.0
      MM=0
    7 DO 8 I=1,NUM
      TH=(AOBS(I)-ACALC(I))/(CON1      *DEN)
      T(I)=T(I)+TH
C     T(I)--THICKNESS OR DEPTH
    8 ACALC(I)=0.0
C     CALCULATION OF ANOMALY USING EXACT FORMULA
      DO 2 I=1,NUM
      DO 2 J=1,NUM
      ABCALC=0.0
      IF(OPT.EQ.0)GO TO 35
   36 X=ABS(XX(J)-XX(I))
      W=WW(J)
      GO TO 37
   35 B = J - I
      X=2.*ABS(B)*W
   37 IF(FLAT.EQ.1)GO TO 66
      ELDIFF=0.0
      GO TO 61
   66 ELDIFF=ELEV(I)-ELEV(J)
      IF(ELDIFF.GE.0.0) GO TO 61
   60 TEMP=T(J)
      T(J)=-ELDIFF
      ABCALC=CON2      *DEN*ABS ((X-W)/2.*ALOG((T(J)**2+(X-W)**2)/(X-W)**
     12)-(X+W)/2.*ALOG((T(J)**2+(X+W)**2)/(X+W)**2)+T(J)*(ATAN((X-W)/T(J
     2))-ATAN((X+W)/T(J))))
      T(J)=TEMP
      GO TO 62
   61 IF(ELDIFF.EQ.0.0)GO TO 62
      FELL=FELEV(X,W,ELDIFF)
      GO TO 63
   62 FELL=0.0
   63 AACALC=CON2      *DEN*ABS ((X-W)/2.*ALOG((T(J)**2+(X-W)**2)/(X-W)**
     12)-(X+W)/2.*ALOG((T(J)**2+(X+W)**2)/(X+W)**2)+T(J)*(ATAN((X-W)/T(J
     2))-ATAN((X+W)/T(J)))-FELL)
    2 ACALC(I)=ACALC(I)+AACALC-ABCALC
      IF (MM. LE. 0) GO TO 10
C     OUTPUT SECTION
      DO 12 I=1,NUM
      ELSL(I) = ELEV(I) - T(I)
   12 ACALC(I)=AOBS(I)-ACALC(I)
      GO TO 42
   42 WRITE(  8,204)DEN,((SYSTN(J),J=KK,KK+1),I=1,4),(XX(I),WW(I),AOBS(I
     1),ACALC(I),T(I),ELEV(I),ELSL(I) , I = 1,NUM)
```

```
      GO TO 9
C     PART 2
C     IN PART 2 THE THICKNESS OR DEPTH IS ADJUSTED TO GIVE A VERY SMALL
C     RESIDUAL ANOMALY
   10 DO 3 K=1,8
    5 DO 4 I=1,NUM
      TT(I)=(AOBS(I)-ACALC(I))/(CON1      *DEN)
    4 T(I)=T(I)+TT(I)
      DO 3 I=1,NUM
      DO 3 J=1,NUM
      IF(OPT.EQ.0)GO TO 38
   39 X=ABS(XX(J)-XX(I))
      W=WW(J)
      GO TO 40
   38 B = J - I
      X=2.*ABS(B)*W
C     APPROXIMATION---HORIZONTAL SHEET OF MASS
   40 AACALC=CON2      *DEN*TT(J)*ABS(ATAN((X-W)/T(J))-ATAN((X+W)/T(J)))
    3 ACALC(I)=ACALC(I)+AACALC
      MM=1  + MM
C     RETURN TO PART 1 FOR FINAL STEPS--CALCULATION OF RESIDUAL WITH
C     CORRECTED DEPTH OR THICKNESS
      GO TO 7
   30 CONTINUE
      CALL EXIT
C
  100 FORMAT(10F)
  103 FORMAT(4I,F)
  200 FORMAT( 20A4)
  203 FORMAT(    '1 PROGRAM FOR DIRECT GRAVITY INTERPRETATION OF SEDIMENT
     1A-Y BAS+NS'//20A4//)
  204 FORMAT(2X,'DENSITY CONTRAST = ',F5.2//2X,'DISTANCE OF ANOMALY',2X,
     1'HALF WIDTH',2X,'OBSERVED ANOMALY',2X,'    ERROR           ',2X,'DEPTH
     2',4X,'ELEVATION'/2X,'VALUES FROM ORIGIN',3X,'OF BLOCK',8X,'MILLIGA
     3LS',9X,'MILLIGALS',1X,2(4X,2A4) /2X,'AT LEFT OF PROFILE',4X,2A4/9X
     4,2A4//(9X,F8.1,7X,F8.1,7X,F8.3,10X,F8.3,3X,F8.1,4X,F8.1, 4X,F8.3))
      END
```

```
C
C
C        GAM 3D IS A PROGRAM DESIGNED TO CALCULATE THE GRAVITATIONAL AND
C    MAGNETIC ANOMALIES ASSOCIATED WITH AN ARBITRARILY SHAPED THREE
C    DIMENSIONAL BODY (GIVEN   SUSCEPTIBILITY AND A DENSITY CONTRAST WITH
C    THE SURROUNDING MATERIALS).  THIS TASK IS FACILITATED BY THE USE OF
C    SOLID ANGLE TECHNIQUES.  THE BODY IS DIVIDED INTO LAMINAE AND EACH
C    LAMINA IS APPROXIMATED B  AN N-SIDED POLYGON.  THE MAGNETIC ANOMALY
C    IS OBTAINED BY CALCULATI G THE DIFFERENCE IN SOLID ANGLE FOR THE TOP
C    AND BOTTOM OF EACH LAYER AND THEN MULTIPLYING THIS DIFFERENCE BY THE
C    PRODUCT OF THE VERTICAL MAGNETIC FIELD AND THE SUSCEPTIBILITY
C    CONTRAST.  THE GRAVITATIONAL ANOMALY PER LAMINA IS OBTAINED BY
C    MULTIPLYING THE SOLID AN LE CONTRIBUTION FROM THAT LAMINA BY THE
C    DENSITY CONTRAST AND THE GRAVITATIONAL CONSTANT.  THE TOTAL ANOMALY
C    IS THEN CALCULATED BY IN EGRATING OVER THE ENTIRE THICKNESS OF THE
C    BODY.  THE RESULTS FROM BOTH THE GRAVITATIONAL AND MAGNETIC
C    CALCULATIONS ARE THEN PRINTED IN TABLE FORM AND ON A 25 X 25 MAP
C    WHICH CAN BE CONTOURED
C
C
C    THE IDENTIFICATION FOR T E FIRST DATA CARD IS AS FOLLOWS
C
C COLUMNS   FORMAT                          ITEM
C
C    1-8      F8.0     XMIN---X  COORDINATE FOR UPPER LEFT HAND MAP CORNER
C    9-16     F8.0     YMIN---Y  COORDINATE FOR UPPER LEFT HAND MAP CORNER
C   17-22     F6.0     FPZ---DEP H OF FIELD POINTS
C   23-28     F6.0     DELTA1---INCREMENT FOR GENERATING FIELD
C   29-34     F6.0     SCALEFM-- THE MAGNETIC VALUE IS MULTIPLIED BY SCALEFM
C                                BEFORE BEING PRINTED ON MAP
C   35-40     F6.0     SCALEFG-- SAME AS SCALEFM EXCEPT FOR GRAVITY VALUES
C   41-55     F15.0    CONVERT1- -CONVERTS (X,Y) COORDINATES FOR PROGRAM USE
C   56-70     F15.0    CONVERT2- -CONVERTS Z COORDINATES FOR PROGRAM USE
C                      CONVERT1  ND CONVERT2---ALL COORDINATES MUST BE IN
C                      KILOMETERS FOR PROGRAM USE.  THEREFORE, IF THEY ARE
C                      READ IN WITH DIMENSIONS
C                                MILES, CONVERT(1,2) = 1.609347219
C                                FEET, CONVERT(1,2) = 0.00030486096
C                                METERS, CONVERT(1,2) = 0.001
C                                KILOMETERS, CONVERT(1,2) = 1.0
C   71-72      I2      FZR---SWI CH--IF NONZERO, Z COORDINATES OF FIELD
C                                POINTS ARE READ IN
C
C
C    THE IDENTIFICATION FOR T E SECOND DATA CARD IS AS FOLLOWS
C
C COLUMNS   FORMAT                          ITEM
C
C    1-2       I2      SOLIDOUT- -SWITCH--IF NONZERO, SOLID ANGLES ARE
C                                PRINTED FOR EACH LAMINA
C    3-4       I2      FPOUT---S ITCH--IF NONZERO, GENERATED FIELD POINTS
C                                ARE PRINTED OUT
C    5-14     F10.0    VMFLD---V RTICAL MAGNETIC FIELD
C   15-24     F10.0    DELTAK--- USCEPTIBILITY CONTRAST
C   25-26      I2      PUNCHG--- WITCH--IF NONZERO, GRAVITY VALUES ARE
```

```
C                                   PUNCHED ON CARDS
C                                   PUNCHED ON CARDS
C                                   ON CARDS
C
C
C    THE THIRD CARD READ IN IS A TITLE CARD FOR THE MODEL.  IT IS READ IN
C          UNDER A 72H FORMAT  PECIFICATION
C
C
C    IDENTIFICATION FOR THE F URTH DATA CARD IS AS FOLLOWS
C
C COLUMNS  FORMAT                      ITEM
C
C    1-3       I3    KK---NUMB R OF FIELD POINTS (=625)
C    4-6       I3    MG---NUMB R OF LAMINAE IN MODEL
C     7        I1    J---SWITCH--IF NONZERO, THE CONTRIBUTION FROM MORE
C                                   THAN ONE BODY GIVEN ON THE SAME MAP
C    8-9       I2    AUX---SWITCH--IF NONZERO, THE VALUES OF TERMS A,B AND
C                                   C GIVEN FOR EACH SIDE OF EACH POLYGON
C   10-11      I2    U---SWITCH--IF NONZERO, TOP OF BODY ENDS IN A POINT
C   12-23    F12.0   ZU---DEPTH TO THE TOP OF THE BODY
C   24-35    F12.0   VU---GRAVITATIONAL ATTRACTION OF TOP POINT IF MODEL
C                                   ENDS IN A POINT
C   36-37      I2    T---SWITCH--IF NONZERO,BOTTOM OF BODY ENDS IN A POINT
C   38-49    F12.0   ZT---DEPT  TO THE BOTTOM OF THE BODY
C   50-61    F12.0   VT---GRAVITATIONAL ATTRACTION OF BOTTOM OF BODY IF
C                                   ENDS IN A POINT
C   62-63      I2    GGG---SWI CH--IF NONZERO,GG(M) IS PRINTED UNDER 9E12.
C
C
C    THERE IS ONE CARD AT THE BEGINNING OF EACH LAMINA AS FOLLOWS
C
C COLUMNS  FORMAT                      ITEM
C
C    1-2       I2    MID(M)---LAMINA IDENTIFICATION NUMBER
C    3-12    F10.0   RHO(M)--- ENSITY CONTRAST FOR THAT LAMINA
C   13-28    F16.0   ZEE(M)--- EPTH TO THAT LAMINA
C   29-36      I8    III(M)---.UMBER OF POLYGON VERTICES FOR THAT LAMINA
C                                   COUNTING THE FIRST ONE TWICE
C   37-42     F6.0   DUM---SWITCH--IF NONZERO, THIS LAMINA HAS THE SAME
C                                   VERTICE COORDINATES AS PREVIOUS LAMINA
C
C
C    THE VERTICE COORDINATES FOLLOW EACH LAMINA ID CARD AND HAVE THE
C                                   FOLLOWING FORMAT
C
C COLUMNS  FORMAT   ITEM
C
C    1-12    F12.0   X(M,I)
C   13-24    F12.0   Y(M,I)
C   25-36    F12.0   X(M,I)
C   37-48    F12.0   Y(M,I)
C   49-60    F12.0   X(M,I)
C   61-72    F12.0   Y(M,I)
C
C
      DIMENSION FX(700),FY(7 0),FZ(700),III(100),RHO(100),ZEE(100),MID(1
```

```
     *00),V(200),DEL(200),DELP(200), X(020, 20),Y(020,020),SIGMA(200),GG
     *(200),PREV(625),ANOM(625),SUM(625),        FFX(700),FFY(700),FFZ(70
     *0),FZ(700),DZ(700),V (200),ZZEE(200)
      COMMON/E/K,M,FX,FY,FZ, ,Y,III,PREV,ANOM,Z,AUX,SFELZ,ALPH1,BETA1,
     *DELTA1,GAMM1,SIGA,FFX,FFY,FFZ,ZEE,ZZEE,SPACE,RHO
      INTEGER AUX,SLIDOU
   10 READ( 5,20, END=1480)XMIN,YMIN,FPZ,DELTA1,SCLEM,SCLEG,VERT1,VERT2,
     * FZR
   20 FORMAT(2F8.0,4F6.0,2F1 .0,I2)
  400 FORMAT(6(5X,F12.5))
C     IF(EOF(60))1480,30
      WRITE(6 ,230)
   30 WRITE(6 ,40) XMIN,YMIN FPZ,DELTA1,SCLEM,SCLEG,VERT1,VERT2
    1 ,FZR
   40 FORMAT(15X,'XMIN =',F1 .2,18X,'YMIN =',F10.2,18X,'FPZ =',F8.2,//,1
     *5X,'DELTA1 =',F8.2,18X 'SCALEFM =',F10.5,15X,'SCALEFG =',F10.5,//,
     *15X,'CONVERT1 =',F15.11,9X,'CONVERT2 =',F15.11,9X,'FZR =',I2,//)
      READ( 5,50)  SLIDOU ,FPOUT,VMFLD,DELTK,PUNG,PUNM
   50 FORMAT (2I2,2F10.0,2I2
      WRITE( 6,60)  SLIDOU ,FPOUT,VMFLD,DELTK,PUNG,PUNM
   60 FORMAT(15X,'SOLIDOUT =',I2,3X,'FPOUT =',I2,3X,'VMFLD =',F10.4,3X,'
     *DELTAK =',F10.5,3X,'PUNCHG =',I2,3X,'PUNCHM =',I2,//)
      NK1 = 1
      NK2 = 625
      K1 = 1
      K2 = 25
      XMIN1 = XMIN
      IF(FZR) 70,110,70
   70 DO 90 I = 1,25
      DO 80 K = K1,K2
      FX(K) = XMIN
      FY(K) = YMIN
      XMIN = XMIN + DELTA1
      A=0.0
   80 CONTINUE
      XMIN = XMIN1
      K1 = K1 + 25
      K2 = K2 + 25
      YMIN = YMIN + DELTA1
   90 CONTINUE
      READ( 5,100) (FZ(K), K = NK1,NK2)
  100 FORMAT(6(F12.7))
  110 DO 130 I = 1,25
      DO 120 K = K1,K2
      FX(K) = XMIN
      FY(K) = YMIN
      FZ(K) = FPZ
      XMIN = XMIN + DELTA1
      A=0.0
  120 CONTINUE
      XMIN = XMIN1
      K1 = K1 + 25
      K2 = K2 + 25
      YMIN = YMIN + DELTA1
  130 CONTINUE
      IF(FPOUT) 140,160,140
  140 WRITE(6 ,150)
```

```
150 FORMAT(//45H          FX( )               FY(K)               FZ(K)          /)
160 DO 200 K = NK1,NK2
    IF(FPOUT) 170,190,170
170 WRITE(6 ,180) FX(K),FY K),FZ(K)
180 FORMAT(3F15.7)
190 FFX(K) = FX(K)
    FFY(K) = FY(K)
    FFZ(K) = FZ(K)
    FX(K) = FX(K)*VERT1
    FY(K) = FY(K)*VERT1
200 FZ(K) = FZ(K)*VERT2
    NK1 = 1
    NK2 = 625
    DO 210 K= NK1,NK2
    SUM(K) = 0
210 FREV(K) = 0
220 READ( 5,250, END=1480)
230 FORMAT(1H1)
C   IF(EOF(60))1480,240
240 WRITE(6 ,250)
250 FORMAT(72H
   *                    )
260 READ( 5,270) KK,MQ,J,A X,U,ZU,VU,T,ZT,VT,GGG
270 FORMAT(2I3,I1,2I2,2F12 0,I2,2F12.0,I2)
    WRITE(6 ,280) KK,MQ,J, UX,U,ZU,VU,T,ZT,VT,GGG
280 FORMAT(//,5X,'KK =',I3 13X,'MQ =',I3,13X,'J =',I3,16X,'AUX =',I2,1
   *3X,'U =',I2,//,5X,'ZU =',F12.6,4X,'VU =',F12.6,4X,'T =',I2,15X,'ZT
   * ='F12.6,4X,'VT =',F12 6,//,5X,'GGG =',I2,//)
    ZZU = ZU
    ZZT = ZT
    ZU = ZU*VERT2
    ZT = ZT*VERT2
290 MM=MQ+1
300 DO420 M=2,MM
    WRITE(6 ,310)
310 FORMAT(////90H  MID(M) RHO(M)                ZEE(M)       III(M)    DUM
   *                                                      /)
    READ( 5,320) MID(M),RHO(M),ZEE(M),III(M),DUM
320 FORMAT(     I2,F10.0,F1 .0,I6,F6.0)
    WRITE(6 ,330) MID(M),RHO(M),ZEE(M),III(M),DUM
330 FORMAT(        I5,F10.4, 16.8,I8,F10.2,//)
    ZEE(M) = ZEE(M)*VERT2
    II=III(M)
    MUM= M-1
    IF(DUM)340,370,340
340 IF(M-2)350,370,350
350 DO 360 I=1,II
    X(M,I)  =  X(MUM,I)
360 Y(M,I)  =  Y(MUM,I)
    GOTO420
370 READ( 5,380) (X(M,I),Y M,I), I = 1,II)
380 FORMAT(6(F12.0))
    WRITE(6 ,390)
390 FORMAT(37X,'X AND Y COORDINATES OF LAMINAE',/,7X,'X(M,I)',11X,'Y(M
   *,I)',11X,'X(M,I)',11X,'Y(M,I)',11X,'X(M,I)',11X,'Y(M,I)',/)
    WRITE(6 ,400) (X(M,I), (M,I), I = 1,II)
    DO 410 I=1,II
```

```
      X(M,I) = X(M,I)*VERT1
  410 Y(M,I) = Y(M,I)*VERT1
  420 CONTINUE
  430 IF(U)440,450,440
  440 MO=1
      ZEE(1)=ZU
      V(1)=VU
      GOTO 460
  450 MO=2
  460 IF(T)470,480,470
  470 MP=MM+1
      ZEE(MP)=ZT
      V(MP)=VT
      GOTO 490
  480 MP=MM
  490 NGO=MP-MO+1
      MES=MM+2
      NGG=NGO-2
  500 IF( SLIDOU ) 510,540,510
  510 WRITE(6 ,520)
  520 FORMAT(72H1                    FIELD  POINT  COORDINATES
     *                                                    /)
      WRITE(6 ,530)
  530 FORMAT(100H    LAMINA           X                Y                Z
     *   SOLID ANGLE                                   //)
  540 DO 870 K = NK1,NK2
  550 DO630 M=2,MM
      SIGA = 0
      SFELZ = 0
  560 IF(AUX)570,590,570
  570 WRITE(6 ,580) MID(M),  II(M), ZEE(M), RHO(M)
  580 FORMAT (1H ///I2,12H   VERTICES=I2,9H   DEPTH=F7.2,11H   DENSITY=F
     *5.2//10H   I     X(I)      Y(I)      X(I+1)      Y(I+1)
     *  B           C            D          PARFEZ      //1H )
  590 SPACE = 10.0
      CALL SLDAN
      SIGMA(M)=SIGA
      IF ( SLIDOU ) 600,620,600
  600 WRITE(6 ,610) MID(M),  FX(K), FFY(K), FFZ(K), SFELZ
  610 FORMAT(I8,3F15.7,F15.6)
  620 V(M) = 6.67*RHO(M)*SFELZ
  630 CONTINUE
  640 IF( SLIDOU ) 650,670,650
  650 WRITE(6 ,660)
  660 FORMAT(1H0)
  670 IF(U) 680,690,680
  680 MO=1
      MID(1)=0
      III(1)=1
      ZEE(1)=ZU
      RHO(1)=RHO(2)
      SIGMA(1)=0.
      V(1)=VU
      GO TO 700
  690 MO=2
  700 IF(T)710,720,710
  710 MP =MM+1
```

```
      MID(MP)=MID(MM)+1
      III(MP)=1
      ZEE(MP)=ZT
      RHO(MP)=RHO(MM)
      SIGMA(MP)=0.
      V(MP)=VT
      GO TO 730
  720 MP=MM
  730 DEL(MO)=0.
      DELP(MO)=0.
      DELP(MO+1)=0.
      DEL(MP)=0.
      ANOM(K)=0
      MN=MP-2
      IF (MO.GE.3) GO TO 760
  740 DO 750 M=2,MM,2
      CVERT    = (DELTK *VWF D)/(6.67*RHO(M))
      SUM(K) = (V(M) - V(M+1.)*  CVERT  + SUM(K)
  750 CONTINUE
  760 DO 770 M = MO,MN
      DEL(M+1) =       (V(M) ((ZEE(M) -ZEE(M+1))/ (ZEE(M) - ZEE(M+2))) *
     *(3.0 * ZEE(M+2) - 2. * ZEE(M) - ZEE(M+1)) + V(M+1) * ((ZEE(M) - ZE
     *E(M+1))/(ZEE(M+1) - ZE (M+2))) * (3. * ZEE(M+2) - 2. * ZEE(M+1) -
     *ZEE(M)) + V(M+2) * ((Z E(M) - ZEE(M+1)) ** 3  )/(( ZEE(M+1) - ZEE
     *(M+2)) * (ZEE(M) - ZEE M+2))))/6.0
      DELP(M+2) =       (V(M, * ((ZEE(M+1) - ZEE(M+2)) ** 3  ) / ((ZEE(M
     *) - ZEE(M+1)) * ( ZEE(    ) - ZEE(M+2)))+ V(M+1) * ((ZEE(M+1) - ZEE
     *(M+2)) / (ZEE(M) - ZEE.M+1))) * ( ZEE(M+2) + 2. *ZEE(M+1) - 3.*ZEE
     *(M)) + V(M+2) * ((ZEE( +1) - ZEE(M+2)) / (ZEE(M) - ZEE(M+2)))* (ZE
     *E(M+1) + 2. * ZEE(M+2) - 3. * ZEE(M)))/6.0
  770 CONTINUE
      ANOM(K)=0.5*(DEL(MO+1) DELP(MP))
      DO780M=MO,MP
      ANOM(K)=ANOM(K)+0.5*(D L(M)+DELP(M))
      GG(M)=ANOM(K)-0.5*DELP MP)
  780 CONTINUE
      GG(MO)=0.0
      GG(MO+1)=0.0
      GG(MP)=GG(MP)+0.5*DELP MP)
  790 PREV(K)=PREV(K)+ANOM(K
  800 IF(GGG) 810,830,810
  810 WRITE(6 ,820) (GG(M),  =MO,MP)
  820 FORMAT(1H 9E12.4)
  830 LIM = MQ-1
      IF(MQ.LE.2) GO TO 870
      DO 840 M = 2, LIM
      MAD = M+1
      ZZEE(M) = ZEE(MAD) - 0 00030486096
  840 CONTINUE
      ZZEE(MQ) = ZEE(MM)
      DO 850 M = 2,MQ
      SIGA = 0
      SEELZ = 0
      SPACE = 20.0
      CALL SLDAN
      SIGMA(M) = SIGA
      VN(M) = 6.67*RHO(M)*SF LZ
```

```
  850 CONTINUE
C       SUM(K) = 0
        DO 860 M = 2, MJ
        CVERT    = (DELTK *VMF_D)/(6.67*RHO(M))
        SUM(K) = (V(M) - U(M)) *  CVERT  + SUM(K)
  860 CONTINUE
  870 CONTINUE
  880 IF(J)220,890,220
  890 IF(PULM)    900,930,900
  900 WRITE(7,250)
      WRITE(7,910)
  910 FORMAT(3X,'VALUES OF T E MAGNETIC ANOMALY',/)
      WRITE(7,920) (SUM(K), K=1,625)
  920 FORMAT(17X,F7.2)
  930 NK1=1
      NK2=25
      WRITE(6 ,1270)
      WRITE(6 ,940)
  940 FORMAT(72H                          VALUES FOR THE MAGNETIC MAP BEFORE RO
     *UNDOFF                                                   //)
      M1 = 1
      M2 = 25
      DO 980 J = 1,25
      WRITE(6 ,950) J
  950 FORMAT(3X,'ROW ON MAP   ',I3,/)
      WRITE(6 ,960) (SUM(K), K = M1, M2)
  960 FORMAT(5(E15.7,4X))
      WRITE ( 6,970)
  970 FORMAT(1H0)
      M1 = M1 + 25
      M2 = M2 + 25
      DZR(J) = 0.0
  980 CONTINUE
      WRITE(6 ,990)
  990 FORMAT(1H1)
      WRITE(6 ,250)
      WRITE(6 ,1260) MG,ZZU,ZT,VMFLD,DELTK
      WRITE(6 ,1000)
 1000 FORMAT(1X,'LAMINA    DE SITY', /)
      DO 1020 M = 2,MM
      WRITE(6 ,1010) MI(M), RHO(M)
 1010 FORMAT(3X, I3,F10.4)
 1020 CONTINUE
      WRITE(6 ,1030)
 1030 FORMAT(100H                                         VERTICAL  MAGNETIC
     *FIELD  IN  GAMMAS                                                   /)
      WRITE(6 ,1040) SCLFM
 1040 FORMAT(30X,'OUTPUT HAS BEEN MULTIPLIED BY SCALE FACTOR = ',F10.5,/
     *         )
      IF(   VERT1 .GT. 1.5 . ND.    VERT1 .LT. 2.0) GO TO 1050
      IF(   VERT1 .GT. 0.000  .AND.     VERT1.LT. 0.0004) GO TO 1070
      IF(   VERT1 .GT. 0.000  .AND.     VERT1 .LT. 0.0012) GO TO 1090
      IF(   VERT1 .GT. 0.9 . ND.    VERT1 .LT. 1.1) GO TO 1110
      GO TO 1130
 1050 WRITE(6 ,1060)
 1060 FORMAT(35X,'THIS MAP H S THE X AND Y DIMENSIONS OF MILES',//)
      GO TO 1130
```

```
1070 WRITE(6 ,1080)
1080 FORMAT(35X,'THIS MAP H S THE X AND Y DIMENSIONS OF FEET',//)
     GO TO 1130
1090 WRITE(6 ,1100)
1100 FORMAT(35X,'THIS MAP H S THE X AND Y DIMENSIONS OF METERS',//)
     GO TO 1130
1110 WRITE(6 ,1120)
1120 FORMAT(35X,'THIS MAP H S THE X AND Y DIMENSIONS OF KILOMETERS',//)
1130 DO 1140 K= 1,625
     SUM(K) = SUM(K)*SCLFM
1140 CONTINUE
     I = 0
1150 I = I + 25
     WRITE ( 6,1440)
     WRITE(6 ,1160) (SUM(K)  K = NK1,NK2)
1160 FORMAT(2X,25(F4.0,1X)/)
     NK1=NK1+25
     NK2=NK2+25
     IF(NK1 - 625)1150,1170 1170
1170 WRITE(6 ,1180) (FFX(I)  I = 1, 25, 2)
1180 FORMAT(/,1X,F6.1,2X,12 F8.1,2X))
     GO TO 1190
1190 NK1=1
     NK2=25
     IF (PHNG)    1200,1220,1200
1200 WRITE(7,250)
     WRITE(7,1210)
1210 FORMAT(3X,'VALUES OF T E GRAVITATIONAL ANOMALY',/)
     WRITE(7,920) (PREV(K), K=1,625)
1220 WRITE(6 ,1230)
1230 FORMAT(72H1                          VALUES FOR GRAVITY MAP BEFORE ROUNDO
    *FF                                                                   //)
     L1 = 1
     L2 = 25
     DO 1260 J = 1,25
     WRITE(6 ,950) J
     WRITE(6 ,1240) (PREV(K , K = L1, L2)
1240 FORMAT(5(E15.7,4X))
     WRITE(6 ,1250)
1250 FORMAT(1H0)
     L1 = L1 + 25
     L2 = L2 + 25
     BZD(J) = 0.0
1260 CONTINUE
1270 FORMAT(1H1)
     WRITE (6 ,1270)
     WRITE(6 ,250)
     WRITE(6 ,1280) MG,ZZU,-ZT,VMFLD,DELTK
1280 FORMAT(1H0,4X,'NUMBER  F LAMINAE =', I3,/,5X,'DEPTH TO TOP OF BODY
    * =',F12.6,/,5X,'DEPTH  O BOTTOM OF BODY =',F12.6,/,5X,'VERTICAL MA
    *GNETIC INTENSITY =',F1 .4,/,5X,'SUSCEPTIBILITY CONTRAST =',F10.4,
    *    /  )
     WRITE(6 ,1000)
     DO 1290 M = 2,MM
     WRITE(6 ,1010) MID(M), RHO(M)
1290 CONTINUE
     WRITE(6 ,1300)
```

```
1300 FORMAT(100H                                              VERTICAL  GRAVITY
    *MAP  IN  MILLIGALS                                                      /)
     WRITE(6 ,1310)  SCLFG
1310 FORMAT(30X,'OUTPUT HAS BEEN MULTIPLIED BY SCALE FACTOR = ',F10.5,/
    *            )
     IF(   VERT1 .GT. 1.5 . ND.    VERT1 .LT. 2.0) GO TO 1320
     IF(   VERT1 .GT. 0.000  .AND.    VERT1.LT. 0.0004) GO TO 1340
     IF(   VERT1 .GT. 0.000  .AND.    VERT1 .LT. 0.0012) GO TO 1360
     IF(   VERT1 .GT. 0.9 . ND.    VERT1 .LT. 1.1) GO TO 1380
     GO TO 1400
1320 WRITE(6 ,1330)
1330 FORMAT(35X,'THIS MAP H S THE X AND Y DIMENSIONS OF MILES',//)
     GO TO 1400
1340 WRITE(6 ,1350)
1350 FORMAT(35X,'THIS MAP H S THE X AND Y DIMENSIONS OF FEET',//)
     GO TO 1400
1360 WRITE(6 ,1370)
1370 FORMAT(35X,'THIS MAP H S THE X AND Y DIMENSIONS OF METERS',//)
     WRITE (6 ,1270)
     GO TO 1400
1380 WRITE(6 ,1390)
1390 FORMAT(35X,'THIS MAP H S THE X AND Y DIMENSIONS OF KILOMETERS',//)
1400 DO 1410 K = 1,625
     PREV(K) = PREV(K)*SCLF
1410 CONTINUE
     I = 0
1420 I = I + 25
     WRITE (6 ,1440)
1430 WRITE (6 ,1450),(PREV( ),K= NK1,NK2)
     NK1=NK1+25
     NK2=NK2+25
1440 FORMAT(4X,24(1H*,4X),1 *,2X)
1450 FORMAT(2X,25(F4.0,1X)/
     IF(NK1-625)1420,1460,1 60
1460 WRITE(6 ,1470) (FFX(I)  I = 1,25,2)
1470 FORMAT(/,1X,F6.1,2X,12 F6.1,2X),//////////)
     GO TO 10
1480 CALL EXIT
     SUBROUTINE SLDAN
     DIMENSION FX(700),FY(7 0),FZ(700),III(100),RHO(100),ZEE(100),MIU(1
    *00),W(200),DEL(200),DEP(200), X(020, 20),Y(020,020),SIGMA(200),GG
    *(200),PREV(625),ANOM(6 5),SUM(625),      FFX(700),FFY(700),FFZ(70
    *0),BZD(700),DZB(700),V (200),ZZEE(200)
     INTEGER AUX
     COMMON/E/K,M,FX,FY,FZ, ,Y,III,PREV,ANOM,Z,AUX,SEELZ,ALPH1,BETA1,
    *DELTA1,GAMM1,SIGA,FFX, FY,FFZ,ZEE,ZZEE,SPACE,RHO
     IF(SPACE .EQ. 10  ) GO TO 2000
     IF(SPACE .EQ. 20.0) GO TO 2010
2000 Z = ZEE(M) - FZ(K)
     GO TO 2020
2010 Z = ZZEE(M) - FZ(K)
2020 ALPH1 = X(M,1) - FX(K)
     BETA1 = Y(M,1) - FY(K)
     R1 = SQRT (ALPH1 ** 2   BETA1 ** 2)
     IF (R1) 2030,2040,2030
2030 GAMM1 = ALPH1 / R1
     DELT1 = BETA1 / R1
```

```
2040 II = III(M)
     DO 2420 I = 2, II
     ALPH2 = X(M,I) -FX(K)
     BETA2 = Y(M,I) - FY(K)
     R2 = SQRT  (ALPH2 **2  + BETA2 ** 2 )
     IF (R2) 2050, 2340, 20 0
2050 GAMM2 = ALPH2 /R2
     DELT2 = BETA2 / R2
2060 IF (R1) 2070, 2340, 20 0
2070 SS=SQRT ((ALPH1-ALPH2) *2 +(BETA1-BETA2)**2 )
     EGA=(ALPH1-ALPH2)/SS
     TAU=(BETA1-BETA2)/SS
     P = TAU * ALPH1 -    EG   * BETA1
     IF(ABS (P)-.00001)2340 2340,2080
2080 IF(P)2090,2340,2100
2090 S = -1.
     GO TO 2110
2100 S = 1.
2110 EMM = BETA1 * ALPH2 - BETA2 * ALPH1
2120 IF (EMM) 2130, 2340, 2140
2130 W = -1.
     GO TO 2150
2140 W = 1.
2150 IF(Z)2160,2170,2160
2160 PSI=S*(Z/SQRT (P**2+Z* 2))
2170 AA=GAMM1*GAMM2+DELT1*D LT2
     EPS = 1.E-10
     DELA = ABS (AA)-1.
     IF(DELA .GT. 0. .AND.  ELA .LE. EPS)  AA= 1.
     IF (AA) 2190, 2180, 22 0
2180 A = W*  1.570796327
     GO TO 2210
2190 A = W * (ATAN ((SQRT (1. - AA ** 2 )) / AA) + 3.141592654)
     GO TO 2210
2200 A = W * ATAN ((SQRT (1. - AA ** 2 )) / AA)
2210 IF(Z)2230,2220,2230
2220 B=0
     C=0
     GO TO 2330
2230 BB=(PSI*(EGA*GAMM1+TAU DELT1))
     IF (BB - 1.) 2250, 224 , 2250
2240 B = 1.570796327
     GO TO 2280
2250 IF ( BB + 1.) 2270,226 ,2270
2260 B = -1.570796327
     GO TO 2280
2270 B = ATAN (BB/(SQRT (1. - BB ** 2 )))
2280 CC =    (PSI * (   EGA * GAMM2 + TAU * DELT2 ))
     IF (CC - 1.) 2300,2290,2300
2290 C = 1.570796327
     GO TO 2330
2300 IF(CC + 1.) 2320,2310,2320
2310 C=-1.570796327
     GO TO 2330
2320 C=ATAN (CC/(SQRT (1.-C **2 )))
2330 D=C-B
     FELZ=A+D
```

```
      GO TO 2350
 2340 FELZ=0
      A=0
      B=0
      C=0
      D=0
 2350 IF(AUX)2360,2400,2360
 2360 PARFEZ=  6.67*RHO(M)*F LZ
 2370 DOG = ALPH1+FX(K)
      DOGS = BETA1+FY(K)
      DOGG=ALPH2+FX(K)
      DOGGS=BETA2+FY(K)
      IRMA=I-1
C     WRITE(6 ,2390) IRMA,DO  ,DOGS,DOGG,DOGGS, A,B,C,D,PARFEZ
C     WRITE(6 ,2380) SS,TAU, GA,P
 2380 FORMAT(4E18.7)
 2390 FORMAT(1H ,I2,3F . 2,F1  .2,4E12.7,F12.6)
 2400 SFELZ=SFELZ+FELZ
      SIGA=SIGA+A
 2410 ALPH1=ALPH2
      BETA1=BETA2
      GAMM1=GAMM2
      DELT1=DELT2
      R1=R2
 2420 CONTINUE
 2430 IF(SIGA)2440,2570,2460
 2440 IF(SIGA+.00001)2470,2450,2450
 2450 SFELZ=SFELZ-SIGA
      GOTO2570
 2460 IF(SIGA-.00001)2450,2450,2520
 2470 IF(SIGA+6.2831754)2510 2510,2480
 2480 IF(SIGA+3.1416027)2570 2500,2490
 2490 IF(SIGA+3.1415827)2500 2500,2570
 2500 SFELZ=SFELZ-SIGA-3.141 927
      GOTO 2570
 2510 SFELZ=SFELZ-SIGA-6.2831854
      GOTO2570
 2520 IF(SIGA-6.2831754)2530 2560,2560
 2530 IF(SIGA-3.1415827)2570 2550,2540
 2540 IF(SIGA-3.1416027)2550 2550,2570
 2550 SFELZ=SFELZ-SIGA+3.141 927
      GOTO 2570
 2560 SFELZ=SFELZ-SIGA+6.283 854
 2570 RETURN
      END
```

```
C
C      ****************************************************************
C                THIS PROGRAM FOLLOWS HENDERSONS ONCE-AND-FOR ALL
C                TECHNIQUE FOR UPWARD AND DOWNWARD CONTINUATION AND
C                FIRST AND SECOND DERIVATIVES.
C                THIS PROGRAM HAS BEEN REVISED FOR USING FTN ON THE CDC
C                6600 SERIES COMPUTER.  THE OUTPUT MAPS ARE NOT 40X40 BUT
C                ARE THE SIZE OF THE INPUT DATA ARRAY.   THE MAXIMUM IS
C                A 40X40 OUTPUT MAP.
C      ****************************************************************
C
C                THESE DIMENSION STATEMENTS PRESUME A MAXIMUM MAP
C                ARRAY OF 40 X 40 .
C      ****************************************************************
C
C
C
       DIMENSION HEAD(10)
       DIMENSION ISLECT(20), C(11,19), P(80,80), R(30,30,11)
       DIMENSION OUTLEV(19)
       DOUBLE PRECISION OUTLEV, HEAD
       COMMON P
        DATA OUTLEV(16)/ 8HSECOND   /
       DATA(OUTLEV(L),L=1,10)/10HUPWARD  1  ,10HUPWARD  2  ,10HUPWARD
      13  ,10HUPWARD  4  ,10HUPWARD  5  ,10HDOWNWARD 1 ,10HDOWNWARD 2
      2 , 10HDOWNWARD 3  , 10HDOWNWARD 4  , 10HDOWNWARD 5  /
       DATA OUTLEV(11)/ 8HFIRST    /
       DATA(OUTLEV(L),L=12,15)/6HDOWN 1,6HDOWN 2,6HDOWN 3,6HDOWN 4/
       DATA(OUTLEV(L),L=17,19)/6HDOWN 1,6HDOWN 2,6HDOWN 3/
C
C      ****************************************************************
C             READ IN HEAD CARD.  READ IN ISLECT CARD WHICH CONTAINS
C          T HE CODED LIST OF THE MAPS DESIRED
C      ****************************************************************
C
       READ 1, (HEAD(I), I=1,10)
     1 FORMAT (10A8)
       READ 2, ( ISLECT(L), L=1,19)
     2 FORMAT (19I1)
C
C      ****************************************************************
C                READ IN MAXIMUM VALUE OF I(=IMAX). I BEGINS AT 26 AND
C                IMAX MUST BE 65 OR LESS. SIMILARLY FOR JMAX. READ IN
C                ON SAME CARD THE VALUE (BASE) TO BE SUBTRACTED FROM
C                MAP VALUES P(I,J)
C      ****************************************************************
C
       READ 3, IMAX, JMAX, BASE
     3 FORMAT (2I,F)
C
C      ****************************************************************
C                READ IN P(I,J) DATA, SUBTRACT BASE, PRINT HEADING
C                AND PLOT ON MAP TYPE OUTPUT.
C                MAP IS PRINTED FROM P(26,26) TO P(IMAX,JMAX).   THE ALGO
C                RITHM IS SUCH THAT EACH SECTION OF THE MAP IS PRINTED
C                BETWEEN THE LIMITS OF J = 26,JMAX AND I = IMINI, IMXT.
C                IMINI IS NOT ALLOWED TO BE GREATED THAN IMAX.
C      ****************************************************************
C
       READ 4, ((P(I,J), I=26, IMAX), J=26, JMAX)
     4 FORMAT (F)
```

```
      DO 6 I=26, IMAX
      DO 5 J = 26, JMAX
    5 P(I,J)=P(I,J)-BASE
    6 CONTINUE
      PRINT 11
      PRINT 101, (HEAD(I) , I=1,10)
  101 FORMAT(20X,10A8/)
      PRINT 8, BASE
    8 FORMAT(/20X,'INPUT DATA LESS BASE OF  'F6.2//)
      DO 9 J=26,JMAX
    9 PRINT 10,(P(I,J), I=26,35)
   10 FORMAT  ((1X,10F10.2/10(9X,1H*)////))
      PRINT 11
   11 FORMAT (1H1)
      DO 12 IMAXI=45,65,10
      IMINI = IMAXI-10
      IF(IMAX.LE. IMINI)  GO TO 1620
      IF(IMAX.LT.IMAXI) 1500,1600
 1500 DO 1520 J = 26, JMAX
      IMAXX = IMAX + 1
      DO 1510 I = IMAXX, IMAXI
 1510 P(I,J) = -999999.99
 1520 CONTINUE
      IMXI = IMAXI
      GO TO 1610
 1600 IMXI= IMAXI
 1610 PRINT 101, (HEAD(I), I=1,10)
      PRINT 8, BASE
      DO 113 J= 26,JMAX
  113 PRINT 13, (P(I,J), I= IMINI,IMXI)
      PRINT 11
   12 CONTINUE
C
C     ****************************************************************
C               NEXT SECTION PREPARES REGIONS BEYOND EDGE OF MAP TO
C               BE USED IN ANALYSIS. APPROACH IS TO FILL THE SURROUNDING
C               SPACE BY EXTENDING EACH EDGE VALUE NORMAL TO THE MAP
C               FOR 25 UNITS.
C     ****************************************************************
C
 1620 IMAX1 = IMAX + 1
      IMAX25 = IMAX + 25
      JMAX1 = JMAX + 1
      JMAX25 = JMAX + 25
      DO 14 J=26,JMAX
      DO 15 I=1,25
   15 P(I,J)=P(26,J)
      DO 16 I = IMAX1, IMAX25
   16 P(I,J)=P(IMAX,J)
   14 CONTINUE
C
C
      DO 17 I=26,IMAX
      DO 18 J=1,25
   18 P(I,J)=P(I,26)
      DO 19 J = JMAX1, JMAX25
   19 P(I,J)=P(I,JMAX)
   17 CONTINUE
C
C
```

```
      DO 20 I=1,25
      DO 21 J=1,25
   21 P(I,J)=P(26,26)
   20 CONTINUE
C
C
      DO 22 I = IMAX1, IMAX25
      DO 23 J=1,25
   23 P(I,J)=P(IMAX,26)
   22 CONTINUE
C
C
      DO 24 I=1,25
      DO 25 J = JMAX1, JMAX25
   25 P(I,J)=P(26,JMAX)
   24 CONTINUE
C
C
      DO 26 I = IMAX1,IMAX25
      DO 27  J = JMAX1, JMAX25
   27 P(I,J)=P(IMAX,JMAX)
   26 CONTINUE
C
C     ****************************************************************
C                CALCULATION OF AVERAGE VALUE OF DATA ON RINGS CENTERED
C                AT EACH MAP POINT. CALL THESE R (I,J,K), WHERE
C                K=1 TO 11
C     ****************************************************************
C
      M=0
      DO 28 I=26,IMAX
      M=M+1
      N=0
      DO 29 J=26,JMAX
      N=N+1
      R(M,N,1)=P(I,J)
      R(M,N,2)=(P(I,J+1)+P(I,J-1)+P(I+1,J)+P(I-1,J))/4.0
      R(M,N,3)=(P(I+1,J+1)+P(I+1,J-1)+P(I-1,J+1)+P(I-1,J-1))/4.0
      R(M,N,4)=(P(I+2,J+1)+P(I+2,J-1)+P(I-2,J+1)+P(I-2,J-1)
     1+P(I+1,J+2)+P(I+1,J-2)+P(I-1,J+2)+P(I-1,J-2))/8.0
      R(M,N,5)=(P(I+2,J+2)+P(I+2,J-2)+P(I-2,J+2)+P(I-2,J-2))/4.0
       R(M,N,6)=(P(I+2,J+3)  +P(I+2,J-3)+P(I-2,J+3)+P(I-2,J-3)
     1+P(I+3,J+2)+P(I+3,J-2)+P(I-3,J+2)+P(I-3,J-2))/8.0
       R(M,N,7)=(P(I+5,J)+P(I-5,J)+P(I,J+5)+P(I,J-5)
     1+P(I+3,J+4)+P(I+3,J-4)+P(I+4,J+3)+P(I+4,J-3)
     2+P(I-3,J+4)+P(I-4,J+3)+P(I-3,J-4)+P(I-4,J-3))/12.0
       R(M,N,8)=(P(I+7,J+1)+P(I+1,J+7)+P(I+7,J-1)+P(I+1,J-7)
     1+P(I-7,J+1)+P(I-1,J+7)+P(I-7,J-1)+P(I-1,J-7)
     2+P(I+5,J+5)+P(I+5,J-5)+P(I-5,J+5)+P(I-5,J-5))/12.0
       R(M,N,9)=(P(I+10,J+6)+P(I+6,J+10)+P(I+10,J-6)+P(I+6,J-10)
     1+P(I-10,J+6)+P(I-6,J+10)+P(I-10,J-6)+P(I-6,J-10))/8.0
       R(M,N,10)=(P(I+7,J+15)+P(I+15,J+7)+P(I-7,J+15)+P(I-15,J+7)
     1+P(I+7,J-15)+P(I+15,J-7)+P(I-7,J-15)+P(I-15,J-7))/8.0
      R(M,N,11)=(P(I,J+25)+P(I,J-25)+P(I-20,J+15)+P(I-15,J+20)  +
     1P(I-20,J-15)+P(I-15,J-15)+P(I+20,J+15)+P(I+15,J+20)
     2+P(I+20,J-15)+P(I+15,J-20)+P(I+25,J)+P(I-25,J))/12.0
   29 CONTINUE
   28 CONTINUE
C
C     ****************************************************************
```

```
C                FOR EACH MAP THERE IS A SET OF COEFFICIENTS C(K,L),
C                WHERE K IS THE RING NOS AND L IS THE CODED INTEGER
C                FOR THE DESIRED MAP.
C          ****************************************************************
C
C                BEGIN FIRST WITH UPWARD CONTINUATION 1 COEFFICIENTS.
C                CODE L=1
C          ****************************************************************
C
           C(1,1)=.11193
           C(2,1)=.32193
           C(3,1)=.06062
           C(4,1)=.15206
           C(5,1)=.05335
           C(6,1)=.06586
           C(7,1)=.06650
           C(8,1)=.05635
           C(9,1)=.03855
           C(10,1)=.02273
           C(11,1)=.03015
C
C          ****************************************************************
C                COEFFICIENTS FOR UPWARD CONTINUATION 2. CODE L=2
C          ****************************************************************
C
           C(1,2)=.04034
           C(2,2)=.12988
           C(3,2)=.07588
           C(4,2)=.14559
           C(5,2)=.07651
           C(6,2)=.09902
           C(7,2)=.11100
           C(8,2)=.10351
           C(9,2)=.07379
           C(10,2)=.04464
           C(11,2)=.05998
C
C          ****************************************************************
C                COEFFICIENTS FOR UPWARD CONTINUATION 3. CODE L=3
C          ****************************************************************
C
           C(1,3)=.01961
           C(2,3)=.06592
           C(3,3)=.05260
           C(4,3)=.10563
           C(5,3)=.07146
           C(6,3)=.10226
           C(7,3)=.12921
           C(8,3)=.13635
           C(9,3)=.10322
           C(10,3)=.06500
           C(11,3)=.08917
C
C          ****************************************************************
C                COEFFICIENTS FOR UPWARD CONTINUATION 4. CODE L=4
C          ****************************************************************
C
           C(1,4)=.01141
           C(2,4)=.03938
           C(3,4)=.03566
```

```
      C(4,4)=.07450
      C(5,4)=.05841
      C(6,4)=.09173
      C(7,4)=.12915
      C(8,4)=.15474
      C(9,4)=.12565
      C(10,4)=.08323
      C(11,4)=.11744
C
C     ****************************************************************
C               COEFFICIENTS FOR UPWARD CONTINUATION 5. CODE L=5
C     ****************************************************************
C
      C(1,5)=.00742
      C(2,5)=.02566
      C(3,5)=.02509
      C(4,5)=.05377
      C(5,5)=.04611
      C(6,5)=.07784
      C(7,5)=.11986
      C(8,5)=.16159
      C(9,5)=.14106
      C(10,5)=.09897
      C(11,5)=.14458
C
C     ****************************************************************
C               COEFFICIENTS FOR DOWNWARD CONTINUATION 1. CODE L=6
C     ****************************************************************
C
      C(1,6)= 4.8948
      C(2,6)=-3.0113
      C(3,6)= 0.0081
      C(4,6)=-0.5604
      C(5,6)=-0.0376
      C(6,6)=-0.0689
      C(7,6)=-0.0605
      C(8,6)=-0.0534
      C(9,6)=-0.0380
      C(10,6)=-0.0227
      C(11,6)=-0.0302
C
C     ****************************************************************
C               COEFFICIENTS FOR DOWNWARD CONTINUATION 2. CODE L=7
C     ****************************************************************
C
      C(1,7)= 16.1087
      C(2,7)=-13.2209
      C(3,7)=  0.4027
      C(4,7)=-01.9459
      C(5,7)= 00.0644
      C(6,7)=-00.0596
      C(7,7)=-00.0522
      C(8,7)=-00.0828
      C(9,7)=-00.0703
      C(10,7)=-00.0443
      C(11,7)=-00.0600
C
C     ****************************************************************
C               COEFFICIENTS FOR DOWNWARD CONTINUATION 3. CODE L=8
C     ****************************************************************
```

```
C
      C(1,8)= 41.7731
      C(2,8)=-38.2716
      C(3,8)= 01.7883
      C(4,8)=-04.7820
      C(5,8)= 00.5367
      C(6,8)= 00.1798
      C(7,8)= 00.1342
      C(8,8)=-00.0560
      C(9,8)=-00.0900
      C(10,8)=-00.0639
      C(11,8)=-00.0891
C
C     ****************************************************************
C               COEFFICIENTS FOR DOWNWARD CONTINUATION 4. CODE L=9
C     ****************************************************************
C
      C(1,9)= 92.5362
      C(2,9)=-89.7403
      C(3,9)= 05.1388
      C(4,9)=-09.9452
      C(5,9)= 01.7478
      C(6,9)= 00.8908
      C(7,9)= 00.6656
      C(8,9)= 00.0718
      C(9,9)=-00.0890
      C(10,9)=-00.0802
      C(11,9)=-00.1173
C
C     ****************************************************************
C               COEFFICIENTS FOR DOWNWARD CONTINUATION 5. CODE L=10
C     ****************************************************************
C
      C(1,10)= 183.2600
      C(2,10)=-183.9380
      C(3,10)= 011.8834
      C(4,10)=-018.6049
      C(5,10)= 004.2324
      C(6,10)= 002.4237
      C(7,10)= 001.7777
      C(8,10)= 000.3606
      C(9,10)=-000.0571
      C(10,10)=-000.0921
      C(11,10)=-000.1444
C
C     ****************************************************************
C               COEFFICIENTS FOR FIRST DERIVATIVE ON SURFACE,CODE L=11
C     ****************************************************************
C
      C(1,11)= 1.87282
      C(2,11)=-1.13625
      C(3,11)=-0.05949
      C(4,11)=-0.30210
      C(5,11)=-0.05857
      C(6,11)=-0.07597
      C(7,11)=-0.07072
      C(8,11)=-0.05758
      C(9,11)=-0.03905
      C(10,11)=-0.02286
      C(11,11)=-0.05020
```

```
C
C      ******************************************************************
C              COEFFICIENTS FOR FIRST DERIVATIVE DOWN 1. CODE L=12
C      ******************************************************************
C
       C(1,12)= 6.62394
       C(2,12)=-5.62446
       C(3,12)= 0.12727
       C(4,12)=-0.88750
       C(5,12)= 0.00361
       C(6,12)=-0.04007
       C(6,12)=-0.04856
       C(7,12)=-0.04007
       C(8,12)=-0.04575
       C(9,12)=-0.03615
       C(10,12)=-0.02233
       C(11,12)=-0.05000
C
C      ******************************************************************
C              COEFFICIENTS FOR FIRST DERIVATIVE DOWN 2. CODE L=13
C      ******************************************************************
C
       C(1,13)= 16.98074
       C(2,13)=-16.05517
       C(3,13)= 00.76135
       C(4,13)=-01.98701
       C(5,13)= 00.23820
       C(6,13)= 00.09219
       C(7,13)= 00.07475
       C(8,13)=-00.00768
       C(9,13)=-00.02726
       C(10,13)=-00.02077
       C(11,13)=-00.04934
C
C      ******************************************************************
C              COEFFICIENTS FOR FIRST DERIVATIVE DOWN 3. CODE L=14
C      ******************************************************************
C
         C(1,14)= 36.11116
       C(2,14)=-35.96237
       C(3,14)= 02.17080
       C(4,14)=-03.83054
       C(5,14)= 00.76745
       C(6,14)= 00.42646
       C(7,14)= 00.32573
       C(8,14)= 00.06859
       C(9,14)=-00.01084
       C(10,14)=-00.01812
       C(11,14)=-00.04832
C
C      ******************************************************************
C              COEFFICIENTS FOR FIRST DERIVATIVE DOWN 4. CODE L=15
C      ******************************************************************
C
       C(1,15)= 67.88049
       C(2,15)=-69.68033
       C(3,15)= 04.76651
       C(4,15)=-06.69004
       C(5,15)= 01.74330
       C(6,15)= 01.05352
```

```
      C(7,15)= 00.77613
      C(8,15)= 00.19699
      C(9,15)= 00.01469
      C(10,15)=-00.01433
      C(11,15)=-00.04693
C
C     ******************************************************************
C               COEFFICIENTS FOR 2ND DERIVATIVE ON THE SURFACE.
C               CODE L=16.
C     ******************************************************************
C
      C(1,16)= 2.82994
      C(2,16)=-2.49489
      C(3,16)= 0.05173
      C(4,16)=-0.39446
      C(5,16)= 0.00932
      C(6,16)=-.00732
      C(7,16)=.00304
      C(8,16)= 0.00219
      C(9,16)= 0.00040
      C(10,16)= 0.00004
      C(11,16)= 0.00000
C
C     ******************************************************************
C               COEFFICIENTS FOR 2ND DERIVATIVE DOWN 1. CODE L=17.
C     ******************************************************************
C
       C(1,17)= 7.08408
      C(2,17)=-6.93715
      C(3,17)= 0.36265
      C(4,17)=-0.80764
      C(5,17)= 0.13050
      C(6,17)= 0.07231
      C(7,17)= 0.06502
      C(8,17)= 0.02312
      C(9,17)= 0.00565
      C(10,17)= 0.00103
      C(11,17)= 0.00043
C
C     ******************************************************************
C               COEFFICIENTS FOR 2ND DERIVATIVE DOWN 2. CODE L=18.
C     ******************************************************************
C
      C(1,18)= 14.15751
      C(2,18)=-14.51327
      C(3,18)= 00.96018
      C(4,18)=-01.42970
      C(5,18)= 00.35907
      C(6,18)= 00.22256
      C(7,18)= 00.17330
      C(8,18)= 00.05501
      C(9,18)= 00.01239
      C(10,18)= 00.00210
      C(11,18)= 00.00085
C
C     ******************************************************************
C               COEFFICIENTS FOR 2ND DERIVATIVE DOWN 3. CODE L=19
C
C
      C(1,19)= 24.74755
```

```
      C(2,19)=-26.02351
      C(3,19)= 01.92719
      C(4,19)=-02.30269
      C(5,19)= 00.72474
      C(6,19)= 00.46253
      C(7,19)= 00.33920
      C(8,19)= 00.09995
      C(9,19)= 00.02070
      C(10,19)= 00.00322
      C(11,19)= 00.00122
C
C     ******************************************************************
C              THIS SECTION MAKES THE FINAL CALCULATIONS FOR THOSE
C              MAPS SELECTED BY THE USER IN HIS ISLECT CODE.
C     ******************************************************************
C
      DO 30 L= 1,19
      IPAGE = 0
      LEVEL=L
      IF (ISLECT(L).LT. 1) 30,31
   31 PRINT 11
   52 PRINT 101, (HEAD(I), I = 1,10)
      IPAGE = IPAGE + 1
      IF( L. LE. 10 ) GO TO 71
      IF (L. EQ. 11 ) GO TO 72
      IF ( L. LE. 15 ) GO TO 73
      IF ( L. EQ. 16 ) GO TO 72
      IF ( L. LE. 19 ) 75, 90
   71 PRINT 171, OUTLEV(L), IPAGE
      GO TO 320
   72 PRINT 172, OUTLEV(L), IPAGE
      GO TO 320
   73 PRINT 173, OUTLEV(L), IPAGE
      GO TO 320
   75 PRINT 175, OUTLEV(L), IPAGE
      GO TO 320
  171 FORMAT (20X,'MAP CONTINUED ',A10,' GRID UNIT '/20X,' SHEET NUMBER'
     1,I2/)
  172 FORMAT(20X,' MAP OF',A8,' DERIVATIVE ON SURFACE'/20X,' SHEET NUMBE
     1R ', I2/)
  173 FORMAT(20X,' MAP OF FIRST DERIVATIVE ',A6,' GRID UNIT'/20X,' SHEET
     1 NUMBER ', I2/)
  175 FORMAT(20X,'MAP OF SECOND DERIVATIVE',A6,' GRID UNIT'/20X,' SHEET
     1NUMBER ',I2/)
  320 DO 33 I = 26, IMAX
      DO 34 J=26,JMAX
      P(I,J)=0.0
      DO 35 K=1,11
   35 P(I,J)=C(K,L)*R(I-25,J-25,K)+P(I,J)
   34 CONTINUE
   33 CONTINUE
C
C    ******************************************************************
C
C     NEXT SECTION PRINTS THE VARIOUS MAPS
C       MAPS ARE PRINTED AS SURFACE MAP. SEE PREVIOUS COMMENT.
C
C    ******************************************************************
C
      DO 36 J = 26, JMAX
```

```
   36 PRINT 10, (P(I,J), I= 26,35)
   13 FORMAT ((1X,11F10.2/11(9X,1H*)////))
      PRINT 11
      DO 1020 IMAXI = 45,65,10
      IMINI = IMAXI - 10
      IF ( IMAX. LE. IMINI)   GO TO 30
      IF(IMAX.LT.IMAXI) 1000,1100
 1000 DO 1040 J = 26, JMAX
      IMAXX = IMAX + 1
      DO 1010 I = IMAXX, IMAXI
 1010 P(I,J) = -999999.99
 1040 CONTINUE
      IMXI = IMAXI
      GO TO 520
 1100 IMXI=IMAXI
  520 PRINT 101, (HEAD(I), I = 1,10)
      IPAGE = IPAGE + 1
      IF( L. LE. 10 ) GO TO 710
      IF (L. EQ. 11 ) GO TO 720
      IF ( L. LE. 15 ) GO TO 730
      IF ( L. EQ. 16 ) GO TO 720
      IF ( L. LE. 19 )750, 90
  710 PRINT 171, OUTLEV(L), IPAGE
      GO TO 3200
  720 PRINT 172, OUTLEV(L), IPAGE
      GO TO 3200
  730 PRINT 173, OUTLEV(L), IPAGE
      GO TO 3200
  750 PRINT 175, OUTLEV(L), IPAGE
 3200 CONTINUE
      DO 39 J = 26, JMAX
   39 PRINT 13, (P(I,J), I= IMINI,IMXI)
 1020 PRINT 11
   30 CONTINUE
 1030 CALL EXIT
   90 PRINT 91
   91 FORMAT(1X,'ERROR, TOO LARGE L VALUE')
      CALL EXIT
      END
```

```
          DIMENSION W(10),V(10),VA(10),ALPH(10),BETA(10),Q(10),
         1 A(10),B(10),TAI(10),TBI(10),HA(10),HB(10),DA(10),DB(10),
         2 P(10), TITLE(8)
          DIMENSION VB(10)
          DOUBLE PRECISION TITLE
C SET M = 1 IF INTERCEPT TIMES ARE IN MEILLISECONDS, M=0 IF IN SECONDS
C N=NUMBER OF LAYERS OR TRAVEL TIME SEGMENTS
C X=PROFILE LENGTH FROM A TO B, IN METERS, KILOMETERS, OR FEET
C VA(I) = APPARENT VELOCITIES FROM END A
C VB(I) = APPARENT VELOCITIES FROM END B
C TAI(I) = INTERCEPT ITMES FROM END A
C TBI(I) = INTERCEPT TIMES FROM END B
C
C
C
  400 READ (2,405, END = 1000) M,N,X,(TITLE(I), I = 1,6)
  405 FORMAT (2I,F,6A8)
      IF (N) 640, 640, 407
  407 READ (2,410) (VA(I), I = 1,N)
  410 FORMAT (9F)
      READ (2,410) (VB(I), I = 1,N)
      READ (2,410) (TAI(I), I = 2,N)
      READ (2,410) (TBI(I), I = 2,N)
      TAI(1) = 0.
      TBI(1) = 0.
,X    PRINT 411, (TITLE(I), I = 1,6)
  411 FORMAT (2X, 6A8,15HSPREAD LENGTH =      ,F8.3,//)
      PRINT 412
  412 FORMAT (2X,10HINPUT DATA //10X,5HLAYER,10X,8HAPPARENT   , 10X,
     18HAPPARENT,10X9HINTERCEPT,9X,9HINTERCEPT / 23X,13HVELOCITIES,A
     25X,13HVELOCITIES, B,7X,8HTIMES,A,10X,8HTIMES, B   //)
      IF (M) 414,417,414
  414 PRINT 415,(I,VA(I),VB(I),TAI(I),TBI(I),I = 1,N)
  415 FORMAT (I12,F22.2,F18.2,F17.2,F18.2)
      DO 416 I = 2,N
      TAI(I) = TAI(I)/1000.
  416 TBI(I) = TBI(I)/1000.
      GO TO 419
  417 PRINT 418, (I,VA(I),VB(I),TAI(I),TBI(I),I = 1,N)
  418 FORMAT (I12,F22.2,F18.2,F17.4,F18.4)
  419 CONTINUE
  421 DO 430 I = 2,N
      TBB = TAI(I) + X*(1./VA(I) - 1./VB(I))
      IF (TBI(I)) 422,422,423
  422 TBI(I) = TBB
      GO TO 430
  423 TAEND = TAI(I) + X/VA(I)
      TBEND = TBI(I) + X/VB(I)
      ERROR = ABS(TAEND/TBEND -1.)
      IF (ERROR - 0.10) 430,424,424
  424 PRINT 425, I
  425 FORMAT (5X,74HAPPATENT VELOCITY AND TIME INTERCEPT DATA ARE IN
     1CONSISTENT AT LAYER NUMBER       ,I2,/7X,56HEND-TO-END TRAVEL
     2TIMES DIFFER BY MORE THAN 10 PERCENT.             ,//)
  430 CONTINUE
      V(1) = (VA(1) + VB(1))*.5
      DO 570 M = 2,N
      K = 1
      ALPH (1) = ASIN(V(1)/VB(M))
      BETA (1) = ASIN (V(1)/VA(M))
```

```
      IF (M -2) 500,500,510
  500 A(1) = (ALPH(1) + BETA(1))*.5
      W(2) = (ALPH(1) -BETA(1))*.5
      V(2) = V(1)/SIN (A(1))
      GO TO 550
  510 A(1) = ALPH(1) - W(2)
      B(1) = BETA(1) + W(2)
  520 K = K + 1
      VV = V(K)/V(K-1)
      P(K) = ASIN (VV*SIN(A(K-1)))
      Q(K) = ASIN(VV*SIN(B(K-1)))
      IF (K+1-M) 530,540,540
  530 A(K) = P(K) -W(K+1) + W(K)
      B(K) = Q(K) +W(K+1) -W(K)
      ALPH(K) = A(K) + W(K+1)
      BETA(K) = B(K) -W(K+1)
      GO TO 520
  540 A(K) = (P(K)+Q(K))*.5
      B(K) = A(K)
      W(K+1) = W(K) + (P(K) - Q(K))*.5
      ALPH(K)  = A(K) +W(K+1)
      BETA(K) = B(K) - W(K+1)
      V(K+1) = V(K)/SIN(A(K))
  550 KK = K-1
      HHA = 0.
      HHB = 0.
      IF (KK) 561,561,551
  551 DO 561 I = 1,KK
      HH = COS(ALPH(I)) + COS(BETA(I))
      HH = HH/V(I)
      HHA = HHA + HH*HA(I)
  560 HHB = HHB + HH*HB(I)
  561 CONTINUE
      R = V(K) /(COS(ALPH(K)) + COS(BETA(K)))
      HA(K) = R*(TAI(K+1) - HHA)
      HB(K) = R*(TBI(K+1) - HHB)
      DA(1) = HA(1)
      DB(1) = HB(1)
      IF (K-1) 570,570,569
  569  DA(K) = DA(K-1) + HA(K)
      DB(K) = DB(K-1) + HB(K)
  570 CONTINUE
      DO 580 J = 2,N
  580 W(J) = W(J)*57.2958 +.001
      PRINT 620
  620 FORMAT (///2X,18HCOMPUTED STRUCTURE  // 9X,5HLAYER, 6X,8HVELOCITY
     1 ,6X,11HTHICKNESS A, 4X,11HTHICKNESS B,8X,3HDIP,10X,7HDEPTH A,
     2 8X,7HDEPTH B     //)
      I = 1
      PRINT 625, I,V(I),HA(I),HB(I),DA(I),DB(I)
  625 FORMAT (I12,3F15.2,15X,2F15.2)
      IF (N-2) 632,632,627
  627 NN = N-1
      PRINT 630,(I,V(I),HA(I),HB(I),W(I),DA(I),DB(I), I=2,NN)
  630 FORMAT (I12,6F15.2)
  632 PRINT 635, N,V(N),W(N)
  635 FORMAT(I12,F15.2,30X,F15.2)
      PRINT 638
  638 FORMAT ('  DECIMAL PLACES DO NOT NECESSARILY HAVE SIGNIFICANCE')
      GO TO 400
```

```
  640 CONTINUE
 1000 CALL EXIT
      END
```

Appendix III

SEISMIC DATA

Bison Data

Ambrose Creek #1B — T9N, R19W, NW¼NW¼SE¼ Sec. 24

Distance	Time
5 ft.	.0036 sec.
10 ft.	.0085 sec.
20 ft.	.0175 sec.
30 ft.	.0175 sec.
40 ft.	.0225 sec.
50 ft.	.0253 sec.
75 ft.	.0323 sec.
100 ft.	.0386 sec.
150 ft.	.0522 sec.
200 ft.	.0606 sec.
250 ft.	.0754 sec.
300 ft.	.0866 sec.

Interpretation (Two layers)

	Velocity	Thickness	Geology
1.	v_1 = 1300'/sec.	8'	Dry recent colluvium
2.	v_2 = 4000'/sec	>75'	Dry Cenozoic deposits

Ambrose Creek #2B — T9N, R19W, on road near section line between Sections 12 and 13

Distance	Time
10 ft.	.0085 sec.
15 ft.	.0130 sec.
20 ft.	.0175 sec.
30 ft.	.0230 sec.
40 ft.	.0245 sec.
50 ft.	.0272 sec.
75 ft.	.0325 sec.
100 ft.	.0365 sec.
150 ft.	.0435 sec.
200 ft.	.0495 sec.

Interpretation (Three layers)

	Velocity	Thickness	Geology
1.	1100'/sec.	10'	Dry recent colluvium
2.	5200'/sec.	35'	Water saturated alluvium
3.	8400'/sec.	>40'	Fractured igneous bedrock

Sheep Creek #1B — T9N, R19W, NW¼SW¼SE¼ Sec. 15

Distance	Time
10 ft.	.009 sec.
20 ft.	.016 sec.
50 ft.	.028 sec.
100 ft.	.048 sec.
150 ft.	.063 sec.
200 ft.	.069 sec.
250 ft.	.098 sec.
300 ft.	.108 sec.
350 ft.	.118 sec.
400 ft.	.128 sec.

Interpretation (Three layers)

	Velocity	Thickness	Geology
1.	1200'/sec.	27'	Dry recent colluvium
2.	4700'/sec.	110'	Dry Cenozoic deposits
3.	8500'/sec.	>75'	Water bearing Tertiary sediments

450 ft.	.136	sec.
500 ft.	.142	sec.
560 ft.	.196	sec.

Sheep Creek #2B T9N, R19W, NW¼NE¼SW¼ Sec. 22

Distance	Time
10 ft.	.016 sec.
20 ft.	.025 sec.
50 ft.	.045 sec.
100 ft.	.058 sec.
150 ft.	.066 sec.
200 ft.	.068 sec.
250 ft.	.074 sec.
300 ft.	.080 sec.
350 ft.	.084 sec.
400 ft.	.089 sec.
450 ft.	.099 sec.
500 ft.	.102 sec.

Interpretation (Three layers)

	Velocity	Thickness	Geology
1.	800'/sec.	13'	Dry recent colluvium
2.	4100'/sec.	47'	Dry Cenozoic deposits
3.	11800'/sec.	>100'	Metamorphic bedrock

Sheep Creek #3B T9N, R19W, NW¼NW¼SW¼ Sec. 15

Distance	Time
10 ft.	.0088 sec.
20 ft.	.0149 sec.
50 ft.	.0262 sec.
100 ft.	.042 sec.
150 ft.	.054 sec.
200 ft.	.056 sec.
250 ft.	.068 sec.
300 ft.	.075 sec.

Interpretation (Three layers)

	Velocity	Thickness	Geology
1.	1000'/sec.	3'	Dry recent colluvium
2.	3300'/sec.	55'	Dry Cenozoic deposits
3.	8500'/sec.	>50'	Water bearing Tertiary sediments

Kootenai Creek #1B T9N, R20W, SE¼SW¼NW¼ Sec. 17

Geophone 2 at west end of survey. Geophone 1 265' east of Geophone 2. Distance with respect to Geophone 1 (- is east, + is west).

Distance	Time(1)	Time(2)
-100 ft.	.0478 sec.	.095 sec.
- 80 ft.	.0414 sec.	.0925 sec.
- 60 ft.	.0366 sec.	.091 sec.
- 40 ft.	.0315 sec.	.087 sec.
- 20 ft.	.0183 sec.	.087 sec.
- 10 ft.	.0093 sec.	-
- 5 ft.	.0043 sec.	-
0 ft.	-	.084 sec.
+ 5 ft.	.0053 sec.	.086 sec.
+ 15 ft.	.0140 sec.	-
+ 25 ft.	.0255 sec.	.079 sec.
+ 40 ft.	.0321 sec.	.077 sec.
+ 60 ft.	.0391 sec.	.0754 sec.
+ 80 ft.	.0426 sec.	.0718 sec.

Interpretation (Four layers)

	Velocity	Thickness (1)	Thickness (2)	Geology
1.	800'/sec.	9'	9'	Dry colluvium
2.	3300'/sec.	40'	47'	Dry Cenozoic deposits
3.	7750'/sec.		69'	Water bearing Tertiary deposits
4.	10600'/sec.			Frontal Zone Gneiss

+100 ft.	.0486 sec.	.0690 sec.
+120 ft.	.0558 sec.	.0662 sec.
+140 ft.	.0580 sec.	.0610 sec.
+160 ft.	.0646 sec.	.0538 sec.
+180 ft.	.0662 sec.	.0482 sec.
+200 ft.	.0694 sec.	.0418 sec.
+220 ft.	.0714 sec.	.0354 sec.
+240 ft.	.0730 sec.	.0302 sec.
+260 ft.	.0762 sec.	.0070 sec.
+280 ft.	.0790 sec.	-

Ambrose Creek 3T f.

T9N, R19W, 1320' west of section corner on section line between Sec. 2 and 11.

Gain = 30
Filters - Broad
LC = 20
HC = 48

Interpretation is in Fig. 19.

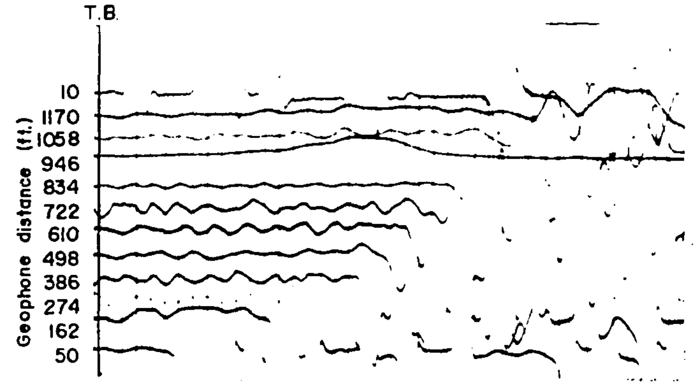

Ambrose Creek 3T r.

Shot point 1180' west of AC3T forward

Gain = 30
Filters - Broad
LC = 20
HC = 48

Interpretation is in Fig. 19.

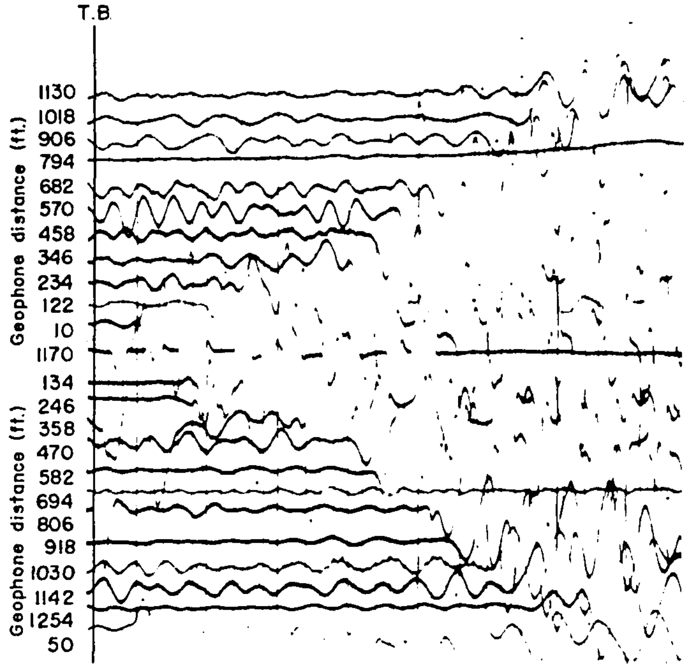

Ambrose Creek 4T f.

Same shot point as AC3T reverse

Gain = 30
Filters - Broad
LC = 20
HC = 48

Interpretation is in Fig. 19.

Kootenai Creek 1T f.

T9N, R20W, SE1/4SW1/4NW1/4 Sec. 17

Line location same as KC1B.

Gain = 20
Filters out

Interpretation is in Fig. 18.

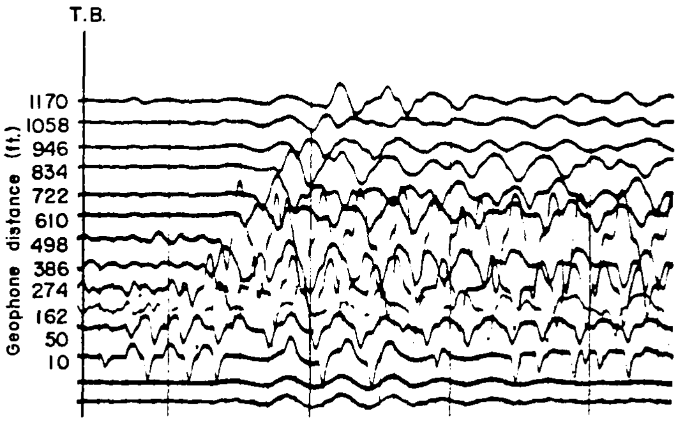

Kootenai Creek 2T r.

T9N, R20W, Sec. 17
Shot location 1170' east of
KC IT f.

Gain = 20
Filters out

Kootenai Creek 3T f.

Same shot point as KC IT r.

Gain = 20
Filters out

Interpretation is in Fig. 18.

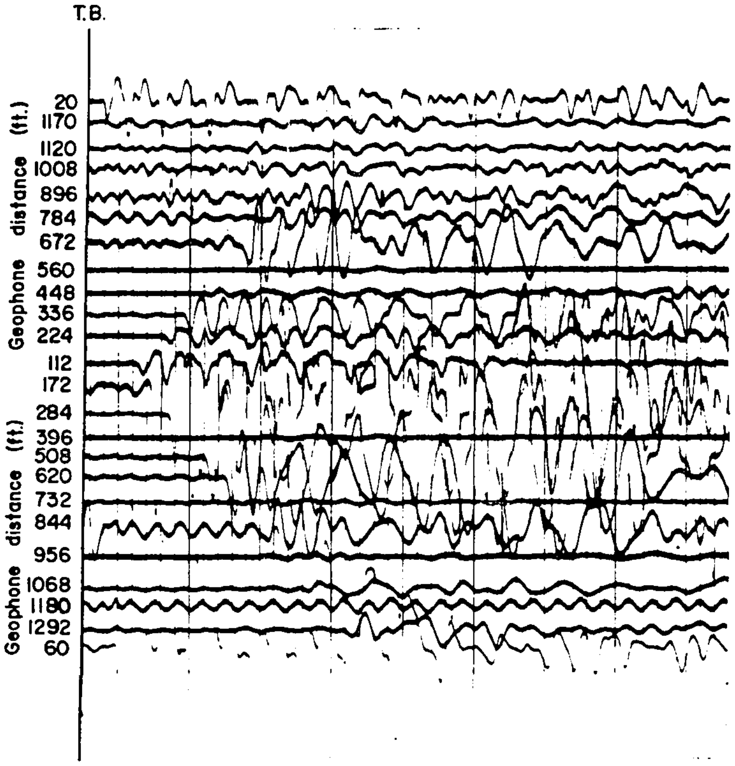

Timing lines on seismic records on p. 106 and 107 are 10 milliseconds apart.

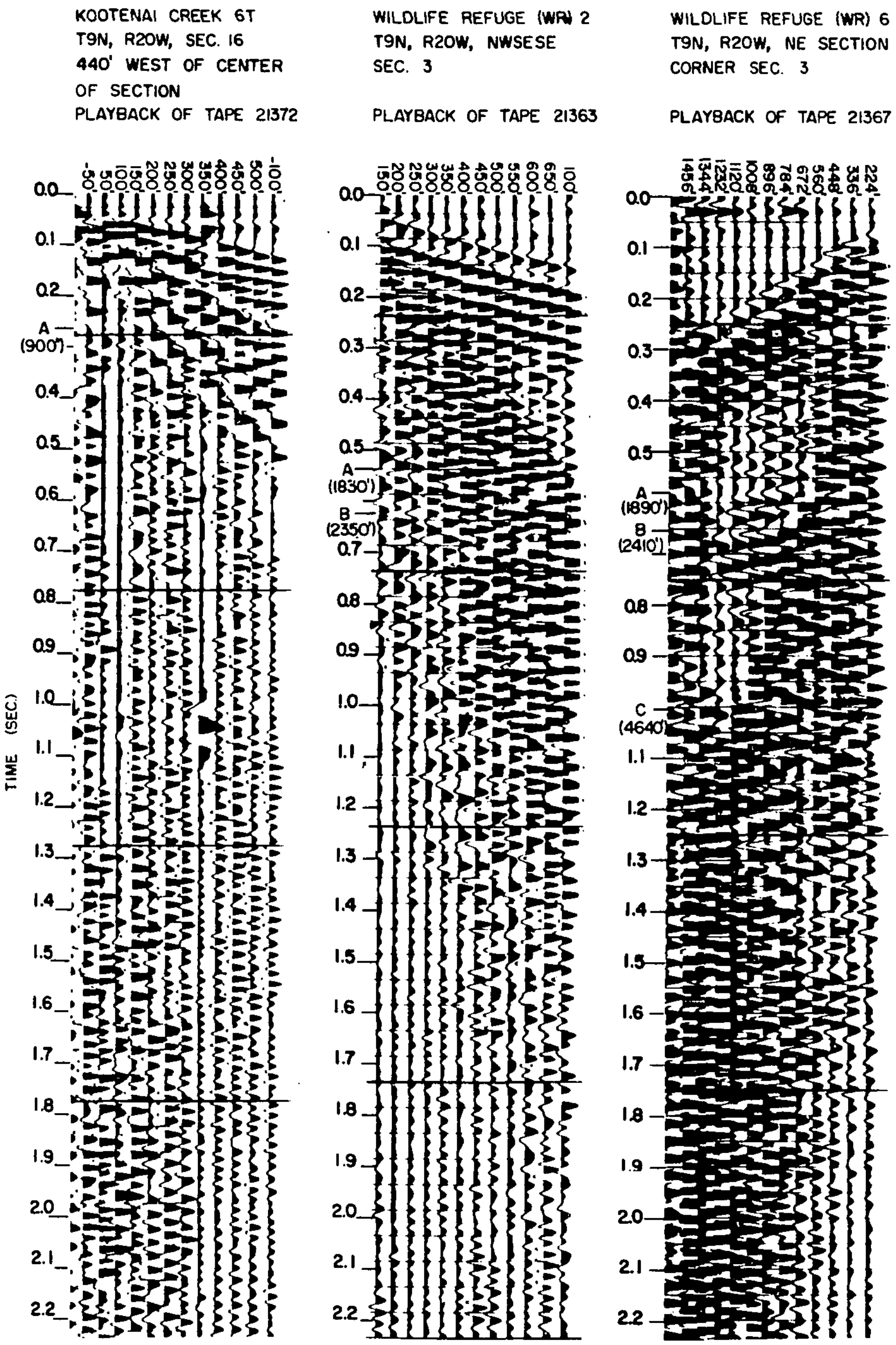

Variable area presentation of three reflection records filtered at 10-45 Hz. Event A. Reflection from base of Cenozoic sediments. Event B. Intra-Frontal Zone Gneiss reflection. Event C. Reflection from base of Frontal Zone Gneiss (?). Calculated depths below surface in parentheses.

BIBLIOGRAPHY

Bonini, W. E., Smith, R. B., and Hughes, D. W., 1973, Complete Bouguer gravity anomaly map of Montana: Mont. State Bur. of Mines and Geol., spec. pub. 62, Butte, 1 p.

Bott, H. M. P., 1960, The use of rapid digital computing methods for direct gravity interpretation of sedimentary basins: Geophys. Jour., v. 3, p. 63-67.

_____________, 1962, A simple criterion for interpreting negative gravity anomalies: Geophysics, v. 27, p. 376-381.

Burfeind, W. J., 1967, A gravity investigation of the Tobacco Root Mountains, Jefferson Basin, Boulder Batholith, and adjacent areas of southwestern Montana: Ph.D. dissertation, Indiana University, Bloomington, 146 p.

Cook, K. L., Berg, J. W., and Lum, D., 1967, Seismic and gravity profile across the northern Wasatch Trench, Utah: Seis. Refrac. Prospecting, Soc. Explor. Geophys., Tulsa, 604 p.

Cooley, J. W. and Tukey, J. W., 1965, An algorithm for the machine calculation of complex fourier series: Math. of Computation, v. 19, p. 297-301.

Cordell, L., and Henderson, R., 1968, Iterative three-dimensional solution of gravity anomaly data using a digital computer: Geophysics, v. 33, p. 596-601.

Davis, T. M., 1974, Theory and practice of geophysical survey design: Ph.D. dissertation, Penn State University, Philadelphia, 137 p.

Dean, W. C., 1952, Frequency analysis for gravity and magnetic interpretation: Geophysics, v. 23, p. 97-127.

Deel, S. A., and Howe, H. H., 1948, United States magnetic tables and magnetic charts for 1945: United States Coast and Geodetic Survey, serial 667, Washington, 137 p.

Dix, C. A., 1955, Seismic velocities for subsurface measurement: Geophysics, v. 20, p. 68-86.

Dobrin, M. B., 1960, Introduction to geophysical prospecting: McGraw-Hill, New York, 446 p.

Douglas, J. K., 1972, Geophysical investigation of the Montana lineament: M.S. dissertation, University of Montana, Missoula, 75 p.

Douglas, J. K., and Prahl, S. R., 1972, Extended terrain correction tables for gravity reductions: Geophysics, v. 37, p. 377-379.

Ferguson, J. A., 1972, Fission track and K-Ar dates on the northeast border zone of the Idaho batholith: M.S. dissertation, University of Montana, Missoula, 32 p.

Fuller, B. D., 1967, Two dimensional frequency analysis and design of grid operators: Mining Geophysics, v. 2, Soc. Explor. Geophys., Tulsa, 708 p.

Grant, F. S., and West, G. F., 1965, Interpretation theory in applied geophysics: McGraw-Hill, New York, 584 p.

Hall, D. H., and Hajnal, Z., 1962, The gravimeter in studies of buried valleys: Geophysics, v. 27, p. 939-951.

Hammer, S., 1939, Terrain corrections for gravimetric stations: Geophysics, v. 4, p. 184-194.

_________, 1974, Approximation in gravity interpretation calculations: Geophysics, v. 39, p. 205-222.

Heiland, C., 1940, Geophysical exploration: Prentice-Hall, Englewood Cliffs, N.J., 1013 p.

Henbest, O. J., Erinakes, D. C., and Hixson, D. H., 1969, Seismic and resistivity methods of geophysical exploration: United States Dept. of Agri. Tech. report 44, 150 p.

Henderson, R. G., 1960, A comprehensive system of automatic computation in magnetic and gravity interpretation: Geophysics, v. 25, p. 569-586.

Hutchison, D. M., 1959, Volcanic ash in the northern part of the Bitterroot Valley, Ravalli County, Montana: M.S. dissertation, University of Montana, Missoula, 62 p.

Keunzi, W. D., and Fields, R. W., 1971, Tertiary stratigraphy, structure, and geologic history, Jefferson Basin, Montana: Geol. Soc. of Amer., v. 18, p. 3373-3394.

Langton, C. M., 1935, Geology of the northeastern part of the Idaho batholith and adjacent region in Montana: Jour. of Geol., v. 43, p. 27-66.

Lankston, R. W., 1975, Depth to magnetic basement in the northern Bitterroot Valley and Sapphire Mountains in western Montana: Geol. Soc. of Amer., abstracts with programs, Rocky Mountain Section, p. 1000.

Manghnani, M., and Hower, J., 1962, Structural significance of gravity profile in the Bitterroot Valley, Ravalli County, Montana (abs.): Geol. Soc. of Amer., spec. paper 68, p. 93.

McMurtry, R. G., Konizeski, R. L., and Stemitz, F., 1959, Geology and water resources of the Bitterroot Valley, Montana: Mont. Bur. of Mines and Geol., bull. v. 9, 45 p.

Montana Almanac, 1957, University of Montana Press, Missoula.

Montana State Geologic Map, 1955, United States Geol. Survey and Mont. Bur. of Mines and Geol., 1 p.

Mooney, H., 1973, Engineering geophysics: Bison, Minneapolis, 45 p.

Musgrave, A. W., 1962, Application of the expanding reflection spread: Geophysics, v. 27, p. 981-993.

Nettleton, L. L., 1942, Gravity and magnetic calculations: Geophysics, v. 7, p. 293-310.

_______________, 1971, Elementary gravity and magnetics for geologists and seismologists: Soc. Explor. Geophys., Tulsa, 75 p.

Nolan, K. M., 1973, Flood hazard mapping of the Bitterroot Valley, Montana: M.S. dissertation, University of Montana, Missoula, 56 p.

Oldenburg, D. W., 1974, The inversion and interpretation of gravity anomalies: Geophysics, v. 39, p. 526-536.

Peters, L. J., 1949, The direct approach to magnetic interpretation and its practical applications: Geophysics, v. 14, p. 290-320.

Peterson, R. A., and Dobrin, M. B., 1966, A pictoral, digital atlas: United Geophys. Corp., Houston, 53 p.

Presley, M. W., 1970, Igneous and metamorphic geology of West Creek drainage basin, southern Sapphire Mountains: M.S. dissertation, University of Montana, Missoula, 64 p.

Rudman, A. J., Mead, J., Whaley, J. F., and Blakely, R. F., 1971, Geophysical analysis in central Indiana using potential field continuation: Geophysics, v. 36, p. 878-890.

Seismograph Service Corporation, Editors, 1969, The Robinson-Treitel reader: Seismograph Serv. Corp., Tulsa, 176 p.

Sheriff, R. E., 1973, Encyclopedic dictionary of exploration geophysics: Soc. Explor. Geophys.c Tulsa, 266 p.

Smith, R. B., 1967, A regional gravity survey of western and central Montana: Ph.D. dissertation, University of Utah, Salt Lake City, 140 p.

Stephens, E. E., 1973, Shallow seismic techniques: Calif. Div. of Highways, Sacramento, 71 p.

Talwani, M., and Ewing, M., 1960, Rapid computation of gravitational attraction of three dimensional bodies of arbitrary shape: Geophysics, v. 25, p. 203-225.

United States Air Force, 1962, Air Force gravity base measuring stations network: Geophysics, v. 27, p. 1035.

United States Department of Defense, 1974, Gravity file: Dept. of Defense Gravity Services Division, St. Louis.

United States Geological Survey, 1966, Three aeromagnetic profiles in the Bitterroot Valley area, Montana and Idaho: United States Geol. Survey, open file report.

Wollard, G. P., and Rose, J. C., 1963, International gravity measurements: University of Wisconsin Press, Madison, 518 p.

Zeitz, I., Hearn, B. C., Higgins, M. W., Robinsion, G. D., and Swanson, D. A., 1971, Interpretation of an aeromagnetic survey across the northwestern United States: Geol. Soc. of Amer., bull., v. 82, p. 33.

Zurflueh, E. C., 1967, Applications of two-dimensional linear wavelength filtering: Geophysics, v. 32, p. 1015-1035.

BOUGUER GRAVITY ANOMALY MAP
OF THE BITTERROOT VALLEY

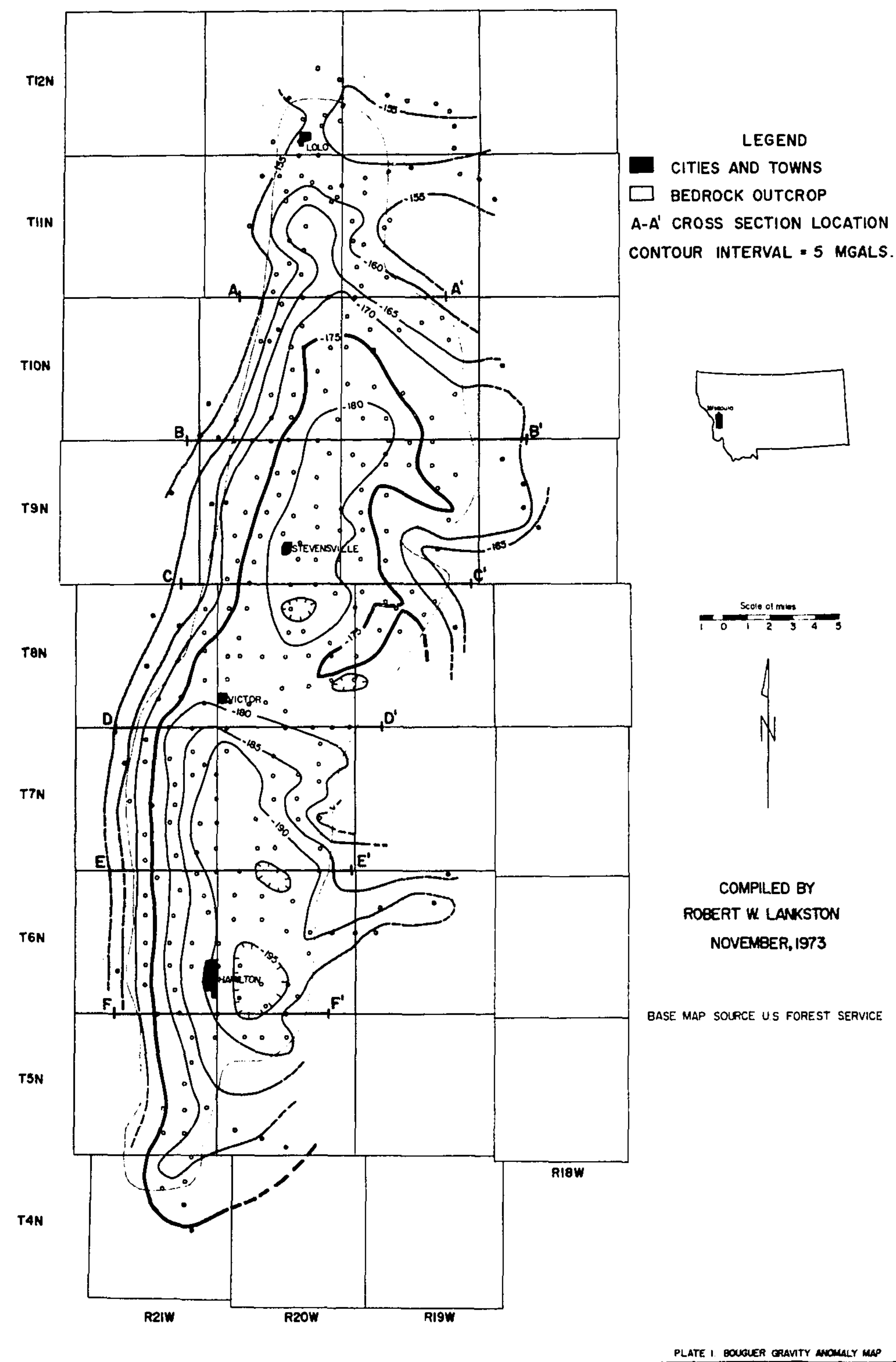

BEDROCK TOPOGRAPHY MAP
OF THE BITTERROOT VALLEY

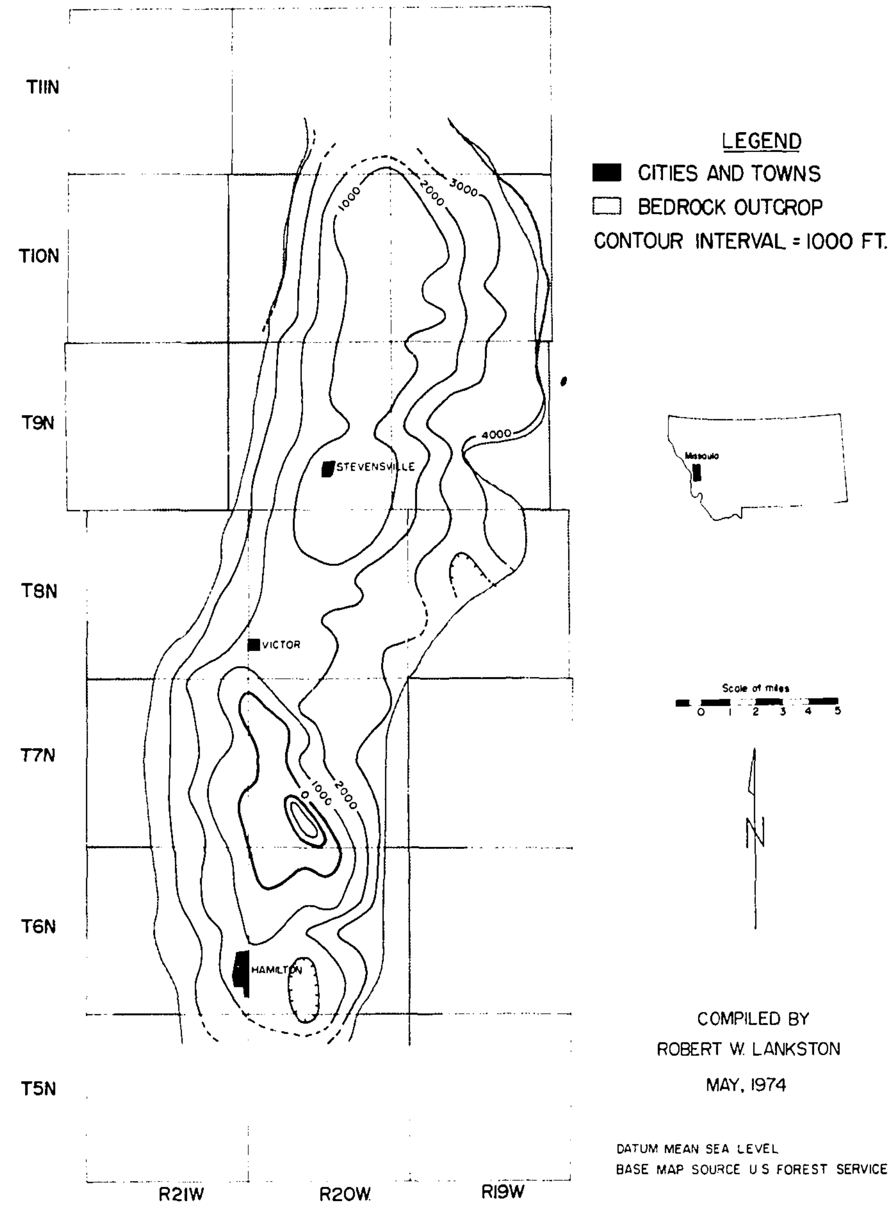

PLATE 2 BEDROCK TOPOGRAPHY MAP

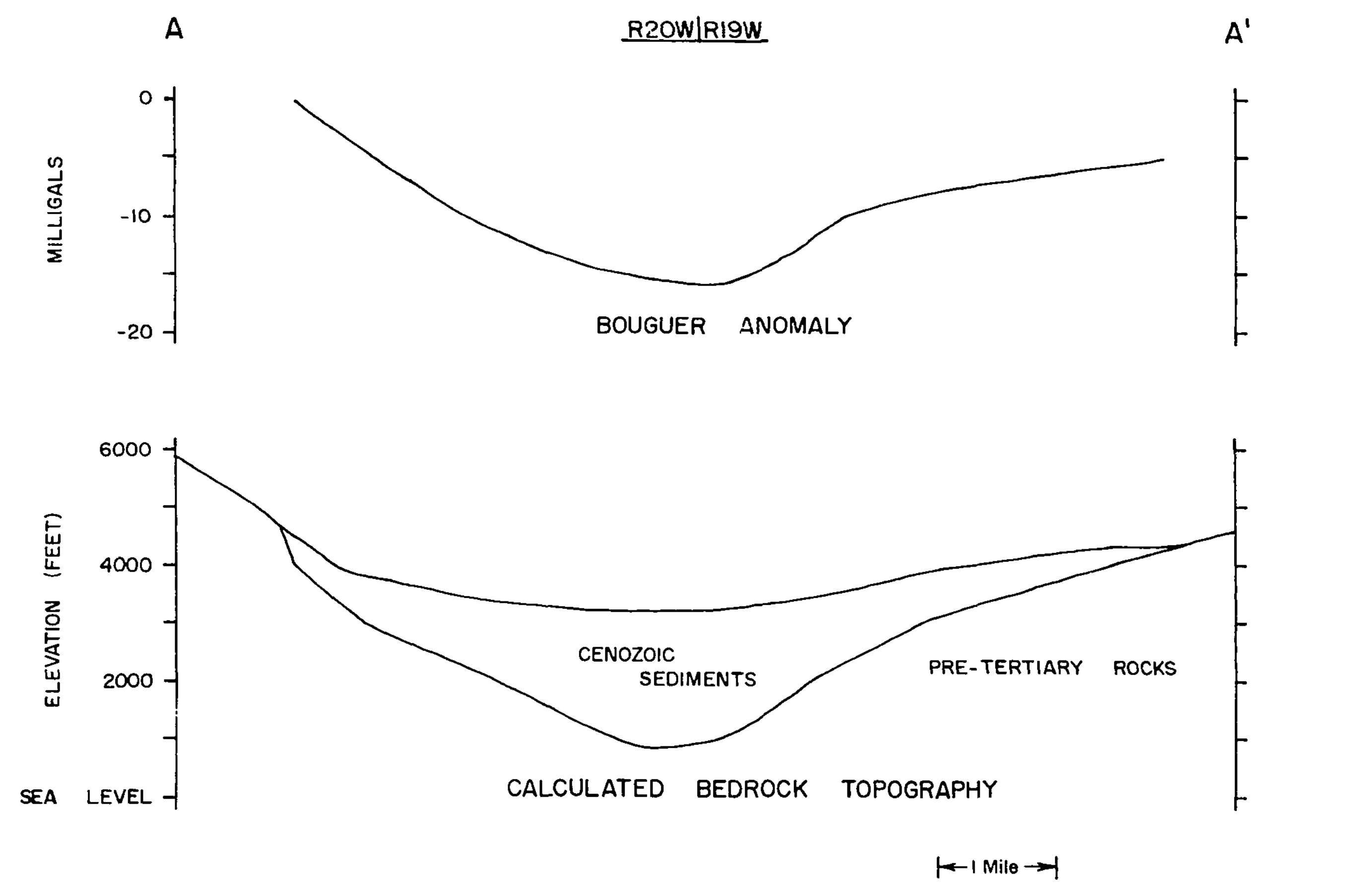

CROSS SECTION A

PLATE 3a

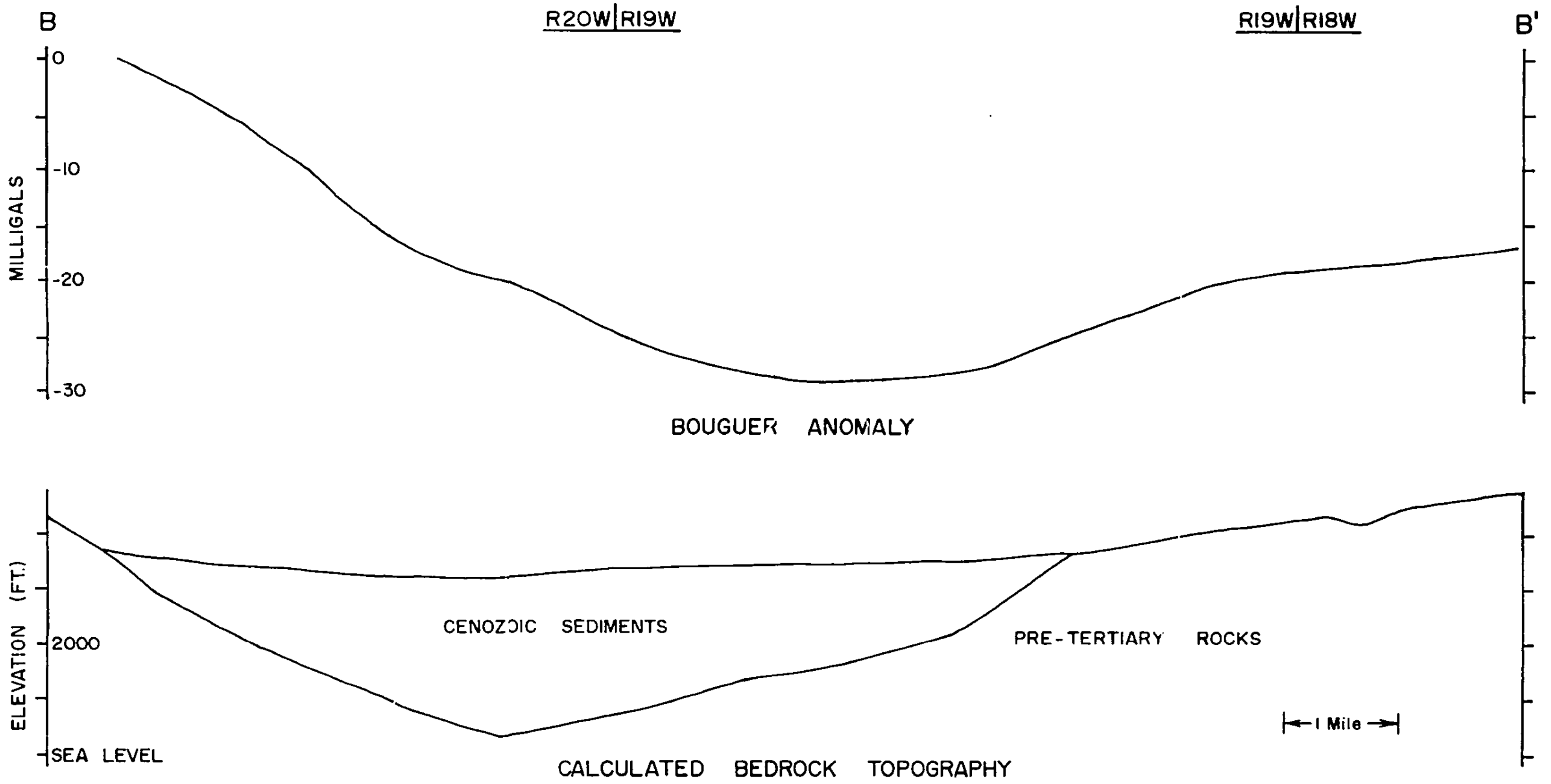

CROSS SECTION B

PLATE 3b

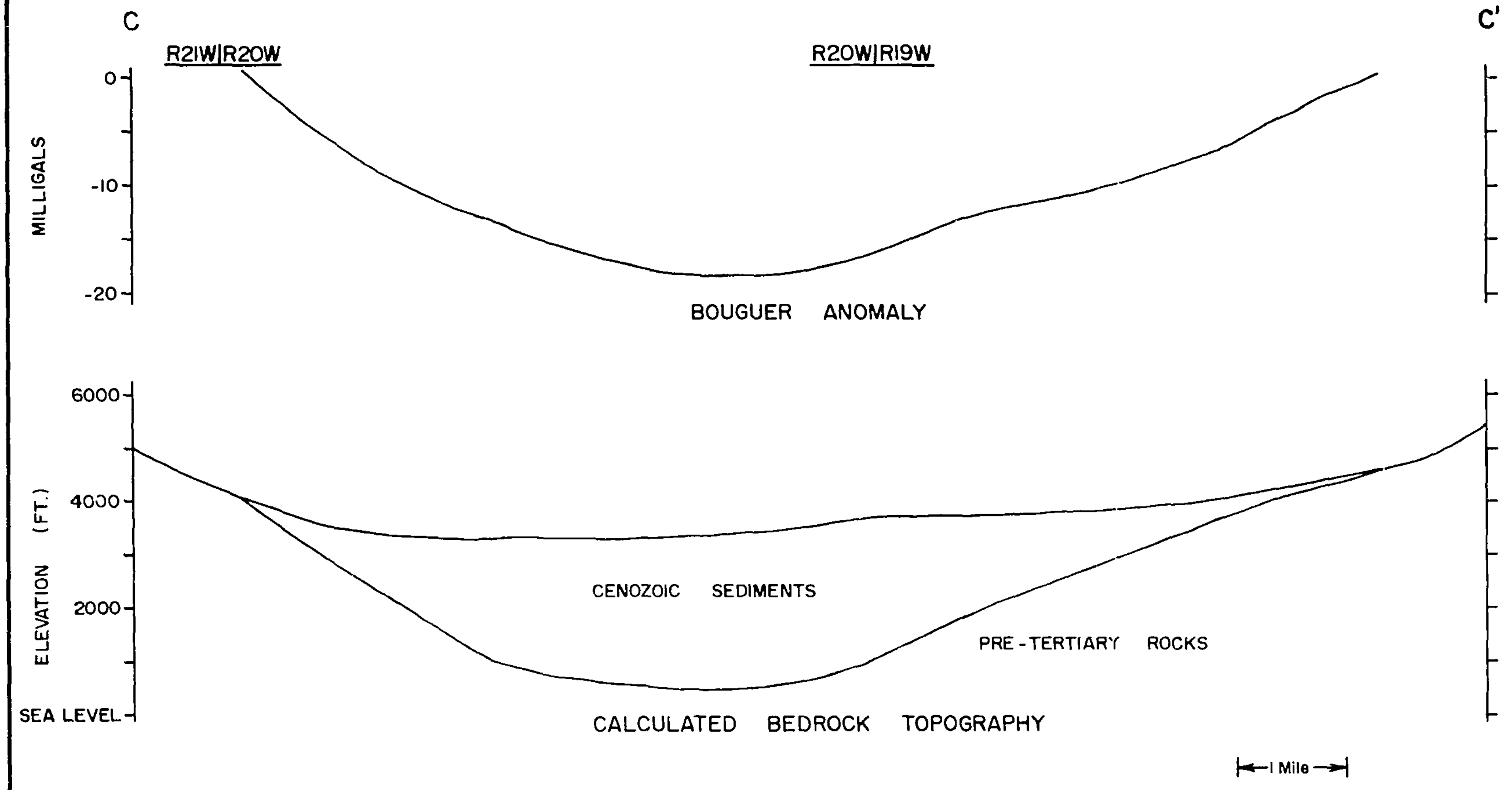

CROSS SECTION C

PLATE 3c

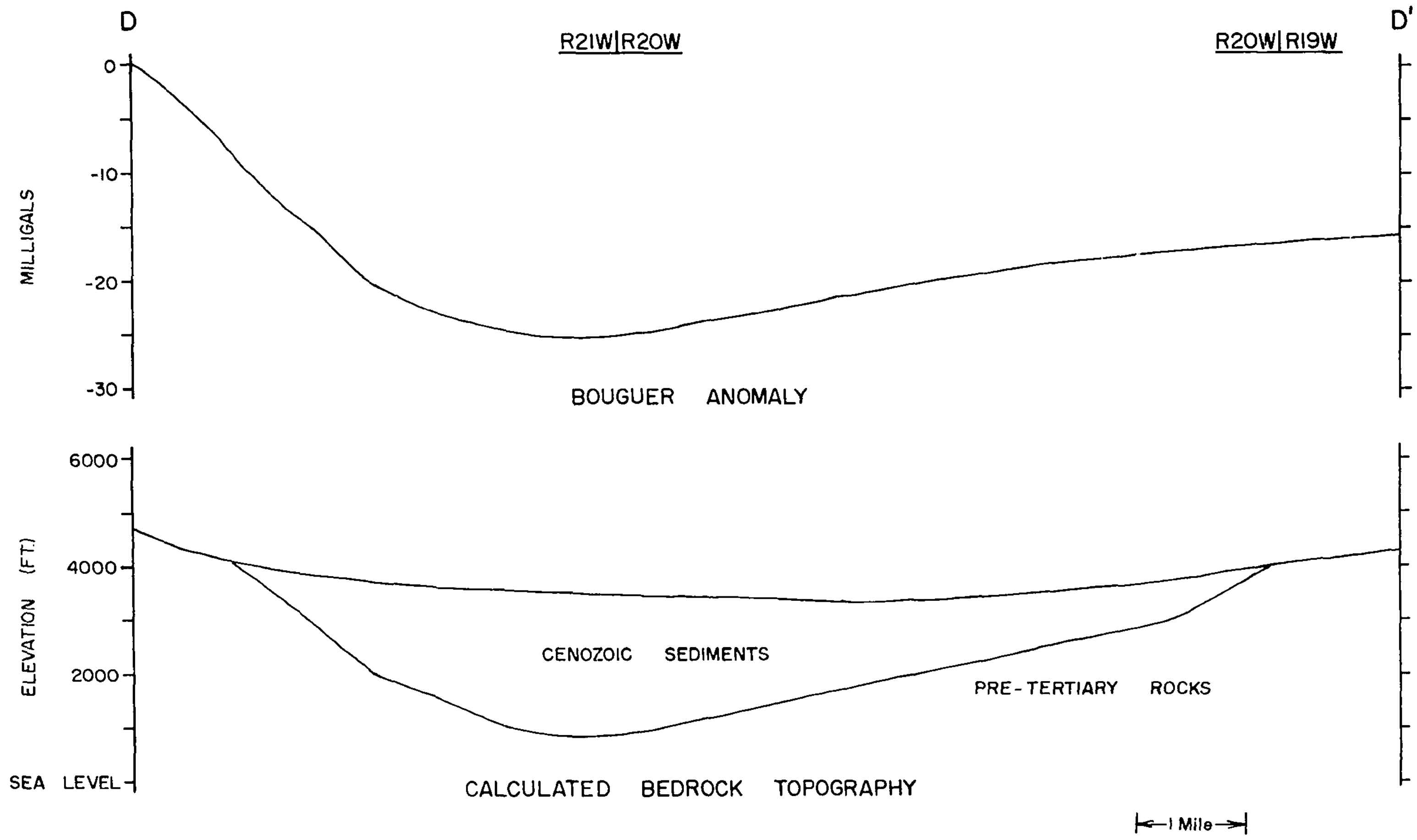

CROSS SECTION D

PLATE 3d

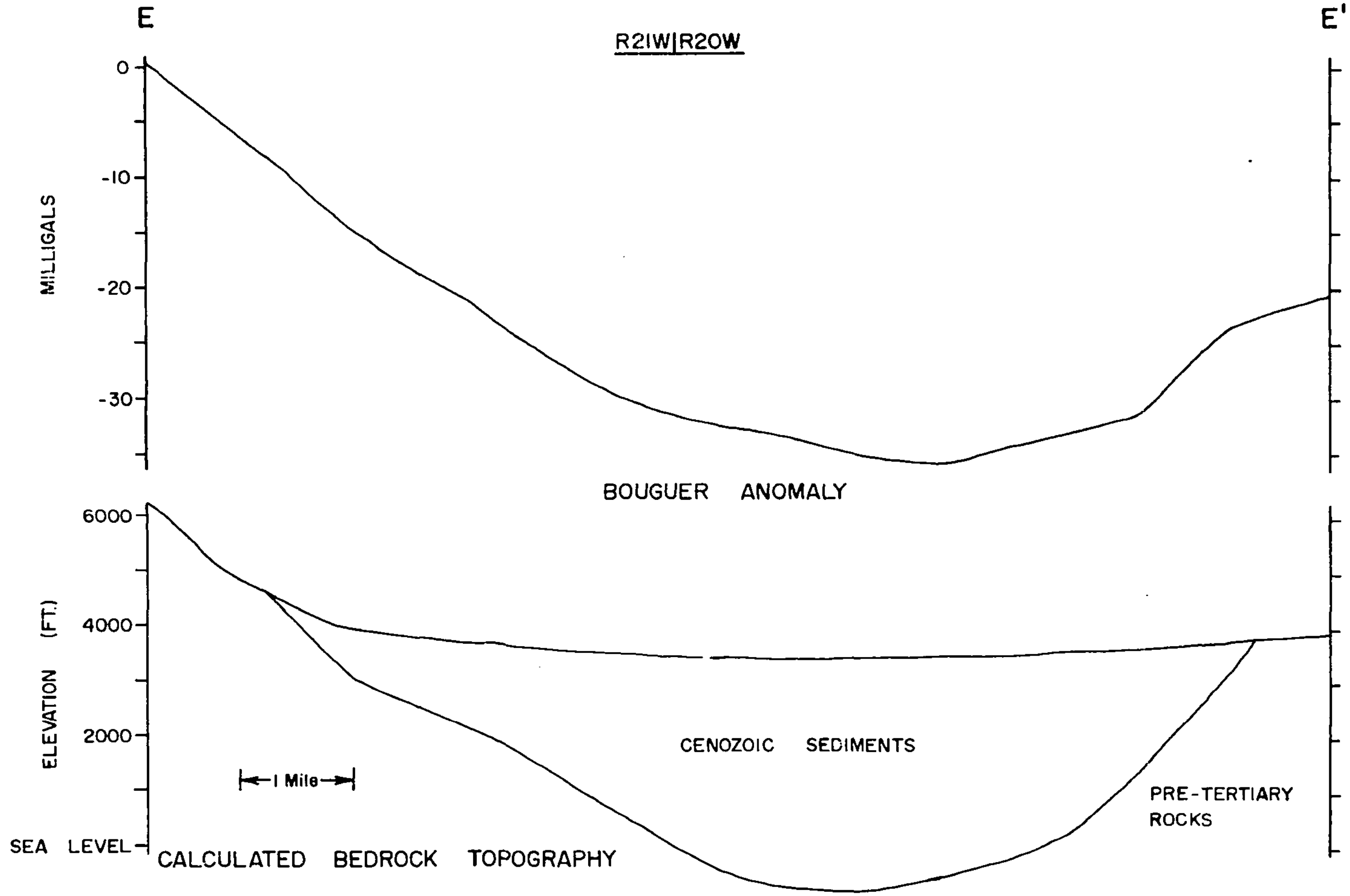

CROSS SECTION E

PLATE 3a

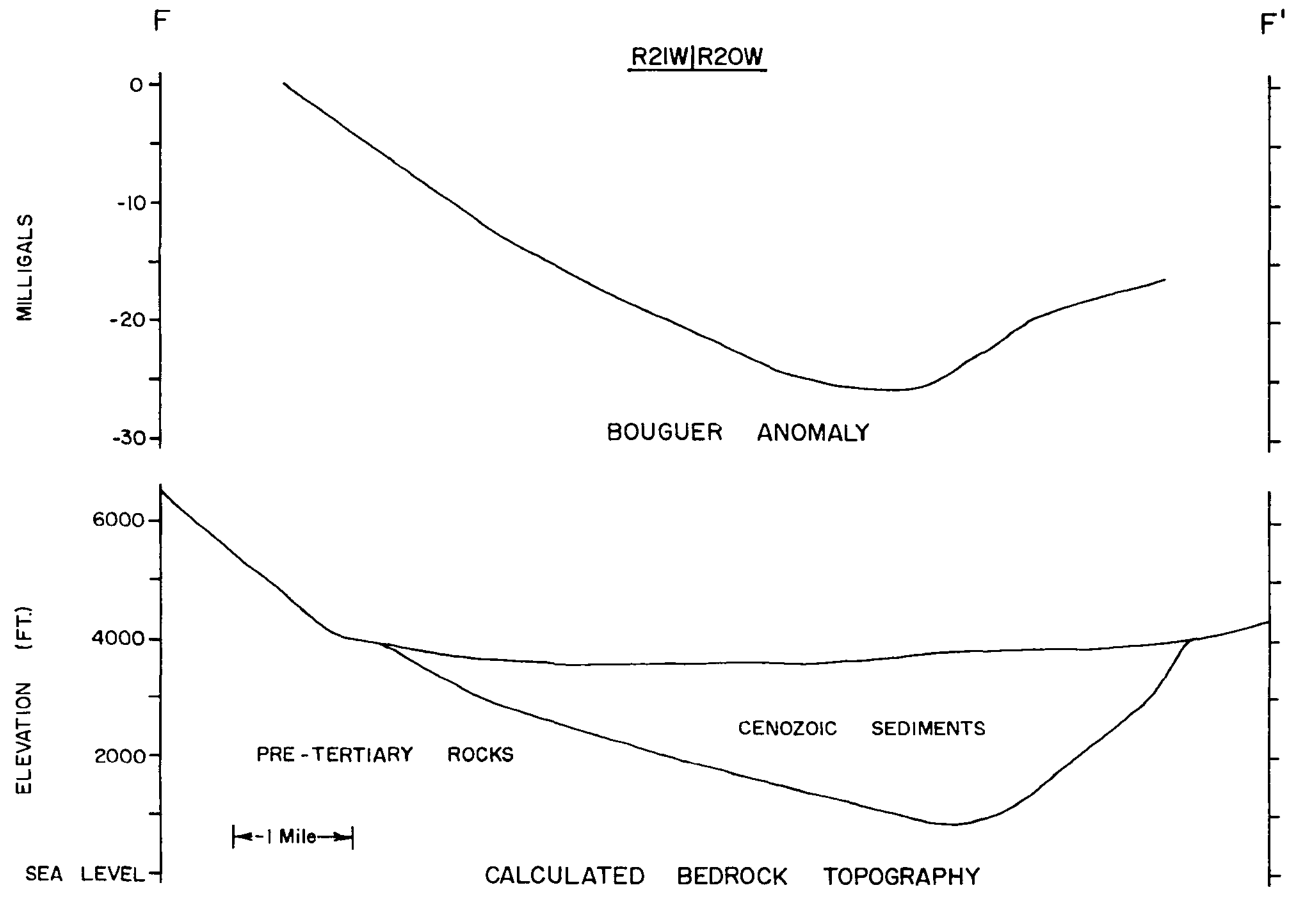

CROSS SECTION F

PLATE 3f